EXPERIMENTAL AND COMPUTATIONAL CHEMISTRY SIMULATION STUDIES ON THE CORROSION INHIBITION POTENTIALS OF SOME AMINO ACIDS

By

AWE, FEMI EMMANUEL B.Sc. (ABU 2008)
M.Sc./SCIEN/00123/08-09

THESIS SUBMITTED TO THE POSTGRADUATE SCHOOL,
AHMADU BELLO UNIVERSITY, ZARIA
NIGERIA

IN PARTIAL FULFILMENT FOR THE AWARD OF MASTER OF SCIENCE IN PHYSICAL CHEMISTRY

DEPARMENT OF CHEMISTRY
AHMADU BELLO UNIVERSITY, ZARIA
NIGERIA

FEBRUARY, 2011

DECLARATION

I declare that the work in this thesis entitled, "Experimental and computational chemistry simulation studies on the corrosion inhibition potentials of some amino acids on mild steel in HCl" has been performed by me in the Department of Chemistry under the supervision of Dr. N. O. Eddy and Prof. C. E. Gimba.

The information derived from the literature has been duly acknowledged in the text and a list of references provided. No part of this project was previously presented for another degree or diploma at the university.

Awe, Femi Emmanuel Signature

CERTIFICATION

The thesis entitled "Experimental and computational chemistry simulation studies on the corrosion inhibition potentials of some amino acids on mild steel in HCl" by Awe, Femi Emmanuel meets the regulations governing the award of the degree of M.Sc. Physical Chemistry of Ahmadu Bello University, and is approved for its contribution to knowledge and literally presentation.

…… ……
Dr. N.O. Eddy Date
Chairman, Supervisory Committee

……. ……...
Prof. C.E. Gimba Date
Member, Supervisory Committee

…….. ……
Prof. C.E. Gimba Date
Head of Department

…….. ……..
Prof. A. A. Joshua Date
Dean, Postgraduate School

DEDICATION

TO

MY PARENTS

ACKNOWLEDGMENTS

I wish to express my profound thanks to the Sovereign Lord for His grace, mercy, love, favours and protection. I am grateful to my dad and mum for being a 'cover' and 'support'. May Lord honour you. I thank my brother and sisters viz Micheal, Oluwakemi, Omowumi and Maria for all their love and care showered on me.

I lack words to express my thanks to my supervisors Dr. N.O. Eddy, and Prof. C. E. Gimba. I must confess I am humbled by the confidence and trust bestowed on me. I am particularly grateful for their corrections, which helped me to straighten the work. I thank them for being patient with me. May the Lord keep them. I also thank the Head of Department, academic, technical staff and students of chemistry department A.B.U., Zaria for all their favours.

To my colleagues Joseph, Omeiza, Ladan, Abdulfatai, Muktar, Dele, Monsurat Shoge, Abubakar, Sunday Moses, Victor, Ibrahim Olaniyi, Paul, Hygenius, Jude, Nkiru and Esther, may God bless you all.

Special thanks go to Mrs., O.R.A. Iyun and Mr. Celetine Ochigbo of M.Sc. laboratory for their technical help and advice.

To my relatives, friends and well wishers too many to mention. I am grateful and may God bless them.

ABSTRACT

Inhibition and adsorption potentials of cysteine, glycine, leucine and alanine have been investigated using experimental and quantum chemical approaches. The experimental study was carried out using gravimetric, gasometric, thermometric and FTIR methods of monitoring corrosion while the quantum chemical study was carried out using semi-empirical and *ab-initio* methods. The results obtained reveal that various concentrations of the amino acids inhibited the corrosion of mild steel in solutions of HCl through the mechanism of physiosorption with activation energy less than $80kJmol^{-1}$. The inhibition potentials of the inhibitors decreased in the order, cysteine >leucine> alanine > glycine and their adsorption was found to be exothermic, spontaneous and fitted the Langmuir adsorption model. Computational chemistry results obtained revealed excellent correlations between quantum chemical parameters (calculated for gas and aqueous phases PM6, PM3, AM1, RM1 and MNDO Hamiltonians) and experimental inhibition efficiencies. Correlations between the experimental and theoretical inhibition efficiencies were also excellent. Application of condensed Fukui and softness functions as well as relative nucleophilicity/electrophilicity (calculated for B3LYP(6-31G) and MP2(STO-5G) paturbations) showed that the sites for electrophilic attack are on the amine bonds (N2-C3) of the amino acids while the sites for nucleophilic attack are on the C-3 atoms of the amino acids. The HOMO and LUMO diagrams of the amino acids as well as the electron density diagrams have also been used to support the information obtained from condensed Fukui function.

Table of content

Title page	i
Declaration	ii
Certification	iii
Dedication	iv
Acknowledgement	v
Abstract	vi
Table of content	viii
List of tables	xii
List of figures	xiii
List of appendices	xvi
List of abbreviation	xxii
CHAPTER ONE	
1.1 Background of the study	1
1.2 Different types of Corrosion in metals	4
1.2.1 Uniform Corrosion	4
1.2.2 Galvanic Corrosion	4
1.2.3 Pitting Corrosion	5
1.2.4 Crevice Corrosion	6
1.2.5 Intergranular Corrosion	6
1.2.6 Erosion Corrosion	6
1.2.7 Cavitations Corrosion	6
1.2.8 Interfilm Corrosion	7

1.2.9 Fretting Corrosion 7

1.3 Environmental Factor affecting the Corrosion of Iron 7

1.4. Inhibition of Corrosion 11

1.4.1 Interphase Inhibitors 12

1.4.2 Passivating/Oxidizing Inhibitors 12

1.4.3 Non Oxidizing Inhibitors 13

1.4.4 Interface Inhibition 13

1.5 Statement of the problem 14

1.6 Aims and objectives of the Study 15

CHAPTER TWO

2.0 Literature review 19

2.1 Green Corrosion Inhibitors 19

2.1.1Plant extractsas green inhibitor 19

2.1.2 Amino acids as green corrosion inhibitor 24

2.2QSAR in corrosion study 29

2.3 Quantum chemical methods in corrosion inhibiton s' studies 30

2.4Quantum chemical parameters 33

2.4.1Atomic charges 34

2.4.2Molecular orbital energies 34

2.4.3Dipole moment (l) 35

2.4.4Energy 35

2.5 Semi-empirical methods 36

2.5.1 MNDO (modified neglect of differential overlap) 37

2.5.2 AM1 (Austin model 1) 37

2.5.3 PM3 (parameterized model number 3) 38

2.6 Study of corrosion inhibitors by semi-empirical methods 38

2.7 Ab initio and density functional theory (DFT) method 46

2.8 Corrosion inhibitors studied by ab initio and DFT methods 47

CHAPTER THREE

3.0 Materials and Method 60

3.1 Material 60

3.2 Experimental Techniques 60

3.2.1 Gravimetric method 60

3.2.2 Thermometric method 61

3.2.3 Gasometric method 63

3.3 Quantum chemical calculation 65

3.4 Infra red analysis 66

CHAPTER FOUR

4.0 RESULTS AND DISCUSSIONS 67

4.1 Experimental 67

4.1.1 Effect of concentration of amino acids on the corrosion of mild steel 67

4.1.2 Gasometric and thermometric studies 73

4.1.3 Kinetic study 73

4.1.4 Effect of temperature 78

4.1.5 Thermodynamics/adsorption study 80

4.1.6 IR study 84

4.2 Quantum chemical study 94

4.2.1 Semi-empirical study 94

4.2.2 Density functional theory (DFT) 108

4.2.2.1 Local selectivity 114

4.2.2.2Quantitative structure activity relation (QSAR) study 126

4.2.2.3Mechanism of inhibition 140

CHAPTER FIVE

5.0 Conclusion and recommendation 143

REFRENCES 144

LIST OF TABLES

Table 4.1: Rates of corrosion of mild steel and inhibition efficiencies of the amino acids in various media 70

Table 4.2: Gasometric and thermometric results for the Inhibition efficiency (%) of some amino acids in various media 75

Table 4.3: Kinetic parameters for the corrosion of mild steel in 0.1 M HCl containing various concentrations of some amino acids 77

Table 4.4: Thermodynamic parameters for the adsorption of various concentrations of some amino acid on mild steel surface 79

Table 4.5: Langmuir parameters for the adsorption of some amino acids on mild steel surface at 303 and 333 K 83

Table 4.6: Frequencies and peaks of IR adsorption by CYS and the corrosion product of mild steel (containing CYS) 88

Table 4.7: Frequencies and peaks of IR adsorption by GLY and the corrosion product of mild steel (containing GLY) 92

Table 4.8: Frequencies and peaks of IR adsorption by LEU and the corrosion product of mild steel (containing LEU) 97

Table 4.9: Frequencies and peaks of IR adsorption by ALA and the corrosion product of mild steel (containing ALA) 100

Table 4.10: Gas phase quantum chemical parameters for the studied amino acids 101

Table 4.11: Aqueous phase quantum chemical parameters for the studied amino acids 102

Table 4.12: Values of R^2 between experimental inhibition efficiencies and some semi-empirical parameters obtained from aqueous phase (gas phase) calculations for different Hamiltonians 107

Table 4.13: Gas phase quantum chemical parameters for the studied amino acids 111

Table 4.14: Aqueous phase quantum chemical descriptors for the studied amino acids 112

Table 4.15 : Fukui and softness functions for electrophilic and nucleophilic attacks on carbon and electronegative atoms in the studied amino acids calculated from Muliken(Lowdin) charges using DFT-B3YLP (6-31G) 117

Table 4.16 : Fukui and softness functions for electrophilic and nucleophilic attacks on carbon and electronegative atoms in the studied amino acids calculated from Muliken(Lowdin) charges using MP2 (STO-5G) 118

Table 4.17: Huckel charges on carbon and electronegative atoms in the studied amino acids 125

Table 4.18: Theoretical inhibition efficiencies (IE_{Theor}) of the studied amino acids for gas phase calculations 129

Table 4.19: Theoretical inhibition efficiencies (IE_{Theor}) of the studied amino acids for aqueous phase calculations 135

LIST OF FIGURES

Fig. 1.1: Optimised and chemical Structures of L-Leucine (LEU), Glycine (GLY), L-cysteine (CYS) and L-alanine (ALA) 16

Fig. 3.1: Diagram of the Thermometric Apparatus 62

Fig. 3.2: Gasometric assembly for the measurement of volume of H_2 evolved 64

Fig. 4.1: Variation of weight loss of mild steel with time for the corrosion of mild steel in 0.1 M HCl containing various concentrations of amino acids at 303 K 68

Fig. 4.2: Variation of inhibition efficiencies of the studied amino acids with concentration at 303 K 69

Fig. 4.3: Variation of inhibition efficiency of cysteine (CYS), glycine (GLY), leucine (LEU) and alanine (ALA) with time 72

Fig. 4.4: Plots of –log(weight loss) versus time for the corrosion of mild steel in 0.1 M HCl containing various concentrations of the studied amino acids 76

Fig. 4.5: Langmuir isotherm for the adsorption of the studied amino acids on mild steel surface at 303 and 333 K 82

Fig. 4.6: FTIR spectrum of the corrosion product of mild steel in 0.1 M HCl 85

Fig. 4.7: IR spectrum of CYS 86

Fig. 4.8: IR spectrum of the corrosion product of mild steel when 0.5 g/l of CYS was used as an inhibitor 87

Fig. 4.9: IR spectrum of GLY 90

Fig. 4.10: IR spectrum of the corrosion product of mild steel when 0.5 g/l of GLY was used as an inhibitor 91

Fig. 4.11: IR spectrum of LEU 95

Fig. 4.12: IR spectrum of the corrosion product of mild steel when 0.5 g/l of LEU was used as an inhibitor 96

Fig.4.13: IR spectrum of ALA 98

Fig. 4.14: IR spectrum of the corrosion product of mild steel when 0.5 g/l of ALA was used as an inhibitor 99

Fig. 4.15: Variation of experimental inhibition efficiency (IE_{exp}) with (a) the HOMO energy, E_{HOMO} (b) the LUMO energy, E_{LUMO} (c) the energy gap, ΔE (d) the dipole moment, μ and with (e) the dielectric energy, $E_{dielect}$ obtained for Aqueous phase calculations using AM1 105

Fig. 4.16: Variation of experimental inhibition efficiency (IE_{exp}) with (a) the HOMO energy, E_{HOMO} (b) the LUMO energy, E_{LUMO} (c) the energy gap, ΔE (d) the cosmo area, cosAr and with (e) the dielectric energy, $E_{dielect}$ obtained for Aqueous phase calculations using AM1 106

Fig. 4.17: Variation of IE with E_{HOMO} and EA with E_{LUMO} for the studied amino acid in aqueous phase 113

Fig. 4.18 Electron density and Fukui function diagrams for L cysteine radical, electrophile and nucleophile 119
\
Fig. 4.19: Electron density and Fukui function diagrams for GLY radical, electrophile and nucleophile 120

Fig. 4.20: Electron density and Fukui function diagrams for LEU radical, electrophile and nucleophile 121

Fig. 4.21 : Electron density and Fukui function diagrams for ALA radical, electrophile and nucleophile 122

Fig. 4.22: Extended Huckel Molecular orbital of the studied amino acids showing the HOMO and the LUMO 124

Fig. 4.23: Variation of experimental and theoretical inhibition efficiencies of CYS in gas phase for the various Hamiltonians 130

Fig. 4.24: Variation of experimental and theoretical inhibition efficiencies of GLY in gas phase for the various Hamiltonians 131

Fig. 4.25: Variation of experimental and theoretical inhibition efficiencies of LEU in gas phase for the various Hamiltonians 132

Fig. 4.26: Variation of experimental and theoretical inhibition efficiencies of ALA in gas phase for the various Hamiltonians 133

Fig. 4.27: Variation of experimental and theoretical inhibition efficiencies of CYS in aqueous phase for the various Hamiltonians 136

Fig. 4.28: Variation of experimental and theoretical inhibition efficiencies of GLY in aqueous phase for the various Hamiltonians 137

Fig. 4.29: Variation of experimental and theoretical inhibition efficiencies of LEU in aqueous phase for the various Hamiltonians 138

Fig. 4.30: Variation of experimental and theoretical inhibition efficiencies of ALA in aqueous phase for the various Hamiltonians 139

Fig. 4.31: (a) the general structure of the studied amino acid. (b) protonation reaction of the inhibitors (c) Adsorption model for the inhibitors 142

LIST OF APPENDICES

Appendix 1: Input file for MOPAC calculations involving CYS

Appendix 2: Input file for MOPAC calculations involving LEU

Appendix 3: Input file for MOPAC calculations involving GLY

Appendix 4: Input file for MOPAC calculations involving ALA

Appendix 5: Input file for GAMESS calculations involving CYS

Appendix 6: Input file for GAMESS calculations involving GLY

Appendix 7: Input file for GAMESS calculations involving LEU

Appendix 8: Input file for GAMESS calculations involving ALA

Chapter 1

INTRODUCTION

1.1 Background of the Study

The great expanded industrial applications of mild steel based on their properties have been recognized by many researchers (Eddy, 2008). However, despite its importance, the problem associated with corrosion, especially pitting corrosion still remains a cause of concern to all and sundry. Huge losses of natural and artificial resources have been noted annually all over the globe as a result of corrosion. In the petroleum and gas industries, more than half of the reported failures of pipelines are caused by corrosion and subsequent rupture of the pipe wall. For, example, between 2002 and 2004, the Nigerian National Petroleum Corporation (NNPC) reported 162 cases of failure due to corrosion (Ajayi, 2003; Eddy, 2008) resulting in large losses of products, environmental pollution and ecological disaster.

Corrosion of metals has been a major industrial problem that has attracted much attention and investigations (Abiola *et al*., 2007; Arora *et al*., 2007; Ashassi-Sorkhabi *et al*., 2005a,2004;Barouni *et al*., 2008;Clark and Varney, 1987; Eddy, 2009a Kumar, 2008; Muralidharan *et al*., 2000; Umoren and Ebenso, 2007,2008; Umoren *et al*., 2008a,b, 2006a,b). Corrosion is one of the major only means through which metals deteriorate. Most metals corrode when they are in contact with aggressive medium such as moisture in the air, either in acids, bases, salts, oils, aggressive metals polishes, and liquid chemicals. Metals will also corrode when they are exposed to gaseous materials such as formaldehyde, acid vapour, and sulphur containing gases.

Corrosion is the degradation of materials due to interactions with their environments. It is an electrochemical process which involves the transfer of electrons between a metal surface and an aqueous solution. When metal atoms are exposed to an aggressive medium such as water, they can give up electrons, becoming themselves positively charged ions provided an electrical circuit can be completed. One of the most familiar corrosion processes is the oxidation of iron (rusting). Iron oxidizes in the presence of oxygen and aqueous electrolyte solution. Physical strains (scratches, dents, etc) on the iron are more easily oxidized than other areas. The result is that these regions are anodic (oxidation occurs) and simultaneously different areas are cathodic regions at which a reduction occurs. When this occurs, iron atom gives up two electrons to form Fe^{2+}:

$$Fe \rightleftharpoons Fe^{2+} + 2e^{-} \qquad 1.1$$

The electrons released during the abovereaction (equation 1.1) flow through the iron metal to the cathodic region leading to a reduction which can be expressed as follows

$$O_2 + 2H_2O(l) \longrightarrow 4OH^{-}(aq) \qquad 1.2$$

Combination of equation 1.1 and 1.2 gives equation 1.3:

$$Fe(s) + 1/2O_2(g) + H_2O(l) \longrightarrow Fe^{2+} + 2OH^{-}(aq) \qquad 1.3$$

Common experiences with this process (e.g., car fenders) reveal that Fe^{2+} is eventually oxidized further to Fe^{3+} , in iron (111) oxide compounds (rust) as shown in equation 1.4 ;

$$Fe^{2+} + O_2 + 4H_2O(l) \longrightarrow 2Fe_2O_{3(s)} + 8H^{+}(aq) \qquad 1.4$$

All corrosion processes exhibit some common features for example, thermodynamic principles can be applied to determine which processes can occur and the

tendency for the changes to take place (Cardoso *et al*., 2007; Eddy and Odoemelam, 2008a;El Ashry *et al*., 2006a,b).

Various studies have been carried out on the inhibition of the corrosion of metals in different environments and most of the well known inhibitors suitable for the corrosion of mild steel in acidic medium are organic compounds having heteroatoms in their aromatic rings or long carbon chains.(Acharya and Upadhyay,2004; Attar and Scantlebury, 2005; Ebenso *et al*., 2004a,b; Elayyoubi *et al*., 2004; Ita, 2004a,b, 2005; Ita and Offiong, 1997; Khavasfar and Iran, 2006; Okafor, 2004; Rajendran *et al*., 2000; Zuchi *et al*., 1978). For these compounds, their adsorption on the metal is the initial step of inhibition (Bilgic and Caliskan, 2001; El Ashry *et al*., 2006a,b; Fang and Li, 2002; Francis and Mercer, 1990; Li *et al*., 1999 a,b; Lukovitis *et al*., 2003, 1998; Quan *et al*., 2002; Yurt *et al*., 2004,2005; Zhenlon *et al*.,2004). The adsorption of inhibitors is linked to the presence of heteroatoms such as N, O, P, and S and long carbon chain as well as triple bonds or aromatic rings in their molecular structure (Ebenso, 2004, 2003a, b; Ebenso *et al*., 2005, Emregul *et al*., 2003; Emregul and Hayvali, 2006; Ehteshanmzade *et al*., 2006; Li *et al*., 1999a, b; Solmaz *et al*., 2005; Umoren *et al*., 2006a,b).

Also studies on the use of green corrosion inhibitors have been intensified. Green corrosion inhibitors are biodegradeable and do not contain heavy metals or other toxic compounds (Eddy and Ebenso, 2008). The successful use of naturally occurring substances to inhibit the corrosion of metals in acidic and alkaline environment has been reported by some group of researchers (Abiola *et al*., 2007; Abdallah, 2004a,b; Bendahou *et al*., 2006).

The adsorption bond strength is dependent on the composition of the metal and that of the corrodent, inhibitor structure and concentration as well as temperature. Despite the broad spectrum of organic compounds, the final choice of appropriate inhibitors for a particular application is restricted by several factors which include: toxicity, cost, ease of availability etc.

1.2 Different Types of Corrosion of Metals

Based on the morphology of attack and the type of the environment the metal is exposed to, corrosion can be classified into the following types.

1.2.1 Uniform corrosion.

Uniform corrosion is the attack of a metal at essentially the same rate at all exposed areas of its surface. It is characterized by laterally constant speed of corrosion. For example, in the atmospheric corrosion of galvanized steel, the speed of corrosion depends on the thickness of the steel and as such the thicker the steel coating, the longer the service life of the metal. Uniform attack is the most common form of corrosion and causes the greatest destruction of metals on a weight loss basis (Moore, 1996).

Uniform corrosion is often expressed in terms of depth of penetration and the units often quoted in literature are ipy (inches of penetration per year), ipm (inches of penetration per month), mg per dm^{-3} per day and $mmyr^{-1}$ (millimetres penetration per year). However, the SI unit is $mmyr^{-1}$ and the conversion factors are as follow,

$$mdd = 10 \text{ X } gm^{-2}d^{-1} \qquad 1.5$$

$$mmy^{-1} = 36.52 \text{ X mdd X } 1/\rho \qquad 1.6$$

$$mdd = \rho \text{ X ipy X } 1/1.44 \qquad 1.7$$

where ρ is the density of the metal (in kgm^{-3})

1.2.2 Galvanic corrosion

Galvanic corrosion is a localized corrosion in which metals are be preferentially corroded. This form of corrosion has the potential to attack junctions of metals, or regions where one construction metal is changed to another. The extent of galvanic corrosion increases with the potential difference of the metal. The relative size of the anode or cathode significantly affects the relationship between the active and inert metals. Therefore a small anode in the presence of a large cathode will corrode more quickly than the reverse. Galvanic corrosion can be prevented by keeping dissimilar metals apart or by the provision of insulating materials between the metals in order to interrupt current flow.

1.2.3 Pitting corrosion

This results from galvanic action, where the metal surface appears to have pinholes. The pit is the anode while the surrounding surface is the cathode (Jones, 1982; Moniz, 1986). Pitting may occur as a result of a change in the acidity of the pit area or differential aeration may also be a contributing factor to the increase in pit because most solutions are in contact with air and because of convection, transportation of oxygen through the solution leads to areas of high or low oxygen concentration. Therefore, where the metal surface contains the solutions, the variation may cause the area with the higher oxygen concentration to become a cathode while an area of lower oxygen concentration becomes anode resulting in a localized attacked.

1.2.4 Crevice corrosion

Crevices are present in all equipments. They occur naturally around bolts, rivets etc. They are also created by scratches on the metal surface. Crevice corrosion absorbs

and draws solution toward the reactive area. Crevice corrosion is influenced by the same factors affecting pitting corrosion and is indeed a specific form of pitting corrosion.

1.2.5 Intergranular corrosion

Intergranular corrosion occurs by localized attack at grain boundaries, which behave as anode to the larger surrounding cathode grains (Moore, 1996). Metals usually are not homogeneous. Impurities or alloying elements may segregate into grain boundaries. Heat treatment or localized heating by welding may provoke a change in composition at localized or near grain boundaries.

1.2.6 Erosion corrosion

Almost all corrosive media can bring about erosion-corrosion and nearly all metals and alloys are susceptible to this except those metals or alloys that are capable of forming hard, dense, adherent and continuous surface film (Moore, 1996). The extent of erosion corrosion increases as the velocity of the corroding medium increases. In some cases, the high velocity increases the supply of oxygen or other gases at the metal surface, which may depolarize the cathodic reaction and consequently increase the corrosion rate (Atkins, 2002).

1.2.7 Cavitations corrosion

Formation and collapse of tiny gas bubbles in a liquid stream called cavitation may mechanically destroy any protective layer, causing a localized corrosion called cavitation corrosion (Moore, 1996). Similarly when an object such as propeller rotates in water, the pressure on the trailing surface of the blade fluctuates continously. At some

points, very low pressures are produced which create tensile forces high enough to exceed the interatomic binding forces of the liquid.

1.2.8 Interfilm corrosion

Coating such as paints, conversion coating or metallic coating may lose their adhesion with substrate due to diffusion through the actual coating or reaction starting from defects like pinholes or scratches (Morgan, 1984). When this happens, residues of soluble salts, acids or bases will attract water through a paint film because of osmotic effect. The blister filled with water will be formed. Fill-form corrosion is a wormlike delamination of a paint film driven by salt residue and high humidity.

1.2.9 Fretting corrosion

Fretting corrosion is a combination of mechanical wear and atmospheric oxidation which frequently occurs between close fitting metal components (Moore, 1996). For fretting corrosion to occur, the surface is usually under load and subject to slight relative movement resulting in damage to the contact surface and formation of an oxide debris such as Fe_3O_4 for iron.

1.3 Environmental factors affecting the corrosion of iron

Exposure of iron to aerated water at room temperature may make the corrosion rate to be pH dependent (Okafor, 2004; Evans, 1981). In the range of pH of 4-10, the corrosion rate of iron is relatively independent of the pH of the environment. In this pH range, the corrosion rate is governed largely by the rate at which oxygen reacts with absorbed atomic hydrogen, thereby depolarizing the surface and allowing the reduction

reaction to continue. For pH values below 4.0, ferrous oxide (FeO) is soluble. Therefore, the oxide dissolves as it is formed rather than depositing on the metal surface to form a film. In the absence of the protective oxide film, the metal surface is in direct contact with the acid solution, and the corrosion reaction proceeds at a higher rate than at higher pH values.

Hydrogen is produced in acid solutions below a pH of 4, suggesting that the corrosion rate no longer depends entirely on depolarization by oxygen**,** but on a combination of the two factors (hydrogen evolution and depolarition). For pH values above 10, the corrosion rate is observed to fall as pH is increased. This is believed to be due to an increase in the rate of the reaction of oxygen with $Fe(OH)_3$ in the oxide layer to form the more protective Fe_2O_3. However, this is not observed in deaerated water at high temperatures.

Like most other chemical reactions, corrosion rates increase as temperature increases (Moore, 1996). Temperature and pressure of the medium govern the solubility of the corrosive species in the fluid, such as oxygen (O_2), carbon dioxide (CO_2), chlorides, and hydroxides. A rule of thumb is that the reaction rate doubles for every 10^0 rise in temperature. This linear increase with temperature does not continue indefinitely due, in part, to a change in the oxide film.

When iron is exposed to high temperature water, the rate of corrosion of the metal is observed to decrease with exposure time during the early period of exposure (Ramachandran *et al*., 2001). After a few thousand hours, the corrosion rate becomes relatively constant during the early period of exposure. While the corrosion rate is decreasing, the oxide film on the surface of the metal grows in thickness. However, the

rate at which the film grows tends to decrease with time. The thickness of the oxide film is soon constant after which film thickness does not change appreciably with further exposure. As might be expected, relatively constant corrosion rate and oxide film thicknesses are attained at about the same time.

The velocity of the surrounding fluid (water) may also affect the rate of corrosion (Okafor, 2004; Soliman and Abdel-Rahman, 2006). When water velocity is extremely high, the impact of the water tends to remove the protective oxides layer and some of the metal under it (erosion), thus exposing more metal to corrosion. Water velocities of 30 to 40ft per second are usually said to cause erosion.

An increase in the concentration of oxygen in water to which iron is exposed increases the corrosion rate. Oxygen promotes corrosion in two ways. First it is a powerful cathode depolarizer. When an acid gas such as hydrogen sulphide or sulphur (IV) oxide or carbon (IV) oxide is present, hydrogen gas tends to be formed at the cathode according to the equation 1.9:

$$2H^+ + 2e^- \rightarrow H_2 \qquad 1.9$$

The associated cathodic reduction is given by equation 1.10:

$$2H^+ + 1/2O_2 \rightarrow H_2O \qquad 1.10$$

Therefore, cathodic reaction resulting in the attendant corrosion is promoted because polarization by hydrogen is minimized in the presence of oxygen. Secondly, the oxygen removes iron by precipitation of iron oxides at the anode and thus prevents anodic polarization by Fe^{2+}.

The presence of carbon (IV) oxide in the surrounding water can also catalyse the corrosion of mild steel (Okafor, 2004). According to Kalman *et al*. (2000), it is evident

that the rate of corrosion can be affect by the partial pressure of CO_2. Increase in CO_2 partial pressure has been observed to increase the concentration of carbonic acid which is known to the cathodic reaction. Okafor (2004) stated that the CO_2 partial pressure affects the pH of the solution which in turn affects the speciation of species involved in the corrosion process and that in a film forming condition, increase in CO_2 partial pressure will lead to increase in CO_3^{2-} concentration.

CO_2 is a stronger acid than H_2S. It combines with hydrogen and trioxocarbonate ions to form trioxocarbonate (IV) acid according to equation 1. 11:

$$CO_2 + H_2O \longrightarrow H_2CO_3 \qquad 1.11$$

The acid formed ionizes to hydrogen and trioxocarbonate ions according to equation 1.12 below:

$$H_2CO_3 \longrightarrow H^+ + HCO_3^- \qquad 1.12$$

The ionization constant for the above reaction is $K_1 = 4.31x\ 10^{-7}$ (Atkins, 2002). However, the major contribution of CO_2 to the corrosion of mild steel is the increase in acidity by H^+ formed in the above reaction and the corrosion product $FeCO_3$(siderite).

The presence of hydrogen sulphide in the surrounding water may also catalyse the corrosion of mild steel. Hydrogen sulphide is a weak acid but is abundant in oil producing areas. The acidity or ability of hydrogen sulphide to generate H^+ is depicted by its first ionization constant. Under standard conditions, each mole of hydrogen sulphide in solution produces only $5.7x\ 10^{-8}$ moles of H^+. However, as the H^+ is removed by cathodic reaction, more is formed and hydrogen gas readily appears on steel exposed to air free water containing H_2S. The anion, SH^- dissociates further to S^{2-} and H^+. The sulphide anion reacts with iron to form the black FeS corrosion product.

Some microorganisms have been found to aid corrosion of mild steel. In an oil producing environment, the major corrosion caused by bacteria is associated with attack by hydrogen sulphide that is generated by metabolic processes of certain organism. The most commonly found sulphide producers are desulfovibrio species such as desulfovibrio desulfuricanes. They are referred to as sulphate reducers because they utilize SO_4^{2-} from salty waters and from H_2S to a limited extent, sulphide corrosion results from the hydrogen sulphide generated by species clostridia from organic sulphur compounds (Eddy, 2008).

1.4 Inhibition of corrosion

According to Hosseini *et al*. (2007), corrosion can be controlled by the addition of chemical substances called inhibitors into acid media. By definition, an inhibitor is a chemical compound which when added in small amounts to the corrosive environment, alters the cathodic and or anodic reaction and subsequently reduces the corrosion rate. This implies that inhibitors can be classified as anodic or cathodic depending on the process (Akpan, 1994). Inhibitors can also be classified as organic or inorganic depending on their chemical nature, oxidizing or non-oxidizing and their redox characteristics. However, one of the most widely applied classification systems for inhibitor is that proposed by Kelly *et al*. (2003).

- Adsorption inhibitors: These are inhibitors which are adsorbed on the metal surface and form protective barrier films. Adsorption inhibitors function by limiting the diffusion of oxygen to the corrosion surface, trapping the metal ion on the surface, stabilizing the double layer and reducing the rate of dissolution.

- Passivation inhibitors: passivating inhibitors function by inducing and maintaining a passive film (consisting of metal oxide) on the surface.
- Surface reaction product inhibitors: these are inhibitors that form sparingly soluble compounds other than an oxide layer. Surface reaction product inhibitors cannot form a protective oxide layer because they are not oxidizing agents but interact with metal on the surface to form insoluble compounds which plug in pores and inhibit corrosion.

1.4.1 Interphase inhibitors

Interphase inhibitors function by facilitating the formation of a 3-D layer which acts as a barrier between the corroding substrate and the electrolyte. The protective film could be a solid film on the surface of the metal or a liquid film adjacent to it. The solid film may be an oxide layer, corrosion product, metallic or non-metallic coating or inhibitor forming a porous layer or non-porous film (Mercer, 1990; Monika *et al*., 2005). However, the liquid film is the electroyte in the interphase which differs from the bulk of the solution in its chemical or physical properties. Based on this model, the inhibition of metal corrosion is governed by the properties of the layer such as its porosity and stability.

1.4.2 Passivating/oxidizing inhibitors

Pourbaix (1981) stated that iron polarizes anodically in the presence of oxidizing inhibitors and passivates as the open circuit potential shifts to more positive potential. It is also possible that the inhibitors are reduced and the reduction product is deposited on the weak points of the films to improve its protective effect.

An oxidizing inhibitor functions by inducing and maintaining a passive surface layer on the metal surface. These inhibitors are effective at certain concentrations (critical concentration, C_{crit}). At concentrations below the critical concentration, corrosion is enhanced but at very high concentrations of the inhibitor, increase in the anodic current density is observed.

1.4.3 Non oxidizing inhibitors

Non oxidizing inhibitors are also capable of passivating metals. They include compounds such as NaOH and the salts of weak acids and strong bases such as Na_3PO_4, Na_2HPO_4, Na_2CO_3, $NaBO_3$ and $Na_2B_4O_7$ (Tarvassoli-Salardini, 2004). These substances are also capable of passivating steel electrochemically.

1.4.4 Interface inhibitions

According to Tavassoli-Salardini (2004), interface inhibition occurs due to a strong interaction between the corroding metal and the inhibitor. The adsorption of the inhibitor depends on the potential of the electrode as well as the charge on the adsorbate molecule. The protective film is a 2-D adsorbate, which can affect the corrosion reaction by one of the following mechanisms.

i. Geometric blocking: In this case, an inert inhibitor blocks the surface of the metal at a high degree of coverage and forms a diffusion barrier which restricts the access of reactants to the metal surface for example, inhibition provided by proteins, polysaccharides or compounds with hydrocarbon chains.

ii. Deactivation coverage: In this process, instead of the complete coverage of the metallic surface, only the active sites are covered by an inert adsorbate and the rates of

the reactions (cathodic and anodic) are reduced in proportion to the extent of coverage of the reactive sites.

iii. Reactive coverage: In this case, the adsorbate undergoes electrochemical reaction and primary or secondary inhibition occurs either by the adsorbate or its reaction product respectively.

Adsorption inhibition is observed when a bare metal is in contact with the adsorbate (inhibitor) and this is usually the case in acidic solutions where the condition is not favourable to oxide formation (Mansfeld, 1987). According to Tarvassolo-Salardini (2004), majority of the very effective interface inhibitors are organic compounds containing nitrogen, sulphur and oxygen. It has been found that some interface inhibitors after initial adsorption onto the metal surface, can be reduced and the reduction product may also posses some inhibitive properties.

1.5 Statement of the Problem

In spite of the broad spectrum of inhibitors synthesized and used for the inhibition of the corrosion of metals including mild steel, it has been found that most inhibitors are toxic thereby posing a problem to the environment. In other to overcome the challenges and find posed by toxic inhibitors, there is need to investigate eco-friendly corrosion inhibitors. Amino acids are products of living things. They are non toxic, cheap and can be readily produced and purified to high quality. Therefore, the present study shall attempt to explore the possibility of using alanine, glycine, leucine and cysteine for the inhibition of the corrosion of mild steel in HCl. The chemical structures of these amino acids are shown in Fig. 1.1. It has been found that the inhibition potentials of any inhibitor are also affected by electronic and molecular properties of the inhibitor.

Therefore, quantum chemical studies shall be used to correlate microscopic and macroscopic properties of the inhibitors.

1.6 Aims and Objectives of the Study

The aims and objectives of the study are as follows,

(i) To study the inhibition of the corrosion of mild steel in solutions of HCl by L-cysteine, alanine, glycine and L-leucine using experimental (gravimetric, gasometric, thermometric and FTIR) and theoretical methods (quantum chemical methodsand Quantitative structure activity relation). From the gravimetric, gasometric and thermometric, experiments, the inhibition efficiencies of the various amino acids used shall be calculated.

(ii) To investigate the effect of temperature and concentration of corrodent and inhibition efficiencies of the amino acids. The activation energy for the uninhibited and inhibited corrosion reactions of mild steel shall be calculated using the Arrhenius equation.

(iii) To study the adsorption characteristics of the inhibitors by fitting adsorption data into different adsorption isotherms. The heat of adsorption and free energy of adsorption shall be calculated using the transition state and Gibb Helmholtz equations respectively.

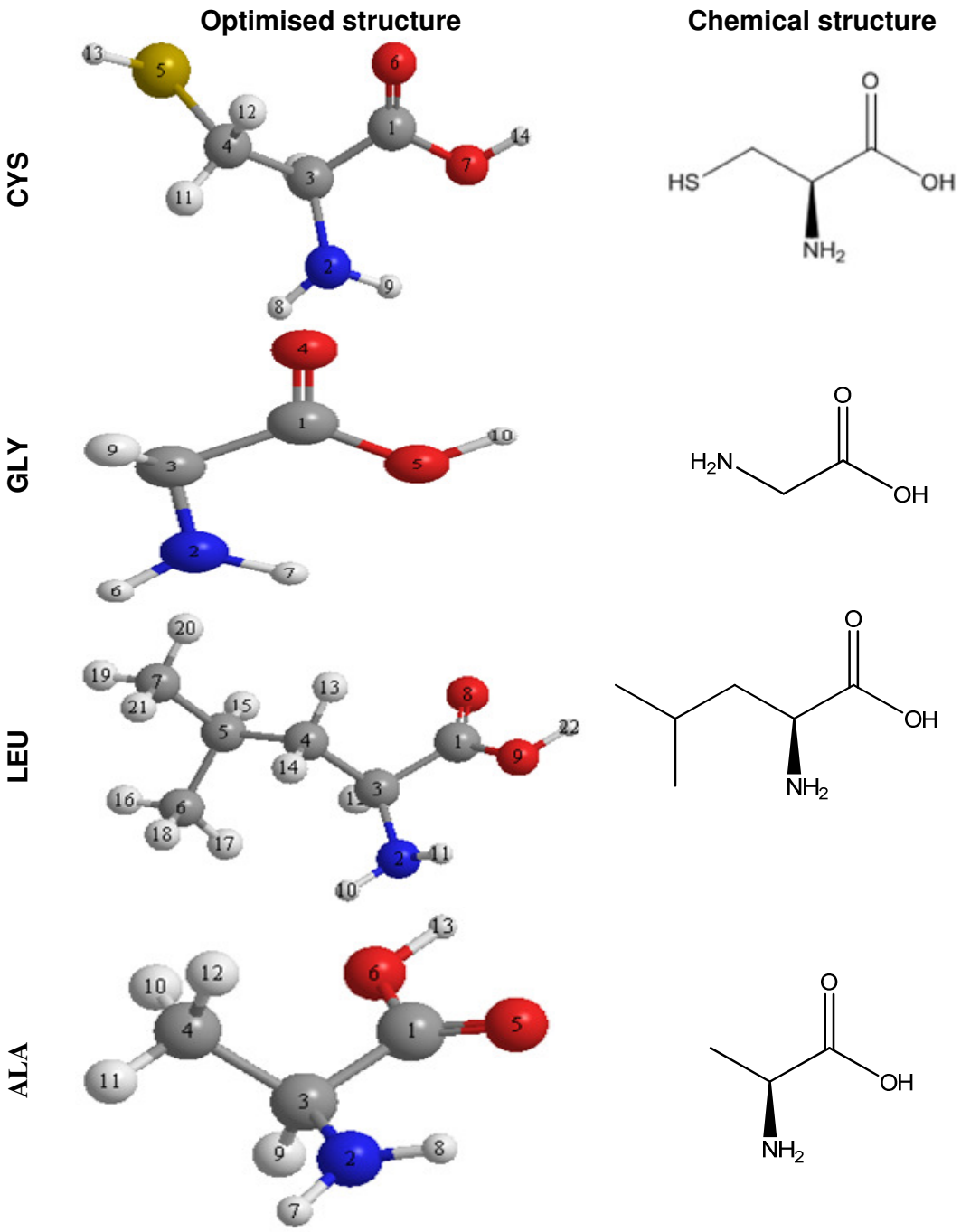


Fig. 1.1: Optimised and chemical structures of L-leucine (LEU), glycine (GLY), L-cysteine (CYS) and L-alanine (ALA)

(iv) To examine the kinetics and effect of immersion time on the stability of the inhibitors. From the kinetic models, the half life of mild steel in HCl solutions containing various concentrations of the inhibitors shall be calculated.

(v) To carry out quantum chemical calculations for the amino acids using Ultra Chem 2008, MOPAC. Semi-empirical parameters to be calculated using MOPAC 2008 shall include the total energy of the molecules (TE), electronic energy of the molecules (EE), core core repulsion energy (CC), ionization potentials (IP), electron affinity (EA), dipole moment (μ), electronegativity (χ), chemical potentials (Υ), energy of the highest occupied molecular orbital (E_{HOMO}), energy of the lowest unoccupied molecular orbital (E_{LUMO}), energy gap (ΔE), cosmo area (CosAr) and cosmo volume (cosvol). Lowdin and Muliken charges on the molecules shall be calculated using GAMESS. From the calculated charges, Fukui and global softness indices (ionization energy, Fukui functions for electrophilic and nucleophilic attacks, global softness, global hardness, electronegativity and fraction of electron transfers) for the various amino acids used shall be calculated. These functions shall be used to predict the sites for electrophilic and nucleophilic attacks of the inhibitors and shall also be expected to furnish information needed for the elucidation of the mechanism of the inhibition process.

(vi) To carry out quantitative structure activity relationship (QSAR) on the various amino acids studied using the quantum chemical descriptors. The results obtained from QSAR calculations shall be used to derive equations for the calculation of theoretical inhibition efficiencies of the amino acids.

(vii) From the results obtained from the experimental studies, recommendations shall be made on the potentials of the various amino acids as inhibitors for the corrosion of mild steel in HCl. Also from theoretical calculations, the synthesization of inhibitors that are structurally related to the various amino acids shall be attempted.

Chapter 2

LITERATURE REVIEW

2.1 Green Corrosion Inhibitors

According to Eddy and Ebenso (2008), green corrosion inhibitors are obtained from plant and animals. They are non toxic and do not contain heavy metals or other toxic substances. Eddy *et al*. (2009b) further stated that green inhibitors are relatively cheap and can be easily produced and purified. In addition, they are biodegradable. Most green corrosion inhibitors are extracts (ethanol, aqueous, methanol, etc) of plants and animal products. The use of green inhibitors is preferred because they are eco-friendly. In view of these, several extracts of plants have been successfully utilized for the inhibition of the corrosion of metals in acidic, neutral or alkaline media.

2.1.1 Plant extracts as green inhibitors

Eddy *et al*. (2009f) investigated the inhibition potentials of ethanol extract of *Lasianthera Africana* for the corrosion of mild steel in H_2SO_4 using gasometric, thermometric, gravimetric and FTIR techniques. The inhibitive properties of the extract were attributed to enhancement in adsorption of the inhibitor on mild-steel surface by saponin, alkaloid, tannin, flavanoid, cardiac glycoside, and anthraquinone (in the extract). Also, adsorption of the inhibitor was found to be exothermic, spontaneous, and fittted the Langmuir and Temkin adsorption models. Synergistic study revealed that among the various halides (KBr, KCl and KI), only KCl enhanced the adsorption of the inhibitor, whereas KBr and KI antagonized its adsorption. Based on the decrease in efficiency of the inhibitor with temperature, activation energies and free energy of adsorption below the threshold values of+80 and - 40kJ mol^{-1}, respectively, a physical adsorption

mechanism was proposed for the adsorption of ethanol extract of *Lasianthera africana* on the surface of mild steel. Ebenso *et al*. (2008) investigated the corrosion inhibition of mild steel by ethanol extract of *Piper guinensis* (EEPG) using gravimetric, gasometric and thermometric methods. The results of the study obtained showed that various concentrations of ethanol extract of EEPG inhibit mild steel corrosion. Inhibition efficiency of the extract was found to vary with concentration, temperature and period of immersion. Activation energiesfor the inhibited corrosion reaction of mild steel were greater than those obtained for the blank. Thermodynamic data indicated that the adsorption of EEPG on mild steel surface is spontaneous and fitted the Langmuir adsorption isotherm. Physical adsorption mechanism was proposed for the adsorption of the inhibitor. Eddy *et al*. (2009e) also investigated the inhibitive and adsorptive characteristics of ethanol extract of *Gnetum Africana* for the corrosion of mild steel in solutions of H_2SO_4 using weight loss, gasometric, thermometric, and IR methods and found that ethanol extract of *Gnetum Africana* is a good adsorption inhibitor for the corrosion of mild steel in H_2SO_4. The inhibitive property of the extract was attributed to the presence of alkaloid, saponin, tannin, terpene, anthraquinone, cardiac glycoside, and alkaloid in the extract. The adsorption of the inhibitor on mild steel surface was exothermic, spontaneous and is consistent with the mechanism of physical adsorption. In addition, Langmuir and Temkin adsorption isotherms best described the adsorption characteristics of the inhibitor. Efforts to improve the adsorption of the inhibitor through synergistic combinations with halides revealed that only KCl may enhance the inhibition efficiency of the inhibitor. The study provides information on the use of ethanol extract of *Gnetum Africana* as a corrosion inhibitor for mild steel.

In their study, Odiongenyi *etal*. (2009) investigated the inhibitive and adsorption properties of ethanol extract of *Vernonia amygdalina* for the corrosion of mild steel in H_2SO_4 using weight loss, thermometric, gasometric and IR methods. The results obtained revealed that ethanol extract of *Vernonia amygdalina* inhibited the corrosion of mild steel. The inhibition efficiency of the extract was found to increase with incease in the concentration of the extract. The inhibitor was found to function by being adsorbed on the surface of mild steel. The adsorption data of the inhibitor fitted the Langmuir adsorption isotherm. IR spectra of the corrosion product before and after adsorption, confirmed that ethanol extract of V*ernonia amygdalina* is an adsorption inhibitor. Phytochemical studies also revealed that ethanol extract of *Vernonia amygdalina* contains tannin, saponnins, flavanoid and anthraquinone, all of which are contributory to the corrosion inhibition. Eddy and Mamza (2009) studied the corrosion of mild steel in H_2SO_4 using gravimetric, gasometric and IR methods. The results obtained showed that the rate of corrosion of mild steel in H_2SO_4 increases with increase in the concentration of the acid and that ethanol extracts of the seeds and leaves of *Azadirachta indica* inhibited the corrosion of mild steel in H_2SO_4. Inhibition efficiencies of the leaves and seeds extract ranged from 82.62 to 94.24% and from 60.55 to 84.78%, respectively. The inhibition potentials of these extracts have been attributed to the presence of tannin, saponin, glycoside, anthraquinone, flavonone and other phytochemicals in the extracts. IR study revealed that the inhibitors are adsorption inhibitors and that the adsorption of the inhibitors on mild steel surface is exothermic, spontaneous and consistent with the assumptions of Flory-Huggins adsorption isotherm. Based on the activation energies, free energy of adsorption and the variation of inhibition efficiency with temperature, a

physical adsorption mechanism was proposed for the adsorption of ethanol extract of leaves and seeds of *Azadirachta indica* on the surface of mild steel surface. Eddy *et al*. (2009a) also investigated the inhibitive and adsorption properties of ethanol extract of *Terminalia catappa* for the corrosion of mild steel in H_2SO_4 using weight loss, hydrogen evolution, and infra red techniques. Ethanol extract of *T. catappa* was found to be a good adsorption inhibitor for the corrosion of mild steel in H_2SO_4. The inhibition efficiency of the inhibitor increased with increasing concentration but decreased with increasing temperature. The inhibition potential of ethanol extract of *T. catappa* was attributed to the presence of saponnin, tannin, phlobatin, anthraquinone, cardiac glycosides, flavanoid, terpene, and alkaloid in the extract. The adsorption of the inhibitor on mild steel surface was exothermic, spontaneous and was best described by Langmuir adsorption model. From the calculated activation energies, free energy of adsorption and the trend in the variation of inhibition efficiency with temperature, the mechanism of adsorption of the inhibitor is physical adsorption. Eddy and Odoemelam (2009) used FTIR, gravimetric and thermometric methods to study the inhibitive properties of ethanol extract of *Aloe vera* and reported inhibition efficiencies ranging from 65.08 to 89.67 %. The adsorption of the inhibitor on mild steel surface was spontaneous and was consistent with the mechanism of physical adsorption. Ethanol extract of *Costur afer* has also been investigated as an inhibitor for the corrosion of mild steeel in HCl by Eddy *et al*. (2009d). The extract was found to be an adsorption inhibitor. Noor (2009) studied the inhibitory potentials of aqueous extract of *Hibiscus sabdariffa* leaves for the corrosion of mild steel in 0.5 M NaOH using chemical and electrochemical techniques. Electrochemical measurements showed that aqueous extract of *Hibiscus sabdariffa* acted as a mixed

inhibitor and the adsorption of the inhibitor on aluminium surface was consistent wiith the mechanism of physical adsorption and was best explained by the Langmuir and Dubinin–Radushkevich adsorption isotherms. Oguzie (2008) also studied the inhibitory potentials of calyx extract of *Hibiscus sabdariffa* for the corrosion of mild steel in HCl and H_2SO_4 solutions, using gasometric (hydrogen evolution) method and found that the inhibition efficiency of the inhibitor increased with increasing concentration. The adsorption of the inhibitor on mild steel surface fitted the Langmuir adsorption model and was consistent with the mechanism of physical adsorption

Apart from the above listed studies, other researchers have successfully used different plant exracts as corrosion inhibitors(Abiola *et al*.,2007; Abdallah, 2004a; Bendahou *et al.,* 2006; Bouyanzer and Hammouti, 2004 ; Chetounane*et al*., 2004; Ebenso *et al*., 1998,2004a,b; Ebenso and Ekpe, 1996; Eddy and Ebenso, 2008 ; Eddy et al., 2010b, 2009a,b; Ekpe *et al*., 1994; El-Etre, 1998, 2003,2006; El-Etre and Abdallah, 2002; Kliskic *et al*., 2000; Krajewka *et al*., 2002;Oguzie,2005,2006a,b,2007, 2008; Oguzie *et al*., 2006,2007; Okafor *et al*., 2005,2007a,b,2008; Okafor and Ebenso, 2007; Umoren *et al*., 2006a,2008a,b;Umoren and Ebenso,2008; Sethuran and Raja*,* 2005*;*Rajendran *et al*., 2000 ; Zucchi and Omar, 1985; Zuchi *et al*., 1978).

Attempts have also been made on the use of waste materials (plant and animal origin) as corrosion inhibitors. For example Eddy *et al*. (2008b) used ethanol extract of *Musa Specie* peel for the inhibition of the corrosion of mild steel in H_2SO_4 and found that it is a good adsorption inhibitor.

2.1.2 Amino acids as green corrosion inhibitors

Some amino acids have been found to be good inhibitors for the corrosion of mild steel in HCl (El-Rabiee *et al*., 2008; Silva et al., 2006). Amino acids are compounds that contain both amino and carboxylic acid functional groups. These acids are non toxic, natural and contain $–NH_2$ and COOH functional groups. Amino acids are completely soluble in aqueous media and can be produced with high purity at reduced costs. They are therefore expected to be good inhibitors for the corrosion of mild steel in H_2SO_4 solutions.

Badawy *et al*. (2006) investigated the inhibition of the corrosion of Cu–Ni alloys in aqueous chloride solutions using some amino acids as environmentally safe materials. The corrosion rate was calculated in the absence and presence of the corrosion inhibitor using polarization and impedance techniques. The inhibition efficiency of the studied amino acids was also calculated. The results obtained showed that a simple amino acid like glycine can be used as efficient corrosion inhibitor for the Cu–Ni alloys in neutral chloride solutions. An inhibition efficiency of about 85% was obtained at very low concentrations of the amino acid (0.1 mM). For low Ni content alloy (Cu–5Ni), 2.0 mM cysteine had a remarkable high (□96%) corrosion inhibition efficiency. The experimental impedance data fitted the theoretical data according to a proposed equivalent circuit model for the electrode/electrolyte interface. Different adsorption isotherms were tested and the corrosion inhibition was found to depend on the adsorption of the amino acid molecules and/or the deposition of corrosion products on the alloy surface. The calculated adsorption free energy for the inhibition of the corrosion of Cu–5Ni by cystine (−37.81 kJ mol−1) suggests a strong physical adsorption of the inhibitor on the alloy

surface.Olivares-Xometl *et al*. (2008) investigated the potentials of new compounds of alkylamides derived from -amino acids as corrosion inhibitors for carbon steel in an aqueous solution of hydrochloric acid. Corrosion testing was carried out using polarization scans and weight loss measurements. Polarization scans indicated that the compounds acted as mixed corrosion inhibitors with an efficiency of 80–90% when dissolved in the test solution (at ≥50 ppm) whereas gravimetric results revealed a similar tendency. Microtox testing indicated a correlation with the molecular structure of inhibitors. Spah *et al*. (2009) used electromotive force measurements to study the inhibition potentials of some amino and carboxylic acids and obtained results which showed that amino acids are potential corrosion inhibitors. Aksot and Bilgic (1992) investigated the inhibitory effect of amino acids on the corrosion of nickel in sulphuric acid medium. Thirteen amino acids with different properties were used. Corrosion current densities were determined by extrapolation of the cathodic Tafel region to the corrosion potential. The effect of the amino acids on the passivity of nickel was examined by anodic current-potential curves. The result obtained revealed that some amino acids are inhibitors to various degrees for nickel but that others accelerated corrosion. El-Rabiee *et al*. (2008) studied the electrochemical behaviour of vanadium in amino acid using open-circuit potential measurements, polarization techniques and electrochemical impedance spectroscopy (EIS). The effect of Cl^- on the corrosion inhibition efficiency especially in acid solutions was investigated. In neutral and basic solutions, the presence of amino acids increases the corrosion resistance of the metal. The electrochemical behaviour of V before and after the corrosion inhibition process indicated that some amino acids like glutamic acid and histidine have promising corrosion inhibition efficiency at low

concentrations. The inhibition efficiency (η) was found to depend on the structure of the amino acid and the constituents of the corrosive medium. The corrosion inhibition was based on the adsorption of the amino acid molecules on the metal surface while the adsorption process was consistent with the Freundlich isotherm. The free energy for the inhibition of the corrosion of V in acidic solutions by valine was found to be −9.4 kJ/mol which indicated a strong physical adsorption of the amino acid molecules on the vanadium surface.

Zhang *et al*. (2008) investigated the inhibition effect of four amino acids (aspartic acid, glutamic acid, asparagine, glutamine) on the corrosion of copper in 0.5 M hydrochloric acid using potentiodynamic polarization and electrochemical impedance spectroscopy (EIS). Both potentiodynamic and EIS measurements revealed that the amino acids have some protective effect against copper corrosion in 0.5M HCl solution. The inhibition efficiency of these compounds was found to increase in the order Gln > Asn > Glu > Asp and tended to increase with increase in the concentration of the inhibitors. Addition of iodide ions to 10mM glutamine solution gives an improvement of the protection efficiency, up to a maximum of 93.74% for 5mM KI. They proposed a mechanism of physical adsorption for the amino acids studied and the adsorption was consistent with the Langmuir adsorption model. .Asshassi-Sorkhabi *et al*. (2005c) investigated the inhibitory effect of three amino acids (alanine, glycine and leucine) on the corrosion of carbon steel in HCl solutions using potentiodynamic polarization method. Corrosion data such as corrosion rate, corrosion potential and corrosion resistance were determined by extrapolation of the cathodic and anodic Tafel region. Adsorption isotherm was investigated using data obtained from weight-loss

measurements. The effect of concentration on the inhibition potentials of amino acidswas also investigated. The inhibition efficiency was found to depend on the type of amino acid and its concentration ranged from 28 to 91%. The adsorption of the amino acids on mild steel surface was consistent with the Langmuir adsorption isotherm. Barouni *et al*. (2008) also investigated the inhibition by five amino acids (valine, glycine, lysine, arginine and cysteine) on the corrosion of copper in solutions of HNO_3 using weight loss and electrochemical polarization measurements. The results obtained by these researchers showed that valine and glycine accelerated the corrosion process; but arginine, lysine and cysteine inhibited the corrosion phenomenon. Cysteine was found to be the best inhibitor. Correlation between calculated quantum chemical parameters and inhibition efficiency was discussed using semi-empirical methods (AM1 and MNDO).

The inhibition by three amino acids (proline, methionine and trytophane) on the corrosion of Pb–Sb–Se–As alloy in solutions of H_2SO_4 was investigated using linear polarization and weight loss measurements (Ghasemi and Tizpar, 2006). The effect of inhibitors' concentration and temperature oncorrosion rate was also investigated. It was found that these inhibitors acted as good inhibitors for the corrosion of lead alloy in H_2SO_4 solution. Increasing inhibitor concentration increases the inhibition efficiency. It was found that adsorption of the amino acids on lead alloy surface fits Langmuir isotherm. Asshassi-Sorkhabi *et al*. (2006) also investigated the inhibition effect of some schiff bases of amino acid on the corrosion of aluminium in 1 M HCl + 1 M H_2SO_4 using weight loss measurement, linear polarization and SEM techniques. The results drawn from the different techniques were comparable. The amino acids used were alanine, leucine, valine, proline, methionine, and tryptophan.The effect of inhibitor'sconcentration

and temperature was also investigated. It was found that these amino acids acted as good inhibitors for the corrosion of aluminium in 1 M HCl + 1 M H_2SO_4 solution. Langmuir and Freundlich adsorption isotherms were the best fitted isotherms.

Moretti *et al*. (2004) investigated the inhibition effects of tryptamine (TA) on the corrosion of ARMCO iron in 0.5M H_2SO_4 using potentiodynamic curves (PCM) and electrochemical impedance spectroscopy (EIS). TA was found to be an effective inhibitor against the corrosion of ARMCO iron, even at higher temperature and after long term exposure. Inhibition efficiencies, calculated from PCM and EIS data, ranged from 90% to 99% and did not diminish over time and as the temperature increased. Adsorption of TA was consistent with the Bockris–Swinkels adsorption isotherm. Silva *et al*. (2006) investigated the effect of cysteine on the corrosion of 304L stainless steel in 1 M H_2SO_4 using open-circuit potential measurements, anodic polarization curves, electrochemical impedance spectroscopy (EIS) and scanning electron microscopy (SEM). The results obtained indicated that inhibition of corrosion by cysteine was concentration dependent. Other studies include those reported by Kiani *et al*. (2008) and Zerfaoui *et al*. (2004). Goa and Liang (2007) evaluated the electrochemical performance of 1-diethylamino-propan-2-ol (EAP) and 1, 3-bis-diethylamino-propan-2-ol (DEAP) for brass in simulated atmospheric water using potentiodynamic curves and electrochemical impedance spectroscopy (EIS). The experimental results obtained showed that the compounds investigated retarded the anodic dissolution of brass. The experimental data were partly supported by density functional theoretical (DFT) and quantum chemical analysis.

In spite of the broad spectrum of information available for corrosion inhibition potentials of amino acids, information on quantum chemical study is scanty. Perhaps few

studies are those reported by Eddy (2010) and Yurt *et al*. (2005). Yurt *et al*. (2005) performed quantum chemical calculations on six amino acids and six hydroxy carboxylic acids. Strong correlations were obtained between experimentalinhibition efficiencies (IE_{exp}) for pitting corrosion of Al 7075 alloy in NaCl solution and quantum parameters such as electronic charges on active centres (qO, qN), dipole moment (m), the energy of the highest occupied molecular orbital (E_{HOMO}), the energy of the lowest unoccupied molecular orbital (E_{LUMO}) and the energy gap ($E_{LUMO} - E_{HOMO)}$. Also, Eddy (2010) performed DFT, QSAR and quantum chemical calculations on four amino acids (aspartic acid, asparagine, glutamine and glutamic acid) for the corrosion of mild steel in HCl. Experimental and theoretical inhibition efficiencies correlated strongly for various Hamiltonians (PM6, PM3, AM1, RM1 and MNDO). From DFT (Using Huckel approximations) calculations, condensed Fukui functions and condensed softness were calculated and were used to predict the sites for electrophilic and nucleophilic attacks on the amino acids molecules studied.

2.2 QSAR in Corrosion Study

The term quantitative structure-activity relationships (QSAR) was first used in pharmacology in 1964, when Hansch and his co-worker (Hansch and Leo,1979) discovered that variation of pharmacological efficiency of (closely-related) drugs might be explained in terms of simple variables and the substituent constants. Substituent constants were invented earlier (Hammett, 1940) and are in fact numbers characterizing various groups (like –OH,-Cl,-NO_2,-COOH,-CH_3, etc). In principle, they do not depend on the parent structure they are attached to. In pharmacology, QSAR research has

produced thousands of papers, and there is even a scientific journal (besides others devoted to QSAR) bearing this abbreviation.

The relationship between efficiency and the structure of corrosion inhibitors has been extensively studied in recent days. For example, Eddy (2010) used QSAR to study the inhibition potentials of some amino acids (glutamine, glutatamic acid, aspargine and aspartic acid) and derived equations for the calculations of theoretical inhibition efficiencies using parametric method 6 (PM 6), parametric method 3 (PM 3), Recife method 1 (RM 1), Austin model 1 (AM 1) and modified neglect of differential overlap (MNDO) Hamiltonians. Correlation coefficients between experimental and theoretical inhibition efficiencies were found to range from 0.879 to 0.9987, indicating a good relationship. Eddy and Ebenso (2010a) also used QSAR to study the inhibition potentials of some penicillin compounds (cloxacillin, penicillin V and ampicilllin) for the corrosion of mild steel in HCl. They obtained equations for the calculation of theoretical inhibition efficiencies for different Hamiltonians (PM6, PM3, AM1, RM1 and MNDO). The results obtained from their study yielded correlation coefficients that were very close to unity. Eddy *et al* (2008a) studied the inhibition potentials of some antibiotics (ampicilin, cloxacillin, tetrcycline, chloramphenicle and ampiclox) for the corrosion of mild steel in H_2SO_4 using QSAR. The results of the investigations also revealed that QSAR can adequately be used to model the inhibition potentials of the antibiotics studied.

2.3 Quantum Chemical Methods in Corrosion Inhibiton Studies.

Quantum chemical methods have been already proven to be very useful in the determination of molecular structure as well as elucidation of electronic structure and reactivity (Kraka and Cremer, 2000). Thus, it has become a common practice to carry out

quantum chemical calculations in corrosion inhibition studies. The concept of assessing the efficiency of a corrosion inhibitor with the help of computational chemistry is to search for compounds with desired properties using chemical intuition and experience in a mathematically quantified and computerized form. Once a correlation between the structure and activity or property is found, any number of compounds, including those not yet synthesized, can be readily screened employing computational methodology (Eddy, 2008; Karelson and Lobanov, 1996) and a set of mathematical equations which are capable of representing accurately the chemical phenomenon under study (Hinchliffe, 1994, 1999). The study of corrosion processes and their inhibition by organic inhibitors is a very active field of research (Bouayed *et al*., 1999). Many researchers have reported that the inhibition effect depends mainly on some physicochemical and electronic properties of the organic inhibitor which relate to its functional groups, steric effects, electronic density of donor atoms, orbital character of donating electrons, and so on (Quraishi and Sardar, 2002; Stupnišek-Lisac *et al*., 1994). The mechanism of inhibition is generally explained by the formation of a physically and/or chemically adsorbed film on the metal surface (Touhami *et al*., 2000; Tang *et al*., 2006). It is well known that organic compounds which act as inhibitors are rich in heteroatoms such as sulphur, nitrogen, and oxygen (Hosseini *et al*., 2003; Subramanyam *et al*., 1993). These compounds and their derivatives are excellent corrosion inhibitors in a wide range of media and are selected essentially from empirical knowledge based on their macroscopic physico-chemical properties. Recently, theoretical prediction of the efficiency of corrosion inhibitors has become very popular in conjunction with the progress in computational hardware and the development of efficient algorithms which have assisted the routine development of

molecular quantum mechanical calculations (Domenicano and Hargittai, 1992; Eddy *et al*., 2009a). In view of the numerous advantages offered by quantum chemical parameters (for the predictions of the reactivity of chemical reactions and for theoretical modeling of certain reactions), some studies have been carried out on corrosion inhibition processes using quantum chemical parameters or descriptors. Arslan *et al*. (2009) used quantum chemical methods to study the inhibition potentials of some sulphonamides. They found that the inhibition potentials of these compounds are strongly related to some quantum chemical parameters and that the inhibition potentials of other members of the sulphonamides family can be easily predicted. Khaled *et al*. (2005) also studied the effect of structures on the inhibition potentials of polymethylene amines for the corrosion of iron in acidic solutions and found a good correlation between the experimental inhibition efficiencies and some quantum chemical parameters. In their study, Sahin *et al*. (2008), found that quantum chemical parameters can be used to predict the direction of the inhibition of the corrosion of low carbon steel in 3.5 % NaCl medium by some heterocyclic compounds. There was a strong correlation between calculated quantum chemical parameters and IE_{exp}.. Bentiss *et al*. (2007a) found that the adsorption of 4 H-1,2,4-triazole derivatives, as corrosion inhibitors for mild steel in solutions of HCl, can be modeled using some quantum chemical parameters. Fang and Li (2002) also used quantum chemical methods to study the relationship between molecular structure and corrosion inhibition efficiency of amides and found that inhibition potentials of the amides studied are related to their chemical structures and were explained, using quantum chemical parameters. Yurt *et al*. (2005) also established strong correlations between inhibition efficiencies of some amino acids and hydroxycarboxylic acids on pitting

corrosion of aluminium alloy 7075 in NaCl solution. Similar findings were reported by Goa and Liang (2007) for some β-amino acids.

2.4 Quantum Chemical Parameters

Quantum chemical methods and molecular modeling techniques enable the definition of a large number of molecular quantities characterizing the reactivity, shape, and binding properties of a complete molecule as well as molecular fragments and substituents (Dewar and Thiel, 1977; Lebrini et al., 2008; Li *et al*., 1999b; Martinez, 2002). According to Levine (1991), the use of theoretical parameters presents two major advantages as follows:

(i) the compounds and their various fragments and substituents can be directly characterized on the basis of their molecular structure only

(ii) the proposed mechanism of action can be directly accounted for in terms of the chemical reactivity of the compounds under study.

Chemically derived quantum parameters are fundamentally different from experimentally measured quantities, although there is some natural overlap. Unlike experimental measurements there is no statistical error in quantum chemical calculations. There is inherent error however, associated with the assumptions required to facilitate these calculations. In most cases the direction but not the magnitude of the error is known (Levine, 1991). In using quantum chemistry-based parameters with a series of related compounds, the computational error is considered to be approximately constant throughout the series. The prominent quantum chemical parameters can be subdivided intoatomic charges, molecular orbital energies and dipole moment.

2.4.1 Atomic charges

All chemical interactions are either electrostatic (polar) or orbital (covalent). Electric charges in the molecule are obviously responsible for electrostatic interactions. The local electron densities or charges are important in many chemical reactions and physicochemical properties of compounds. Therefore, charge-based parameters have been widely employed as chemical reactivity indices or as measures of weak intermolecular interactions. Despite its usefulness, the concept of a partial atomic charge is somewhat arbitrary, because it depends on the method used to delimit between one atom and the next. As a consequence, there are many methods for estimating the partial charges. Muliken population analysis is mostly used for the calculation of the charge distribution in a molecule(Murrell *et al*., 1985). These numerical quantities are easy to obtain and provide at least a qualitative understanding of the structure and reactivity of molecules (Grüber and Buss, 1989). Furthermore, atomic charges are used for the description of the molecular polarity of molecules.

2.4.2 Molecular orbital energies

The energy of the highest occupied molecular orbital (E_{HOMO}) and that of the lowest unoccupied molecular orbital (E_{LUMO}) are important quantum chemical parameters. These orbitals, also called the frontier molecular orbitals, determine the way the molecule interacts with other species (Ogretir *et al.*, 2003). The HOMO is the orbital that could act as an electron donor, since it is the outermost (highest energy) orbital containing electrons (Parr et al., 1950; Yan *et al*., 2008). The LUMO is the orbital that could act as the electron acceptor, since it is the innermost (lowest energy) orbital that has room to accept electrons. According to the frontier molecular orbital theory, the

formation of a transition state is due to an interaction between the frontier orbitals (the HOMO and the LUMO) of the reacting species (Fukui, 1975). The energy of the HOMO is directly related to the ionization potential (IP) while the LUMOenergy is related to the electron affinity (EA). The HOMO–LUMO gap, i.e. the difference in energy between the HOMO and LUMO, is an important stability index (Lewis *et al*., 1994). A large HOMO–LUMO gap implies high stability for the molecule in chemical reactions (Zhou and Parr, 1990). The concept of ‘‘activation hardness” has also been defined on the basis of the HOMO–LUMO energy gap. The qualitative definition of hardness is closely related to polarizability, since a decrease of the energy gap usually leads to easier polarization of the molecule (Eddy, 2009a, Pearson, 1989).

2.4.3 Dipole moment (l)

The most widely used quantity to describe polarity is the dipole moment of the molecule (Kikuchi, 1987). Dipole moment is the measure of polarity of a polar covalent bond. It is defined as the product of charge on the atoms and the distance between the two bonded atoms (Eddy, 2008). The total dipole moment, however, reflects only the global polarity of a molecule. For a complete molecule, the total molecular dipole moment may be approximated as the vector sum of individual bond dipole moments.

2.4.4 Energy

The total energy calculated by quantum chemical methods is also a beneficial parameter. The total energy of a system is composed of the internal, potential, and kinetic energy. Hohenberg and Kohn (1964) found that the total energy of a system including that of the many body effects of electrons (exchange and correlation) in the presence of static external potential (for example, the atomic nuclei) is a function of the charge

density. The minimum total energy is the ground state energy of the system. The electronic charge density which yields this minimum energy is then the exact single particle ground state energy.

2.5 Semi-Empirical Methods

In principle, any observable property of an atomic or molecular system can be obtained from the Schrödinger equation (Young, 2004). Over the past decades the semi-empirical molecular orbital methods have been used widely in computational studies. Semi-empirical approaches neglect many smaller integrals to speed up the calculations. In order to compensate for the errors caused by these approximations, empirical parameters are introduced into the remaining integrals and calibrated against reliable experimental or theoretical reference data. This strategy can only be successful if the semi-empirical model retains the essential physics to describe the properties of interest. Provided that this is the case, parameterization can account for all other effects in an average sense, and it is then a matter of validation to establish the numerical accuracy of a given approach. In current practice, semi-empirical methods serve as efficient computational tools which can yield fast quantitative estimates for a number of properties. This may be particularly useful for correlating large sets of experimental and theoretical data, for establishing trends in classes of related molecules, and for scanning a computational problem before proceeding with higher level treatments.

Over the years, a large number of methods with different acronyms have been developed, including the modified neglect of diatomic overlap (MNDO) (Dewar and Thiel, 1977), the Austine model 1 (AM1) (Dewar *et al*., 1985), the parametric method 3 (PM3) (Stewart, 1989). Semi-empirical methods differ in details of approximations (e.g.

the core–core repulsion functions) and in particular in the values of the parameters. The semi-empirical methods can be optimized for different purposes. The MNDO, the AM1 and the PM3 were designed to reproduce heats of formation and structures of a large number of organic molecules. Other semiempirical methods are specifically optimized for spectroscopic properties (e.g. complete neglect of diatomic overlap,i.e CNDO).

2.5.1 MNDO (modified neglect of differential overlap)

It is based on the NDDO (neglect of diatomic differential overlap) approximation and in turn NDDO is an improved version of INDO (intermediate neglect of differential overlap) method. INDO itself is an improvement over the CNDO (complete neglect of differential overlap) approximation. There are several such semi-empirical linear combinations of atomic orbital-molecular orbital (LCAO MO) methods, developed for specific purposes

2.5.2 AM1 (Austin model 1)

AM1 is a semi-empirical method based on the neglect of differential diatomic overlap integral approximation. Specifically, it is a generalization of the modified neglect of diatomic differential overlap approximation. AM1 was developed by Dewar *et al*.(1985). AM1 is an attempt to improve the MNDO model by reducing the repulsion of atoms at close separation distances. The atomic core–atomic core terms in the MNDO equations were modified through the addition of off-center attractive and repulsive Gaussian functions. The complexity of the parameterization problem increased in AM1 as the number of parameters per atom increased from seven in MNDO to 13–16 per atom in AM1.

2.5.3 PM3 (parameterized model number 3)

PM3 is another semi-empirical method based on the neglect of differential diatomic overlap integral approximation. The PM3 method uses the same formalism and equations as the AM1 method. The only differences are: (a) PM3 uses two Gaussian functions for the core repulsion function, instead of the variable number used by AM1 (which uses between one and four Gaussians per element); (b) the numerical values of the parameters are different. The other differences lie in the philosophy and the methodology used during the parameterization: whereas AM1 takes some of the values of the parameters from spectroscopic measurements, PM3 treats them as optimised values. The method was developed by Stewart (1989).

2.6 Study of Corrosion Inhibitors by Semi-Empirical Methods

The inhibition of corrosion in acid solutions can be affected by the addition of a variety of organic molecules. Compounds containing nitrogen, oxygen and sulphur have shown vast applications as corrosion inhibitors. Studies by Vosta and Eliásek (1971) and Chakrabarti (1984) appear to be the first theoretical studies on corrosion inhibitors in the literature. Subsequently, Costa and Lluch (1984) reported the results of quantum mechanical calculations of different compounds, such as linear-chain diols, diamines and aliphatic aminoalcohols as corrosion inhibitors for metals. They calculated HOMO and LUMO energies using the semi-empirical MINDO/3 method. A good agreement was found between their theoretical predictions and experimental data. Sayós *et al*. (1986) performed theoretical calculations on several aromatic organic compounds as corrosion inhibitors for titanium and its alloys employing the MNDO method. They also concluded that the agreement with the experimental data was quite good. In the following decades,

several studies on various compounds were reported which dealt with correlations of quantum chemical properties obtained with semi-empirical tools with experimental findings. For instance, the influence of some heterocyclic compounds, i.e. some oxadiazole derivatives, on the corrosion of mild steel in acid solutions, has been investigated by Lagrenée *et al*. (2001) and Bentiss *et al*. (2003,2004). Apart from using experimental methods, AM1 semi-empirical method was used to obtain the electronic properties of those compounds. They calculated E_{HOMO}, E_{LUMO}, $\Delta E(E_{LUMO} - E_{HOMO})$ and dipole moment (μ) and found a highly significant multiple correlation coefficient between experimental and theoretical data. Semi-empirical calculations to evaluate the efficiency of some imidazole derivatives as acidic corrosion inhibitors for zinc and iron have been performed by Bereket *et al*. (2002) using AM1, PM3, MNDO and MINDO/3 methods. Charges on nitrogen atoms, total energy, ionization potential, E_{HOMO}, E_{LUMO}, ΔE (E_{LUMO} - E_{HOMO}) and dipole moment were calculated and correlated with experimental results. A satisfactory agreement was found between theoretical and experimental data. Similar studies on these compounds have been carried out by Ögˇretir *et al*. (2003) in order to probe the inhibition mechanism of corrosion via metal–ligand interaction using semi-empirical methods. According to their conclusion, semiempirical calculations can be used to elucidate the mechanism of inhibition. Popova *et al*. (2007) investigated the effect of molecular structure of some different triazole derivatives as corrosion inhibitors for mild steel in acidic medium using the AM1 method. The effects of some triazole derivatives (triazole (TA), 3-amino-1,2,4-triazole (ATA) and 3,5-diamino-1,2,4-triazole (DTA)) on copper corrosion in 0.5 M HCl have been studied by El Issami *et al*. (2007) using AM1, MNDO and PM3 Hamiltonians. They showedthe

formation of the copper-ATA or copper-DTA complexes and established a correlation between the E_{HOMO} and inhibition efficiencies. From a comparison of their experimental and theoretical results, they concluded that high values of E_{HOMO} indicated a tendency of the molecule to donate electrons to appropriate acceptor molecules with low energy of empty atomic orbitals, while the energy of the lowest unoccupied molecular orbitals indicated the ability of the molecule to accept electrons. Also, the less negative E_{HOMO} and the smaller ΔE reflected stronger chemisorbed bond and greater inhibitor efficiency. Zhang *et al*. (2004) also studied some triazole derivatives using Parker, Parr and Pople (PPP) method and concluded that E_{HOMO}, E_{LUMO} and p-electron density were consistent with the inhibition efficiencies of the compounds. The adsorption behaviour of some thiazole derivatives at Fe surface was studied by Zhang *et al*. (2007) through molecular dynamics simulation and quantum chemical calculations. Furthermore, some pyrazole (Gad Allah and Moustafa, 1992; Bouklah *et al*., 2005; Benabdellah *et al*., 2007) and pyridine (Xiao-Ci *et al*., 2000; Sastri and Perumareddi, 1997; Ögˇretir *et al*., 1999; Szeptycka and Kwiatkowski, 2000) derivatives have been investigated as corrosion inhibitors in acidic media by means of semi-empirical quantum chemical methods. Due to the presence of the –C=N– group, electronegative nitrogen, sulphur and/or oxygen atoms in the molecule, Schiff bases should be good corrosion inhibitors. Recently, some Schiff bases as effective corrosion inhibitors for steel (Ashassi-Sorkhabi *et al*., 2005b,c), aluminium (Ashassi-Sorkhabi *et al*., 2006; Yurt *et al*., 2006) and copper (Li *et al*., 1999a; Sheikhshoaie and Mashhadizadeh, 2003) in acidic media have been investigated using semi-empirical molecular orbital methods. El Ashry *et al*. (2006a,b) correlated the structural characteristics of hydrazides and Schiff bases with their corrosion inhibition

efficiency at different inhibitor concentrations in aqueous acid solutions. They also investigated the relation between the inhibition efficiency and quantum chemical parameters such as E_{HOMO}, E_{LUMO}, dipole moment, total negative charge on molecules (TNC), intrinsic volume (V_i), polarizabilty (p*) and linear solvation energy (LSER). These researchers used a non-linear regression analysis to correlate quantum chemical parameters (E_{HOMO}, E_{LUMO},μ, TE, TNC, LSER, V_i, and p*) and inhibitor concentrations (Ci) with the experimental inhibition efficiencies obtained by mass loss methods for the compounds. From their results, the inhibition efficiency of the Schiff bases increases with increasing E_{HOMO} and decreasing E_{LUMO}, while an opposite trend was observed for the hydrazides. A highly significant multiple correlation coefficient ($r > 0.96$) was obtained between experimental and calculated efficiencies. Some amides and their derivatives, e.g. urea, thiourea, thioacetamide, and thiosemicarbazide have also been found to be good inhibitors for mild steel in acid solutions (Awad, 2004; Lukovits *et al*., 1998; Stoyanova and Peyerimhoff, 2002; Fang and Li, 2002; Kutsán *et al*., 2000; Zhang *et al*., 2006). Several quantum chemical studies (Awad, 2004; Lukovits *et al*., 1998; Stoyanova and Peyerimhoff, 2002; Fang and Li, 2002; Kutsán *et al*., 2000; Zhang *et al*., 2006) have been carried out on these compounds by using semi-empirical methods. Zhang *et al*. (2006) and Fang and Li (2002) found a strong relationship between inhibition effect andΔE (E_{LUMO} - E_{HOMO}), whereas Kutsán *et al*. (2000) found a relationship between the dipole moment (μ) and corrosion parameters. According to the reported theoretical data, the inhibition efficiency decreased as the E_{HOMO} level decreased. The urea molecule has the lowest E_{HOMO} value, and, therefore, the lowest inhibition efficiency. Imidazoline-based corrosion inhibitors are well known as efficient corrosion inhibitors and are used

extensively to prevent oilfield corrosion. A considerable number of experimental studies of imidazoline inhibitors have been reported (Cheng and Zhou, 1993; He *et al*., 1997). However, there were relatively few theoretical studies (Edwards *et al*., 1994; Wang *et al*., 1999). Wang *et al*. (1999) measured the averaged percentage protection experimentally and obtained molecular geometry and charge density in MNDO calculations. Their theoretical predictions were in good agreement with experimental results.

The environmental requirements that are currently imposed on the development of ‘‘green” chemical inhibitors represent a strong motivation for the study of inhibition by natural tannins. Although anti-corrosive action of natural tannins was known for a long time, only in the past decade have tannins been investigated as corrosion inhibitors for some metalsin various media both experimentally and theoretically (Martinez, 2002; Martinez and Štagljar, 2003; Rahim *et al*., 2007). Martinez (2002) and Martinez and Štagljar, (2003) calculated molecular properties of chestnut and mimosa tannins that are most relevant to their action as corrosion inhibitors. These were the geometrical structure of the molecule, the dipole moment (l), HOMO and LUMO energies, and the energy gap. From the results obtained from their work, analysis of the action of metal corrosion inhibitors by quantum chemical tools may, to a great extent, eliminate an empirical approach to research in this field (Chittendon, 1951; Jiang and Geng, 1998). Li *et al*. (2005) used experimental and quantum chemical methods to explain the correlation of the inhibition effect and molecular structure of berberine. The authors predicted that the adsorption of berberine on the mild steel surface in sulphuric acid may be achieved by the interaction between iron atoms, cyclic molecular p-orbital and calculated E_{HOMO} and E_{LUMO}. The density distribution of HOMO/LUMO suggested that there were several

feasible absorption sites in one berberine molecule which favoured strong adsorption and high inhibition efficiency. Attempts to correlate corrosion inhibition with structural properties of prospective molecules using semi-empirical quantum chemical methods were developed together with the theories of reactivity. Various compounds were investigated i.e. zinc di-alkyl-di-thiophosphates (Armstrong *et al*., 1997;1998), potassium ethyl xanthate (Scendo, 2005), phthalocyanines (Zhao *et al*., 2005), polymethylene amines (Khaled *et al*., 2005), benzyl triphenyl phosphonium bromide (Bhrara and Singh, 2006), nicotinic acid (pyridine 3-carboxylic acid) (Kanojia and Singh, 2005), hydrazine carbodithioic acid derivatives (Khaled, 2006), aliphatic amines (Sastri and Perumareddi, 1994), pyrimidine derivatives (Bereket *et al*., 2003b), piperazine derivatives (Bereket *et al*., 2003a), amino acids and hydroxy carboxylic acids (Yurt *et al*., 2005a), phenyl-N,N dimorpholinemethanes (Kouznetsov *et al*., 2000), aniline trimers (Sein Jr. *et al*., 2001), triblock copolymers (Yurt *et al*., 2007), quarternary ammonium salts (Bereket *et al*., 2006), organophosphorus compounds (Mutombo and Hackerman, 1998), para-chlorobenzene nitriles (Xuejun *et al*., 2004), maleimide and its derivatives (Lazarova *et al*., 1995), anhydrides and imides (Lazarova *et al*., 2000) and substituted catechols and pyrogallols (Affrossman *et al*., 2001). Parameters of electron structure have been extensively used for correlation with corrosion inhibition effect of these organic compounds. Although there is no general rule to predict the potential of a compound to be good corrosion inhibitor or to find a universal type of correlation, Babic´-Samardz˘ija *et al*.(2005a) attempted to correlate some molecular parameters of N-heterocyclic amines (piperidine (pip), 2-methyl piperidine (2mp), 3-methyl piperidine (3mp), 2,6- dimethyl piperidine (26dp), and 3,5-dimethyl piperidine (35dp)) with their corrosion inhibition

efficiency. For this purpose, PM3, AM1 and MNDO semi-empirical methods were used. The effect of the molecular structure of these compounds on their inhibiting properties has been considered in terms of their electronic and chemical structure. Firstly, the effect of electron density, i.e. charge on the nitrogen atom and on the entire heterocyclic ring was obtained. Secondly, the effect of structural changes in terms of bond distances and angles was investigated. The total energy (TE) was obtained after geometric optimization with respect to all nuclear coordinates. From the results of their computational study, a relationship between some molecular parameters and the inhibition properties of amino compounds was found. Nevertheless, a number of neglected parameters that could be involved in such correlations, such as surface and solution characteristics, give at least a simplified explanation, although correlation is not so simple and straightforward as might be expected. However, it is clear that the inhibition properties of these N-heterocyclic amines could be related to the charge on nitrogen atom and sum of the net charge of the six atoms from the cyclic ring.

Babic´-Samardzˇija and Hackerman (2006) also used molecular modeling to gain insights into structural and electronic effects of polypyrazolylborates, dihydrobis (1-pyrazolyl) borate (Bp) and hydrotris(1-pyrazolyl)borate (Tp) in relation to their inhibition efficiencies and adsorption behaviour. From the findings of their electrochemical measurements, both polypyrazolylborates were relatively efficient inhibitors against acidic iron corrosion. Such parameters as the E_{HOMO}, E_{LUMO},ΔE total and binding energies and the heat of formation were obtained by the MNDO method. It was obvious that Bp had a lower binding energy (8.231 kJ mol^{-1}) and heat of formation (268kJmol^{-1}) as well as lower total energy (171.677 kJ mol^{-1}) than did Tp. The energy

gap (ΔE) showed that the greater inhibition effect could be related to the lower energy difference, i.e. to the Bp molecules that could be more readily excited and undergo a charge transfer interaction with the metal surface. Babic´-Samardzˇija *et al*. (2005b) also studied the inhibition properties of macrocyclic cobalt (III) complexes in the corrosion of iron in perchloric acid solutions. They used semi-empirical PM3 and ZINDO/1 methods was used to correlate structural properties of the complex species and their inhibition efficiency. Their theoretical predictions were in good agreement with experimental results. Detailed experimental and theoretical investigations of 23 different compounds including amines, thiourea derivatives, and acetylenic alcohols as corrosion inhibitors for 22% Cr stainless steel (austenitic-ferritic, duplex) in hydrochloric acid solutions were carried out by Cardoso *et al*. (2006, 2007) using quantitative structure- property relationship (QSPR) prediction analysis. The AM1 method was used to calculate quantum chemical parameters and obtained excellent correlations. Recently, Khaled (2008) applied molecular simulation tools to optimize the structure of adsorbed triazole derivatives. The iron/ inhibitor/solvent interfaces were simulated and the charges on the inhibitor molecules as well as their structural parameters were calculated in the presence of solvent effects. From the experimental and theoretical data, aminotriazole was the best inhibitor among triazole, aminotriazole and benzotriazole. Several studies on corrosion inhibitors employing semi-empirical methods have been reviewed up to date. As mentioned previously, the use of semi-empirical methods has been a subject of special intense interest in corrosion inhibitor studies in recent years. Consequently, it can be said that in such studies two different approaches have been used. In the first empirical approach, each functional group in an inhibitor molecule is assumed to contribute a

unique, independent and additive increment of corrosion protection determined from the corrosion rates by correlation of the molecular fragments with inhibitor performance. In the second semi-empirical approach, quantum chemical properties are correlated with inhibitor performance; determining the descriptor parameters is a most important aspect of this approach (Khalil, 2003).

2.7 Ab initio and Density Functional Theory (DFT) Methods

Quantum mechanical methods (ab initio, density functional theory (DFT) and semi-empirical methods) are all based on solving the time independent Schrödinger equation for the electrons of a molecular system as a function of the positions of the nuclei. The term ab initio indicates that the calculation is from first principles and that no empirical data is used. The simplest type of ab initio electronic structure calculation is the Hartree–Fock (HF), in which the instantaneous coulombic electron–electron repulsion is not specifically taken into account and only its average effect is included in the calculation. This is a variational procedure, and, therefore, the approximate energies obtained expressed in terms of the system wave function, are always equal to or greater than the exact energy, and approach a limiting value called the Hartree–Fock limit as the size of the basis is increased (Parr *et al*., 1950). Many types of calculations (Møller-Plesset perturbation theory and coupled cluster theory) begin with a Hartree–Fock calculation and subsequently correct for electron–electron repulsion, referred to also as electronic correlation. DFT is used to investigate the electronic structure, principally the ground state of many-body systems, in particular atoms, molecules and the condensed phases (Eddy and Ita, 2010b).

The main objective of DFT is to replace the many-body electronic wave function with the electronic density as the basic quantity (Jensen, 2007). Any exchange functional can be combined with any correlation functional in DFT calculations.

2.8 Study of Corrosion Inhibitors by Ab initio and DFT Methods

Some studies have been carried out on corrosion inhibition mechanism using ab initio methods. For example, Ma *et al*. (2006) attempted to determine theoretical parameters to characterize inhibition property of three nitrogen-heterocyclic compounds, namely 3,5-dimethyl-1H-pyrazole, pyridine and 2- (3-methyl-1H-pyrazol–5-yl)pyridine for steel corrosion using an ab initio method employing the HF/LANL2DZ basis set. From the results obtained, corrosion inhibition efficiency is related to the HOMO energy. The interaction between inhibitor molecules and one iron atom was also investigated. It was found that the lower the combined energy, the more stable the complex formed, with the inhibitor having better inhibitive property. A similar interaction energy approach was used for the theoretical study of some aniline derivatives toward the corrosion of copper in hydrochloric acid. Henríquez-Román *et al*. (2005) also performed ab initio SCF-HF calculations using D95 and D95 V basis sets for aniline derivatives and copper clusters, respectively. The results obtained showed that corrosion inhibition by aniline molecules can be associated mainly with local properties acting on active sites are in the copper surface. The electronic and molecular structures of several heterocyclic compounds, 1,3,4-thiadiazole and its derivatives have been calculated by Rodríguez-Valdez *et al*. (2005) using of B3LYP/STO-3G* method. Parameters such as total energy, ΔE E_{HOMO} and E_{LUMO}, dipole moment (μ) and global hardness (g) were calculated for each of the derivatives of 1,3,4-thiadiazole, both in the gas and liquid phases. No significant

differences were found for the structures of these compounds in gaseous and liquid phases. Rodríguez-Valdez *et al*. (2004) performed calculations for 4-amino-1,2,3,5-thiatriazole and 5-amino-1,2,3,4-thiatriazole using a modified density functional theory (DFT) called PBEg, with 3-21G*, CBSB2**, CBSB7, CBSB4 and CBSB1 basis sets. Because of lack of experimental data for these compounds, they made a comparison of their results with the previous computational results was made. There was a good agreement between experimental and theoretical data and indicating that accurate results could be obtained in a reasonable time using their new DFT method. A similar study on the efficiency of hydroxyethyl, aminoethyl and amidoethyl was also carried out by Rodríguez-Valdez *et al*. (2006) using the PBEg functional with the CBSB2** basis set. Feng *et al*. (2006) performed calculations of a self-assembled monolayer of 2-mercaptobenzothiazole (MBT) in order to investigate the adsorbate-surface interactions by the B3LYP/6-31+G* method. They calculated such parameters as the atomic charges for two tautomeric forms of the MBTmolecule (i.e. thiol and thione), the HOMO and LUMO energies and the interaction energy between MBT and iron. They chose benzothiazole to compare the results obtained by MBT. The HOMO energies of two forms of MBT (-624.1 kJ mol^{-1} for thiol form and -583.5 kJ mol^{-1} for thione form) were larger than that of benzothiazole (-647.9 kJ mol^{-1}). These results show the importance of the heterocyclic sulphur atom in forming the self-assembled monolayers on iron. The interaction energy calculations also predicted that MBT can be chemically adsorbed on the iron surface through the heterocyclic sulphur atom. For further insights into the adsorbent-surface interactions, Feng *et al*. (2007) also applied B3LYP/6-31+(d,p) method for 5,10,15,20-tetraphenylporphyrin (TTP) and

5,10,15,20-tetra-(4- chlorophenyl)porphyrin (TCIPP) inhibitors for iron corrosion. They computed the HOMO and LUMO energies of these two molecules was computed and found to be higher (- 505.67 kJ mol^{-1}) for TTP than that for TCIPP (-543.69 kJ mol^{-1}). They concluded that the interaction between TTP and iron will be stronger than that between TCIPP and iron. In order to probe the interactions between methionine molecules and metal surface, theoretical calculations were performed by Özcan *et al*. (2008) using B3LYP/6-311**G(d,p) method. A local type reactivity criterion (Fukui index) was considered and Fukui indices were determined for N + 1 and N- 1 electron species at the geometry of the reference N-electron methionine molecule. From their results, it was shown that localization of frontier molecular orbitals (HOMO and LUMO) and condensed Fukui indices (f^- and f^+) analysis of the reactive regions are very useful in characterization of organic adsorbates.

Li *et al*. (2007) computed the HOMO and LUMO energies, energy gap, molecular orbital densities and dipole moment of newly synthesized three triazole derivatives: 4-chloro-acetophenone- O-10-(10,30,40-triazolyl)-metheneoxime (CATM), 4-methoxyl-acetophenone-O-10-(10,30,40-triazolyl)-metheneoxime (MATM) and 4-fluoro-acetophenone-O-10-(10,30,40-triazolyl)-methenoxime (FATM) as corrosion inhibitors of mild steel in acid media by ab initio method employing 3-21G* basis set. They could not find a direct relationship between the inhibition efficiency and the E_{HOMO}, E_{LUMO} and dipole moment of the molecules. Therefore, they tried to reduce the complexity of adsorption process using just the values of ΔG^{o}_{ads} obtained from thermodynamic calculations. From ΔG^{o}_{ads} and calculated quantum parameters, two types of interactions, chemisorption and physisorption, were responsible for the inhibition behaviour of these

triazole derivatives. Gao and Liang (2007) investigated the inhibition efficiency of 1-diethylamino-propan-2-ol (EAP) and 1, 3-bis-diethylamino-propan- 2-ol (DEAP) as corrosion inhibitors for brass in simulated atmospheric water. The Milliken charges, HOMO and LUMO energies, total energy and dipole moment were calculated using the B3LYP/6-311G** methodology. From the results obtained their calculation show, the E_{HOMO} of DEAP (- 0.205 a.u.) was higher than that of EAP (-0.222 a.u.) and the values of ΔE for EAP and DEAP were -0.258 and -0.242 a.u., respectively. They found a good correlation between the inhibition efficiency of DEAP and values of E_{HOMO}, and lower values of ΔE and dipole moment which was a good agreement with the experimental findings. In order to understand the formation of protective film on iron by alkynol inhibitors (oct-1-yn-3-ol and 2-2-(1,1,-dimethyl-prop- 2-ynyloxy)-ethoxy-ethanol) in acidic solutions, Lendvay-Györik *et al*. (2003) calculated the binding energy of both dative iron-triple bond and the iron-alcoholic oxygen bond using B3LYP/3-21G* and HF/6-311G** methods. They also calculated vibrational frequencies characteristic of the iron-bonded alkynol molecules for comparison with experimental IR spectra. Their results supported the formation of a dative bond between the iron and the carbon–carbon triple bond.

Qafsaoui *et al*. (2001) compared the inhibitive effect of 3-amino 1, 2, 4-triazole (ATA) with benzotriazole (BTAH) and 1-hydroxybenzotriazole (BTAOH) on the pitting corrosion of copper induced by sulphate and chloride ions by the Hartree–Fock method. Calculations were carried out to estimate interaction energies between these aggressive anions and ATA supported by Cu^{+} ions. Small Cu^{2+} clusters were used to model the copper surface. The binding energy of Cl^{-} on the ATA-Cuþn system was found to be13 kJ

mol^{-1} higher than the binding energy of Cl^- on clusters of Cu^{2+} ions. In contrast, the binding energy of SO_4^{2-} on the ATA-Cuþn system was found to be 19 kJ mol^{-1} lower than the interaction energy between SO_4^{2-}ions and the clusters of Cu^{2+}. These calculations showed a significant inhibitive effect of ATA in the presence of chloride ions and that in contrast to the two other inhibitors, ATA was less efficient in sulphate medium than in chloride solution because of the strong interaction with chloride ions. The correlation between the molecular structures and corrosion inhibition efficiencies of thioacetamide (TAcA), thiourea (TU) and thiobenzamide (TBA) was investigated by Özcan and Dehri (2004) using the ab initio 6-31G(d) method. To investigate the effect of substituents on the inhibition mechanism and efficiency, the HOMO and LUMO energies, energy gap, the volumes of molecules and molecular orbital densities were computed. Although there was no correlation between the LUMO energy and inhibition efficiency for TU molecule, an increase in inhibition efficiencies of molecules was observed when the molecules had higher HOMO energies. Their HOMO energies increased in the order of thiobenzamide > thiourea > thioacetamide, which was in agreement with experimental data.

The effects of the concentration of thiourea (TU), methylthiourea (MTU) and phenylthiourea (PTU) on the corrosion of mild steel in 0.1 M H_2SO_4 were also investigated by Özcan *et al*. (2004). The electronic properties of these compounds were calculated by ab initio RHF/6-31G (d) method. The highest E_{HOMO} and the lowest E_{LUMO} and ΔEvalues were found for PTU which was the most efficient inhibitor based on the experimental data. Stoyanova *et al*. (2002) investigated the geometrical and electronic molecular structures of a- and c-pyrophtalone as inhibitors for copper corrosion using a SVP (split valence plus polarization quality) basis set which is equivalent to 6-31G*.

Bond distances, bond angles, ionisation potentials, dipole moments and net atomic charges were calculated from the result of their calculations, it was found that the ionisation potential and the dipole moments of the molecules are parameters that had the strongest influence on the adsorption and inhibition properties of these compounds. It was shown that a decrease in the ionisation potential of the inhibitor molecule and an increase in the dipole moment produce a higher inhibition efficiency on corrosion. Lebrini *et al*. (2006) investigated the effect of 2,5-bis(4-pyridyl)- 1,3,4-thiadiazole (4-PTH) and some of its derivatives (n-PTH; for n = 2 and n = 3) on the corrosion of mild steel in acidic media by the HF/ 3-21G method. The energies of HOMO and LUMO and dipole moments (μ) were computed. A linear resistance model (LR) relying on dipole moment, E_{HOMO} and E_{LUMO} was developed. Significant multiple correlation coefficients ($R > 0.93$) that indicated the variation of the corrosion inhibition with the structure of the inhibitors were obtained.

Sahin *et al*. (2008) investigated the dependence of inhibition efficiencies of three heterocyclic compounds, 3-amino-1,2,4-triazole (3-ATA), 4-hydroxy-2H-1-benzopyran-2- one (4-HQ) and 4-hydroxy-3-(1H-1,2,4-triazole-3-ylazo)-2H-1- benzopyran-2-one (3-ATA-Q), using the B3LYP/6-31G(d) method. Such parameters as the E_{HOMO}, E_{LUMO}, ΔE, net atomic charges(q), μ, total and interaction energies were calculated. A good agreement was found between experimental and theoretical data. Bentiss *et al*. (2002) carried out theoretical calculations for 2,5- bis(n-methoxyphenyl)-1,3,4-oxadiazoles (n-MOX) as corrosion inhibitors for mild steel in 1 M HCl and 0.5 M H_2SO_4 to show if any structural differences induced by different positions of the methoxy group may be related to the experimentally observed differences of corrosion efficiency. They used Monte

Carlo method for conformational search and found two conformers of 2-MOX. They calculated the HOMO and LUMO energies, energy gap, and charges on nitrogen atoms for these two conformers of 2-MOX, 3-MOX and 4-MOX were calculated using the RHF/3-21G* method. The electrostatic potential map calculations were employed to determine the effect of hydrogen bonding on the cationic form of the 2-MOX molecule. The results obtained revealed that the experimentally found superior inhibition efficiency 2-MOX can be explained in terms of electronic densities in the neutral molecules and by the cationic form of this molecule highly stabilised by hydrogen bonding.

Bentiss *et al*. (2007b) also investigated some new 2,5-disubstitued 1,3,4-thiadiazoles as corrosion inhibitors for mild steel corrosion in 1 M HCl using the B3LYP/ 6-31G(d,p) (2d,2p) method. In order to obtain any correlation between experimentally determined corrosion inhibition data and a number of quantum molecular properties, inhibition efficiency of six thiadiazole compounds (2,5-bis(phenyl)-1,3,4-thiadiazole (DPTH), 2,5-bis(4-methoxyphenyl)-1,3,4-thiadiazole (4-MTH), 2,5-bis(4 dimethylaminophenyl)-1,3,4-thiadiazole (4-DATH), 2,5-bis(4-methylphenyl)- 1,3,4-thiadiazole (4-MPTH), 2,5-bis(4-nitrophenyl)-1,3, 4-thiadiazole (4-NPTH) and 2,5-bis(4-chloroxyphenyl)-1,3,4-thiadiazole (4-CPTH)) was subjected to correlation analysis with calculated quantum chemical parameters (E_{HOMO}, E_{LUMO}, ΔE and dipole moment (μ)) using linear and non-linear models in order to establish any direct links between them. The linear model was not found to be satisfactory for correlation. A good correlation ($R = 0.98$) was found for the non-linear model. The same authors investigated the inhibition properties of 3,5-bis(n-pyryridyl)-4-amino-1,2,4-triazoles (Bentiss *et al*., 2008), isomers of 3-pyridyl-substitued 1,2,4 and 1,3,4-thiadiazoles (Bentiss *et al*., 2004a), some 4H-

triazole derivatives (Bentiss *et al*., 2007a) and some new macrocyclic polyether compounds as corrosion inhibitors for the corrosion of mild steel using the HF/3-21G*, HF/6-21G*, and B3LYP/6-31G(d,p) methods, respectively. The results of theoretical calculations carried out in these studies supported experimental findings. Allam (2007) tried to establish a quantitative relationship between inhibition efficiency and the electronic structure of some triazole derivatives (4-amino– 5-mercapto-3-methyl 1,2,4-triazole (AMMT), 4-amino-5-mercapto-3-ethyl 1,2,4-triazole (AMET) and 4-amino-5-mercapto-3-propyl 1,2,4-triazole (AMPT)) as new corrosion inhibitors for Cu-Zn alloy (60Cu–40Zn) in acidic and neutral solutions. Such parameters as the HOMO and LUMO energies, energy gap, total energy, dipole moment for AMMT, AMET and AMPT compounds were calculatedusing the RHF/3-21G method. A correlation between the E_{HOMO}, energy gap, the charge on nitrogen atom and the inhibition efficiency was found by regression analysis. However, no clear relationship between the E_{LUMO}, dipole moment and the inhibition efficiency could be established from the results. A similar study was carried out for two tautomeric forms of 2-mercapto-1-methylimidazole (MMI) employed to retard corrosion of carbon steel in 1 M $HClO_4$ by Benali *et al*. (2007) using DFT methods. The HOMO and LUMO energies, energy gap and dipole moment were calculated for the thiol and thione forms of MMI. From the theoretical data, the thione form of MMI was found to be more efficient inhibitor than the thiol form because the thione form has the highest E_{HOMO} and dipole moment, and the lowest E_{LUMO} and energy gap values. Ma *et al*. (2008) studied the inhibition efficiency of self-assembled films of 1-methyl-5-mercapto-1,2,3,4-tetrazole (MMT) for the corrosion of iron using the B3LYP/LANL2DZ method. In order to investigate the adsorption between MMT and

iron, the enthalpies, entropies and free energy changes of the MMT/iron system were calculated. From the results of these calculations, it was concluded that MMT molecule is bound to the iron surface by sharing electrons between the nitrogen and iron atoms.

Blajiev and Hubin (2004) investigated the efficiency of 2-amino- 5-mercapto-1,3,4-thiadiazole (AMTD) and 2-methyl-5-mercapto- 1,3,4-thiadiazole (MMTD) as copper corrosion inhibitors in neutral chloride environments. Soler *et al*. (2002) carried out calculations using SIESTA method, based on DFT, to reflect the relaxation and adsorption interactions of ions and inhibitors on the Cu_2O surface. Their results with benzotriazole inhibitor were compared suggesting that AMTD and MMTD are better corrosion inhibitors than benzotriazole. The inhibitive action of some thiadiazole derivatives namely 2,5-bis(2-thienyl)-1,3,4-thiadiazole (2-TTH) and 2,5-bis(3-thienyl)-1,3,4-thiadiazole (3-TTH) against the corrosion of mild steel in 0.5 M H_2SO_4 was investigated by Lebrini *et al*. (2007a) using the B3LYP/6-31+G(d,p) (2d,2p) method. The HOMO and LUMO energies, energy gap and the dipole moment of the molecules were calculated. Since a small energy difference was found between E_{HOMO} and E_{LUMO} and no direct correlation could be seen between the dipole moment, energy gap and inhibition efficiency, a linear resistance model (LR) was used to correlate the corrosion inhibition properties with the calculated quantum chemical parameters. A good correlation (R= -0.91) was found between the coefficient of E_{HOMO}, E_{LUMO}, and inhibition efficiency.

Zhang *et al*. (2005)studied the inhibition efficiencies of imidazole, benzimidazole and their derivatives using the B3LYP/6-31G* method. A number of quantum chemical parameters such as E_{HOMO}, E_{LUMO}, ΔE, charge distribution, dipole moment, and molecular connectivity index (MCI) which reveal the stearic hindrance effect of the molecule were

calculated. From their results, the E_{HOMO} was the most statistically significant term influencing the corrosion inhibition efficiencies The greater the E_{HOMO}, the greater the inhibition efficiency. Wang *et al*. (2003) studied the protection offered by self-asssembled films of carbazole (CZ) and N-vinylcarbazole (NVC) against copper corrosion in NaCl solution using ab initio HF/LANL2DZ method. The HOMO and LUMO energies and total atomic charges of the molecules were calculated. Their calculations showed that the HOMO energy (-743.6 kJ mol^{-1}) of NVC was higher than that of CZ (-754.7 kJ mol^{-1}). The LUMO energy (230.68 kJ mol^{-1}) was lower than that of CZ (245.7 kJ mol^{-1}). These results provided a theoretical confirmation that NVC has stronger bonding affinity for copper than CZ, which was consistent with the experimental results.

Kandemirli and Sagdinc (2007) carried out detailed quantum chemical studies for urea (U), thiourea (TU), acetamide (A), thioacetamide (TA), semicarbazide (SC), thiosemicarbazide (TSC), methoxybenzaldehyde thiosemicarbazone (MBTSC), 2-acetylpyridine-(4-phenyl)thiosemicarbazone (2AP4PTSC), 2-acetylpyridine-(4-methyl)thiosemicarbazone (2AP4MTSC), benzointhiosemicarbazone (BZOTSC) and benzylthiosemicarbazone (BZITSC) using ab initio RHF/6-31G(d) and MP2/6-31G(d) methods and B3LYP/STO-3G, B3LYP/3-21G and B3LYP/6-31G(d) DFT methods. The results obtained from quantum chemical calculations and experimental efficiencies of inhibitors were subjected to correlation analysis. On the basis of the HOMO and LUMO energies, HOMO and LUMO coefficients, polarizability, Muliken population analysis, it was concluded that consideration of one parameter is not sufficient and that the synthesis of better corrosion inhibitors can be achieved by controlling all electronic properties and

parameters of a selected group of molecules. Szeptycka (2005) investigated the effect of saccharin, 2-butyne -1,4-diol, 1-4-b,b0-dihydroxyethoxy-2-butyne, 4-(b-hydroxypropoxy)- 2-butyne-1-ol, 1-methylenedipyridinium chloride and 1,1'-methylenedipyridinium dichloride, on the corrosion inhibition of steel in two acids, 6.3 N hydrochloric acid and 4.28 N sulphuric acid using ab initio and PM3 methods. All quantum chemical calculations were carried out using the ab initio method with full geometrical optimization using a STO-3G basis set. The HOMO, LUMO energies and energy gap were calculated and correlated with experimental data. Good fit of data was obtained and it was concluded that such calculations appear to be useful in assessing the degree of pickling inhibition since the use of polyaniline (PAni) as an alternative anti-corrosion material is well known,

Sein *et al*. (2004) investigated the electronic behaviour of aniline oligomers which is similar to that of PAni. They determined the thermodynamic parameters for several competing reaction sequences occurring during the interaction of an iron (or aluminium) surface and aniline trimers using B3LYP/6-311G(2d,p) and B3LYP/6-31G+ methods. The calculation of thermochemical properties of aniline trimers in various oxidation states, in conjuction with similar calculations on cluster models of iron and aluminium surfaces, has shown that the emeraldine dihydrochloride is the most effective form for corrosion inhibition. Furthermore, it was shown that a model based on the analysis of equilibrium and rate of corrosion inhibition by aniline trimers can be supported by density functional theory. A detailed calculation of the molecular structure of benzimidazoles was carried out by El Ashry *et al*. (2008) using the B3LYP/6-31G* method to explore possible correlations between corrosion inhibition efficiencies and a

number of quantum molecular properties such as E_{HOMO}, E_{LUMO}, total negative charge on molecules and linear solvation energy relationship parameters. Furthermore, bivariate correlations using two trial personal correlation coefficient and linear regression analyses were performed by stepping method. A comparison of the inhibition efficiencies of a series of benzimidazoles revealed that their inhibition effect has been closely related to the orbital energies (E_{HOMO} and E_{LUMO}), Log P, dipolar-polarizability factor (p*) and the total negative charge on the molecule. It has been concluded that a composite index of more than three quantum chemical parameters should be considered to characterize the inhibition efficiency of molecules. Quantum chemical studies of corrosion inhibition of steel in acidic medium by some triazole, oxadiazole and thiadiazole derivatives were also carried out by El Ashry *et al*. (2006a) in a similar manner. Increased attention has been paid in recent years to Schiff bases as corrosion inhibitors for various metals in typical acidic environments.

Hasanov *et al*. (2007) investigated the inhibition effects of two Schiff base compounds, (2-{[(4 methoxyphenyl)imino]- methyl}phenol and 1-{[(4-methoxyphenyl)imino]methyl}-2-naphthol), on steel corrosion in sulphuric acid solution. Such parameters as frontier orbital energies, Muliken charges of possible adsorption sites and dipole moments were calculated using B3LYP/6-31G (d) method. All theoretical data were found to be in good agreement with the experimental findings. Furthermore, Ju *et al*. (2008) presented a theoretical study of electronic and molecular structures of aminic nitrogen-containing polydentate Schiff base compounds and calculated their HOMO and LUMO energies, charge distributions, the absolute electronegativity (v) values, and the fraction of electrons (DN) transferred from inhibitors to iron by the B3LYP/6-31G*

method. It was concluded that the inhibition efficiency increased with an increase in E_{HOMO} and decrease in E_{LUMO}- E_{HOMO}. This conclusion simply supports the results of various studies on different inhibitors, such as macrocyclic polyether compounds (Lebrini *et al*., 2007b), thiadiazole derivatives (Lebrini *et al*., 2005) and pyridine derivatives (Lashgari *et al*., 2005). In a very recent study, purines and their derivatives such as guanine, adenine, 2,6-diaminopurine, 6-thioguanine and 2,6-dithiopurine, were investigated as corrosion inhibitors for mild steel in 1 M HCl solution by Yan *et al*. (2008) using the 6-31G* DFT method. The Milliken partial charges, HOMO and LUMO energies, energy gap and dipole moments were calculated and the inhibition efficiency was correlated with the energy gap and the electron density of the frontier orbital. It was concluded that purines were physically adsorbed by p stacking on mild steel. For the inhibition of aqueous metallic corrosion with an organic compound, it is necessary to design a ligand that adsorbs strongly on the metal. There are some theoretical studies in the literature on the corrosion inhibition of metals taking into account the role of the metallic surface (Shapovalova *et al*., 2005; Pokhmurs'kyi *et al*., 2003; Arshadi *et al*., 2004; Lashkari and Arshadi, 2004; Lukovits *et al*.,2003; Yan *et al*., 1999; Lashgari *et al*., 2006; Bartley *et al*., 2003; Pradip, 2002; Ramachandran and Jovancicevic, 1999).

Chapter 3

MATERIALS AND METHODS

3.1 Materials

Materials used for the study were mild steel sheet of composition (wt %, as determined by quantiometric method) Mn (0.6), P (0.36), C (0.15), Si (0.03) and Fe (98.78). The sheet was mechanically pressed cut into different coupons, each of dimension, 5x4x0.11cm. Each coupon was degreased by washing with ethanol, cleaned with acetone and allowed to dry in the air before preservation in a desiccator. All reagents used for the study were analar grade and double distilled water was used for their preparation. Concentrations of HCl used for gasometric, thermometric and weight loss studies were 2.5, 2.5 and 0.1 M respectively. The amino acids used for the study were provided by Department of Chemistry, Ahmadu Bello University, Zaria. They were used without further purification.

3.2 Experimental Techniques

3.2.1 Gravimetric method

In the gravimetric techniques, a previously weighed metal (mild steel) coupon was completely immersed in 250 ml of the test solution in an open beaker. The beaker was covered with aluminium foil and inserted into a water bath maintained at 303 K. After every 24 hours, the corrosion product was removed by washing each coupon (withdrawn from the test solution) in distilled water containing 50 % NaOH and 100 g l^{-1} of zinc dust. The washed coupon was rinsed in acetone and dried in the air before re-weighing. The experiment was repeated at 333 K. In each case, the difference in weight for a period of 168 hours was taken as the total weight loss. From the average weight loss

(mean of three replicate analysis) results, the inhibition efficiency (%I) of the inhibitor, the degree of surface coverage (θ) and the corrosion rate of mild steel (CR) were calculated using equations 3.1, 3.2 and 3.3 respectively;

$$\%I = (1 - W_1/W_2) \times 100 \quad (3.1)$$

$$\theta = 1 - W_1/W_2 \quad (3.2)$$

$$CR = \Delta W/At \quad (3.3)$$

where W_1 and W_2 are the weight losses (g) for mild steel in the presence and absence of the inhibitor, θ is the degree of surface coverage of the inhibitor, $\Delta W = W_2 - W_1$, A is the area of the mild steel coupon (in cm^2), t is the period of immersion (in hours) and W is the weight loss of mild steel after time, t.

3.2.2 Thermometric method

In other to determine the corrosion rate in the different reagents, a three-neck flask (shown in Fig. 3.1) with provisions for the introduction of chemicals and for insertion of thermometer was used for thermometric study.

For each study, the mild steel coupon was introduced into the flask. Enough quantities of the test solution were in turn transferred into the flask until the mild steel coupon was completely immersed. Once this was done, the temperature of the reacting solution was read at one-minute interval until a constant temperature was obtained.The reaction number (RN) of each system was calculated by dividing the difference between the highest and lowest temperature attained by the time interval.

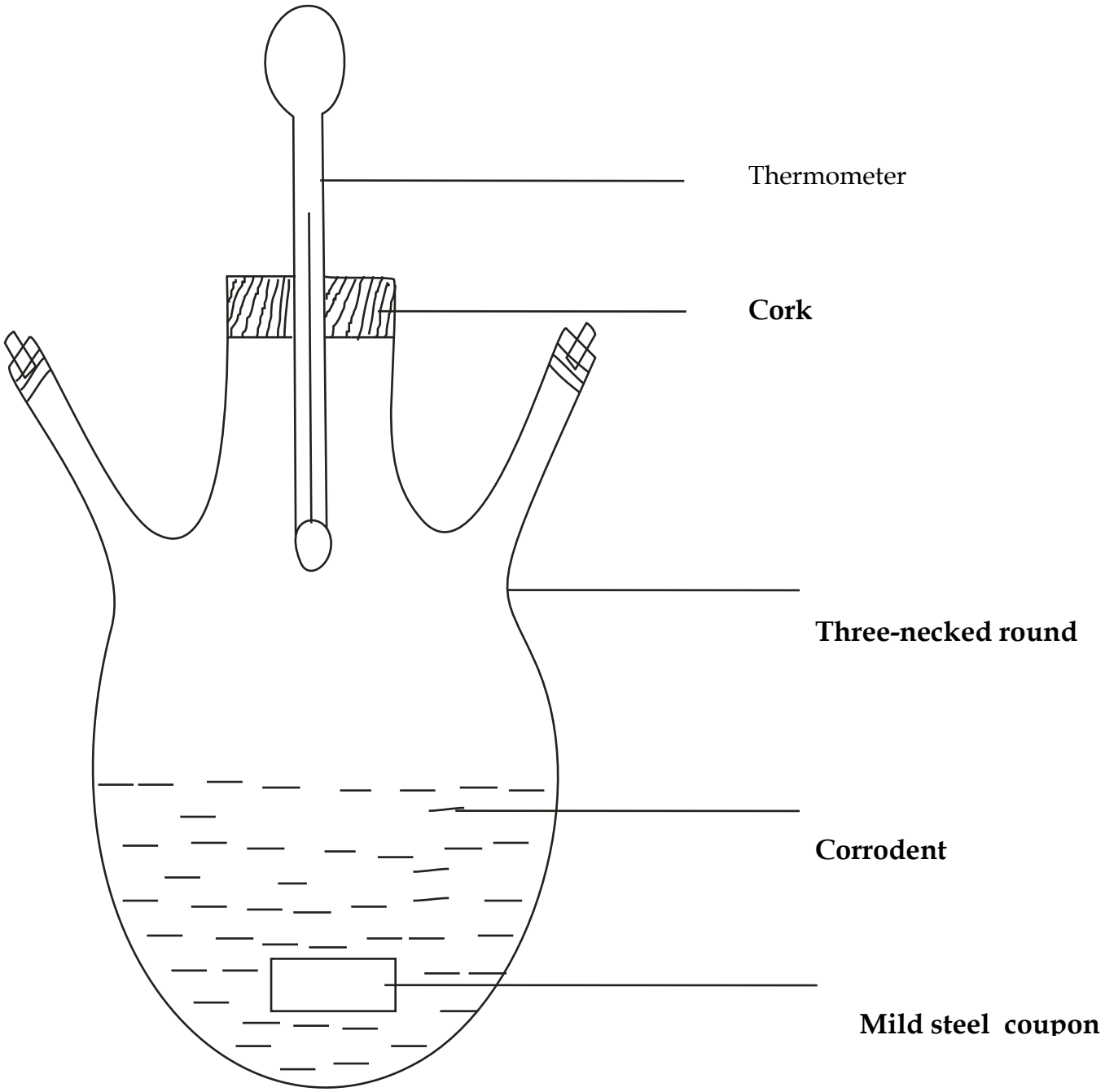


Fig. 3.1: Diagram of the Thermometric Apparatus

From the reaction number, the inhibition efficiency (%I) of the inhibitor was calculated using equation 3.4:

$$\%I = \frac{RN_{aq} - RN_{wi}}{RN_{aq}} \times 100 \qquad 3.4$$

where $RN_{aq}$is the reaction number in the absence of inhibitors (blank solution) and $RN_{wi}$is the reaction number of 2.5 M HCl containing the studied inhibitor.

3.2.3 Gasometric method

The apparatus used for hydrogen evolution measurement is shown in Fig. 3.2. The test solution (different concentrations of halides, inhibitor, acid or their mixtures) was transferred into the reaction vessel. Upon the introduction of mild steel, the flask was quickly corked and the rise in volume of the paraffin due to hydrogen evolution was noted after every minute until a constant volume was observed.

From the volume of hydrogen gas evolved per minute, inhibition efficiencies were calculated using equations 3.5.

$$\%I = \left(1 - \frac{V_{Ht}^{1}}{V_{Ht}^{o}}\right) x\,100 \qquad 3.5$$

where V_{Ht}^{1} and V_{Ht}^{o} are the volumes of H_2 gas evolved at time, 't' for inhibited and uninhibited solutions respectively.

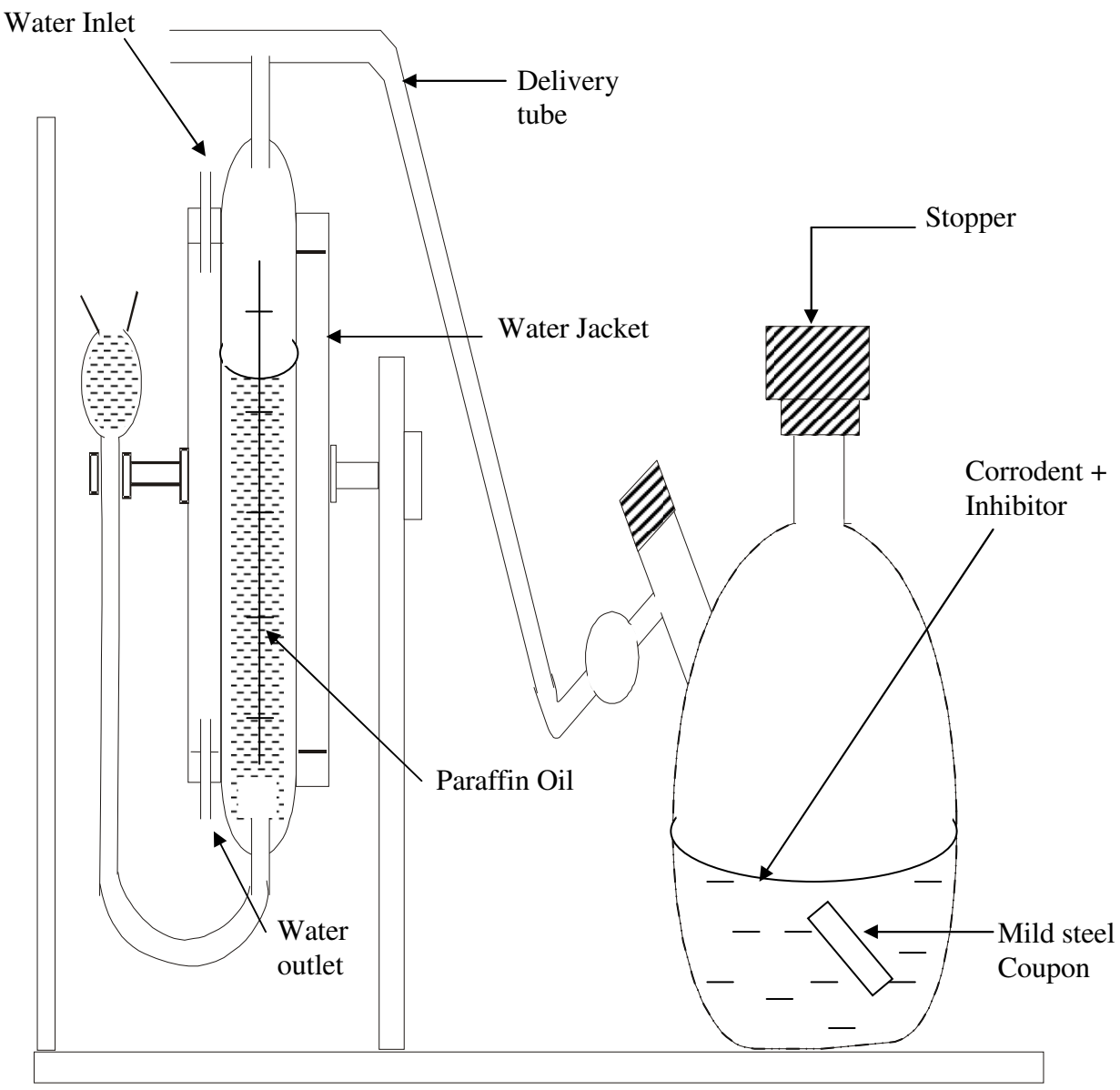


Fig. 3.2: Gasometric assembly for the measurement of volume of H_2 evolved.

3.3 Quantum Chemical Calculation

The input programmes (input file) for all computational calculations were developed by Dr. Nnabuk Okon Eddy of the Department of Chemistry, AhmaduBelloUniversity, Zaria (some of the input programmes are presented in Appendices 1 to 8). Single point energy calculations were carried out using AM1, PM6, PM3, MNDO and RM1 Hamiltonians in the MOPAC 2008 software for Windows (Steward, 2009). Calculations were performed on an HP compatible Intel Pentium V (4.0 GHz, 4 GB RAM) computer. The following quantum chemical indices were calculated: the energy of the highest occupied molecular orbital (E_{HOMO}), the energy of the lowest unoccupied molecular orbital (E_{LUMO}), the dipole moment (μ), the total energy (TE), the electronic energy (EE), the ionization potential, the cosmo area (cosAr) and the cosmo volume (CosVol). The Muliken and Lowdin charges (q) for nucleophilic and electrophilic attacks were computed using GAMESS computational softwares (Schmidt *et al*., 1993). The programme settings for the density functional theory calculations (DFT) were:Corelation.: DFT, correlation type: B3YLP, Basis set: 6-31G but for Moller-Plesset perturbation theory calculations (MP2) the programme settings were, correlation: MP2, correlation type: MP2 and Basis set: STO-5G.

Statistical analyses were performed using SPSS program version 15.0 for Windows. Non-linear regression analyses were performed by unconstrained sum of squared residuals for loss function and estimation methods of Levenberg-Marquardt using SPSS program version 15.0 for Windows.

3.4 Infra red Analysis

FTIR analysis of the corrosion product for the corrosion of mild steel and those of the amino acids were carried out at National Research Institute of Chemical Technology (NARICT), Zaria, Kaduna State, Nigeria using Fourier Transform Infra RedSpectrophotometer.

Chapter 4

RESULTS AND DISCUSSIONS

4.1 Experimental

The results obtained from various experiments are presented and discussed under different sub headings. The results are discussed based on established chemical principles.

4.1.1 Effect of concentration of amino acids on the corrosion of mild steel

Fig. 4.1 shows the variation of weight loss of mild steel with time for the corrosion of mild steel in 0.1 M HCl containing various concentrations of amino acids. From Fig.1, it is evident that weight loss of mild steel decreases with increase in the concentration of the amino acid but increases with increasing period of contact. These indicate that the rate of corrosion of mild steel in HCl solutions increases with increase in the period of contact but decreased with increase in the concentration of the amino acids. The findings also indicate that the amino acids studied inhibited the corrosion of mild steel in HCl solutions. Fig. 4.2 shows the variation of inhibition efficiencies of L-cysteine (CYS), glycine (GLY), L-leucine (LEU) and alanine (ALA) with concentration. From the figure, it can be seen that the inhibition efficiency of the various amino acids is concentration dependent and that the order of increasing inhibition efficiency is CYS > LEU > ALA > GLY.

Table 4.1 presents the corrosion rates andinhibition efficiencies of mild steel in various media at 303 and 333 K. The results obtained reveal that the rate of corrosion

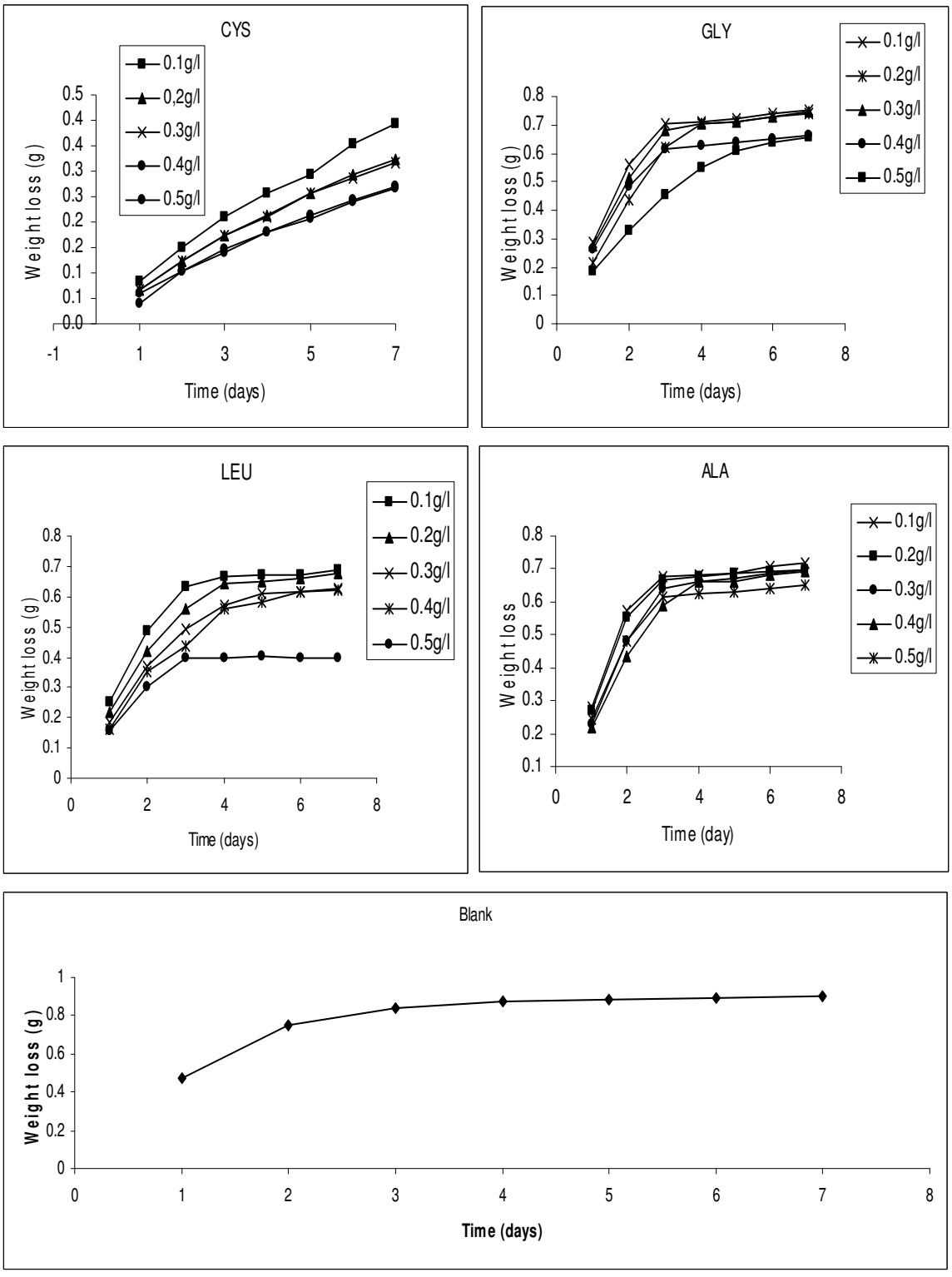


Fig. 4.1: Variation of weight loss of mild steel with time for the corrosion of mild steel in 0.1 M HCl containing various concentrations of amino acids at 303 K

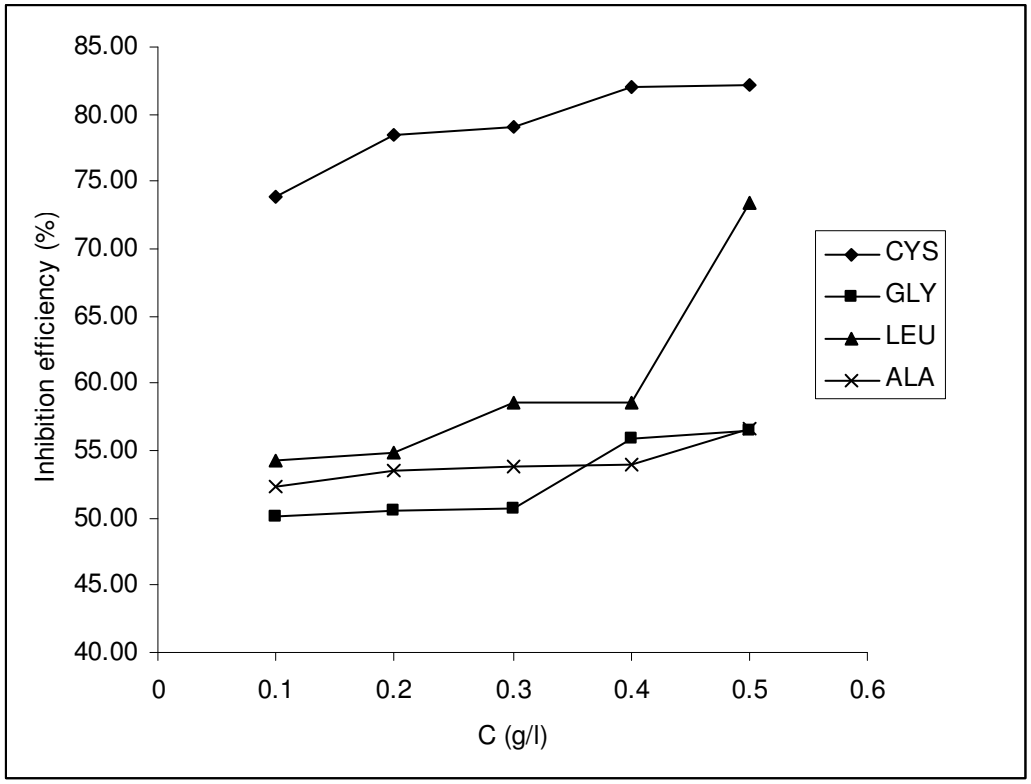


Fig. 4.2: Variation of inhibition efficiencies of the amino acids with concentration at 303 K

Table 4.1: Rates of corrosion mild steel and inhibition efficiencies of the amino acids in various media.

System	Inhibition efficiency (%)				Corrosion rate ($gh^{-1}cm^{-2}$)			
	CYS	**GLY**	**LEU**	**ALA**	**CYS**	**GLY**	**LEU**	**ALA**
Blank at 303 K	**-**	-	**-**	**-**	0.000448	0.000448	0.000448	0.000448
0.1g at 303K	78.42	50.06	54.22	52.30	0.000117	0.000224	0.000219	0.000214
0.2 g at 303 K	73.93	50.56	55.83	53.58	9.66E-05	0.00022	0.000174	0.000208
0.3 g at 303 K	79.00	54.75	59.50	53.75	9.4E-05	0.000221	0.000172	0.000207
0.4 g at 303 K	82.09	55.91	60.59	54.02	8.02E-05	0.000197	0.000163	0.000206
0.5 g at 303 K	82.21	56.50	64.42	56.56	7.96E-05	0.000195	0.000161	0.000194
Blank at 333 K	-	-	-	-	0.002686	0.002686	0.002686	0.002686
0.1g at 333K	69.59	41.75	43.05	44.36	0.000817	0.001565	0.00153	0.001495
0.2 g at 333 K	74.82	42.33	57.47	45.85	0.000676	0.001549	0.001219	0.001454
0.3 g at 333 K	75.51	42.56	54.55	46.06	0.000658	0.001543	0.001221	0.001449
0.4 g at 333 K	79.10	48.57	54.62	46.37	0.000561	0.001381	0.001142	0.001441
0.5 g at 333 K	79.25	49.26	57.95	49.33	0.000557	0.001363	0.00113	0.001361

mild steel decreases with increase in the concentration of the amino acid while the inhibition efficiency increases with increasing amino acid concentration. The results also indicate that the amino acids are adsorption inhibitors for the corrosion of mild steel in HCl solutions. According to Eddy *et al*. (2010a), the inhibition efficiency of an adsorption inhibitor tends to increase with increase in the concentration of the inhibitor. From Table 4.1, it is also evident that the inhibition efficiencies of the amino acids decreased with increase in temperature indicating that the adsorption of the amino acids supports the mechanism of physical adsorption. For the mechanism of physical adsorption, the inhibition efficiency is expected to decrease with increasing temperature but for a chemical adsorption mechanism, the inhibition efficiency increases with increasing temperature (Eddy and Mamza, 2009).

The stability of the inhibitive properties of the studied amino acids over 168 hours of immersion was studied by plotting inhibition efficiencies against time as shown in Fig. 4.3. The plots revealed that after 168 hours of immersion, CYS can retain more than 70 % of its inhibition potentials while the other inhibitors (GLY, LEU and ALA) can retain more than 40 % of their respective inhibition potentials. From the plots, it is also evident that the inhibition efficiency first decreased with time until a critical value was attained after which it started to decrease. These trends suggest that at first, there was competition between the forces of adsorption and desorption and that after the critical zone, adsorption facilitated the formation of a protective layer and thus protected the metal against further corrosion attack.

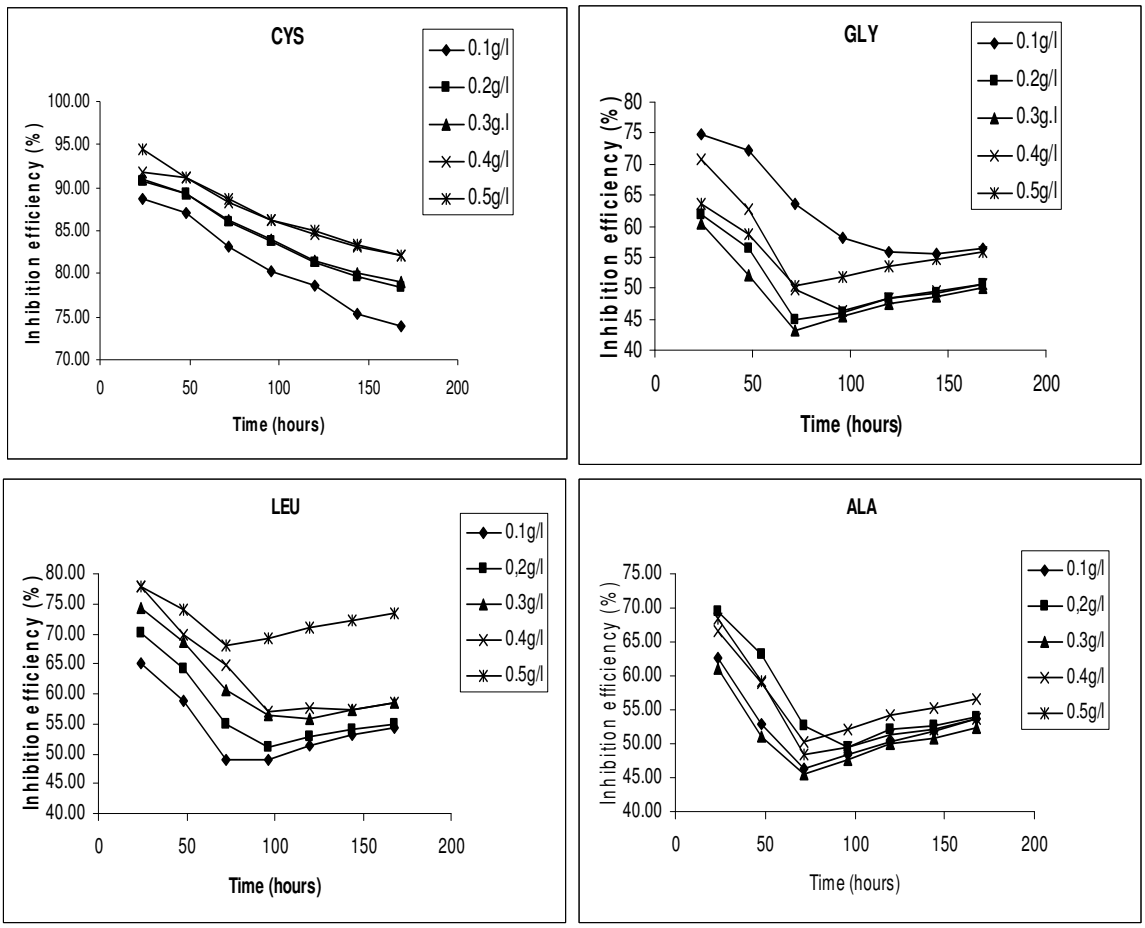


Fig. 4.3: Variation of inhibition efficiency of cysteine (CYS), glycine (GLY), leucine (LEU) and alanine (ALA) with time.

4.1.2 Gasometric and thermometric studies

Table 4.2 also presents inhibition efficiencies obtained from gasometric and thermometric measurements. The results obtained are comparable to those obtained from gravimetric measurements. However, the inhibition efficiencies obtained from the later are relatively higher than those obtained from gravimetric measurements indicating that the instantaneous efficiencies of the amino acids are better than their average inhibition efficiencies.

4.1.3 Kinetic study

The kinetic of mild steel corrosion in the solution of HCl was studied by fitting data obtained from weight loss measurements into different kinetic equations. The test revealed that the corrosion of mild steel in solutions of HCl is consistent with a first order kinetic which can be derived as follows. If the initial concentration of Fe in the mild steel is a_0 and after time, t, x mole of the corrosion product is formed, then the kinetic equation of the reaction can be represented according to the equation 4.6:

$$dx/dt = k_1(a_0 - x) \quad 4.6$$

where k_1 is the first order reaction rate constant. Rearrangement of equation 4.6 yields equation 4.7 and upon integration, equation 4.8 and equation 4.9 are obtained

$$dx/(a_0 - x) = k_1 dt \quad 4.7$$

$$-\ln(a_0 - x) = k_1 t \quad 4.8$$

$$-\log(\text{weight loss}) = k_1 t/2.303 \quad 4.9$$

Also, for a first order reaction, the half life is related to the rate constant as follows

$$t_{1/2} = 0.693/k_1 \quad 4.10$$

The plots of –log(weight loss) versus time were linear and are presented in Fig. 4.4. Values of kinetic parameters deduced from the plots are presented in Table 4.3. From the results obtained, its is evident that the half lives of mild steel in solutions of HCl containing various concentrations of the inhibitors are greater than the half life of mild steel in the blank solution (i.e 0.1 M HCl, without any inhibitor). Therefore, CYS, GLY, LEU and ALA increase the half life of mild steel in HCl solutions.

Table 4.2: Inhibition efficiency (%) of some amino acids in various media by gasometric and thermometric methods.

System	Gasometric				Thermometric			
	CYS	**GLY**	**LEU**	**ALA**	**CYS**	**GLY**	**LEU**	**ALA**
0.1g/l at 303K	82.34	60.23	60.02	61.23	80.21	59.34	61.02	59.08
0.2 g/l at 303 K	84.44	63.21	63.45	64.22	83.45	62.34	63.24	63.43
0.3 g/l at 303 K	87.03	64.34	63.55	66.90	86.32	64.33	66.22	66.39
0.4 g/l at 303 K	90.00	64.44	64.43	67.00	88.94	68.39	69.01	69.87
0.5 g/l at 303 K	93.42	66.22	70.21	69.21	92.01	72.98	70.54	73.21

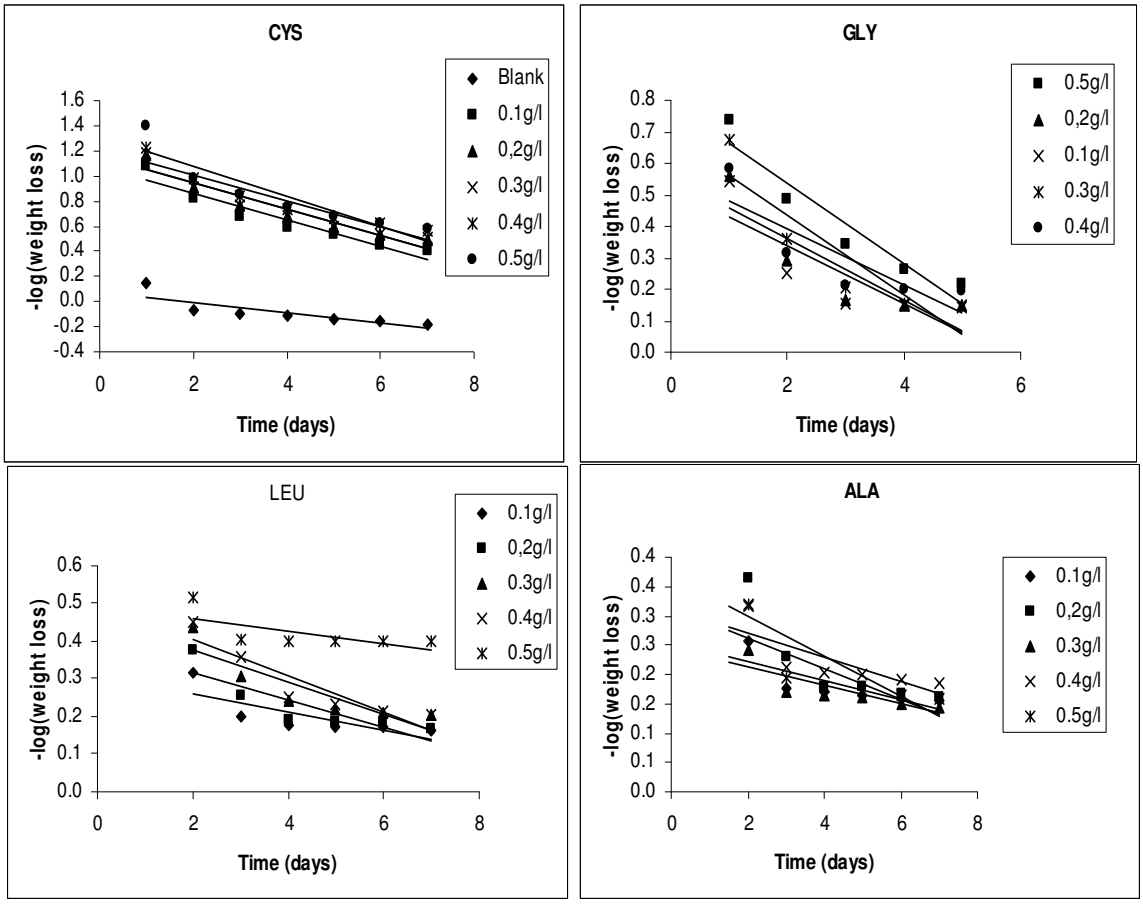


Fig. 4.4: Plots of –log(weight loss) versus time for the corrosion of mild steel in 0.1 M HCl containing various concentrations of the some amino acids

Table 4.3: Kinetic parameters for the corrosion of mild steel in 0.1 M HCl containing various concentrations of the some amino acids.

System	K_1	$t_{1/2}$ (days)	R^2
Blank	0.5571	1	0.7167
0.1g/l CYS	0.2411	3	0.9072
0.2 g/l CYS	0.2439	3	0.9041
0.3 g/l CYS	0.2418	3	0.8954
0.4 g/l CYS	0.2367	3	0.9068
0.5 g/l CYS	0.2773	2	0.8360
0.1g/l GLY	0.2087	3	0.6984
0.2 g/l GLY	0.2218	3	0.7477
0.3 g/l GLY	0.2890	2	0.8059
0.4 g/l GLY	-0.2045	-3	0.7307
0.5 g/l GLY	0.2923	2	0.7902
0.1g/l LEU	0.1331	5	0.6121
0.2 g/l LEU	0.1603	4	0.6930
0.3 g/l LEU	0.1746	4	0.7221
0.4 g/l LEU	0.1951	4	0.7415
0.5 g/l LEU	0.1188	6	0.5516
0.1g/l ALA	0.0368	19	0.6287
0.2 g/l ALA	0.0792	9	0.6934
0.3 g/l ALA	0.0362	19	0.6980
0.4 g/l ALA	0.0474	15	0.6071
0.5 g/l ALA	0.0599	12	0.6334

4.1.5 Effect of temperature

The effect of temperature on the corrosion of mild steel in the absence and presence of various concentrations of the some amino acids was investigated using the Arrhenius equation which can be written as follows (Eddy, 2009b)

$$CR = A\exp(-E_a/RT) \quad 4.11$$

where CR is the corrosion rate of mild steel, A is the Arrhenius or pre-exponential factor, E_a is the activation energy (i.e the minimum energy needed before the corrosion reaction of mild steel can proceed), R is the universal gas constant and T is the temperature of the system. Taking logarithm of equation 4.11, equation 4.12 is obtained,

$$\log CR = \log A - E_a/2.303RT \quad 4.12$$

If the corrosion rates of mild steel at two temperatures T_1(303 K) and T_2 (333 K) are known, (i.e CR_1 and CR_2 respectively), then equation 4.12 can be transformed to equation 4.13:

$$\log(CR_2/CR_1) = E_a/2.303R\,(1/T_1 - 1/T_2) \quad 4.13$$

The activation energies calculated from equation 4.13 are presented in Table 4.4 and are within the range of values expected for physical adsorption mechanism. According to Eddy *et al*., (2010a,b) the mechanism of physical adsorptionis favoured, if values of $E_a$is less than 80 $kJmol^{-1}$ as distinct from the mechanism of chemical adsorption where E_a values are expected to be greater than 80 $kJmol^{-1}$. Therefore the adsorption of some amino acids on mild steel surface is consistent with the mechanism of charge transfer from the inhibitors' molecule to the metal surface, which represents physiosorption.

Table 4.4: Thermodynamic parameters for the adsorption of various concentrations of the some amino acids on mild steel surface.

System	E_a (kJmol^{-1})	Q_{ads} (kJmol^{-1})
Blank	49.66	**-**
0.1g/l CYS	53.94	-4.50
0.2 g/l CYS	53.54	-5.38
0.3 g/l CYS	55.85	-4.64
0.4 g/l CYS	57.64	-8.69
0.5 g/l CYS	58.99	-7.80
0.1g/l GLY	55.85	-23.84
0.2 g/l GLY	57.64	-17.33
0.3 g/l GLY	58.66	-14.09
0.4 g/l GLY	59.64	-14.47
0.5 g/l GLY	60.90	-8.66
0.1g/l LEU	55.10	-26.44
0.2 g/l LEU	57.29	-11.21
0.3 g/l LEU	57.64	-8.77
0.4 g/l LEU	60.90	-5.61
0.5 g/l LEU	61.51	-16.14
0.1g/l ALA	54.72	-19.40
0.2 g/l ALA	55.85	-14.37
0.3 g/l ALA	57.29	-9.88
0.4 g/l ALA	58.32	-11.85
0.5 g/l ALA	60.59	-7.96

4.1.5 Thermodynamics/adsorption study

The heat of adsorption of the inhibitors was calculated using equation 4.14 (Eddy, 2009a,b),

$$Q_{ads} = 2.303R\left[\log\left(\frac{\theta_2}{1-\theta_2}\right) - \log\left(\frac{\theta_1}{1-\theta_1}\right)\right] x\left(\frac{T_{1X}T_2}{T_2 - T_1}\right) kJmol^{-1} \qquad 4.14$$

Values of Q_{ads} calculated from equation 4.14 are also presented in Table 4.4. The values are negative, indicating that the adsorption of the amino acids studied on mild steel surface is exothermic. It should also be noted that since the corrosion reactions were carried out at constant pressure, calculated values of Q_{ads} are expected to be approximately equal to the enthalpies of adsorption.

The adsorption characteristics of the amino acids were investigated by fitting data obtained for the degrees of surface coverage (from weight loss experiments) into different adsorption isotherms. The results obtained reveal that the adsorption of the amino acids on mild steel surface is best described by Langmuir adsorption isotherm. According to Langmuir adsorption model, the degree of surface coverage is related to the concentration of the inhibitor in the bulk electrolyte according to equation 4.15 (Eddy and Odoemelam, 2009).

$$\theta = k_{ads}C/(1+ k_{ads}C) \qquad 4.15$$

where θ is the degree of surface coverage of the inhibitor, C is the concentration of the inhibitor in the bulk electrolyte and k_{ads} is the adsorption equilibrium constant. Simplification of equation 4.15 yields equations 4.16 and 4.17.

$$k_{ads}C = \theta(1 + k_{ads}C) \qquad 4.16$$

$$C/\theta = 1/k_{ads} + C \qquad 4.17$$

Also, from the logarithm of equation 4.17, equation 4.18 is obtained

$$\log(C/\theta) = \log C - \log k_{ads} \quad 4.18$$

From equation 4.18, a plot of log(C/θ) versus logC should be linear provided the assumption establishing the Langmuir model is valid. Fig. 4.5 shows Langmuir isotherms for the adsorption of the some amino acids on mild steel surface. Values of adsorption parameters deduced from the plots are presented in Table 4.5. The results obtained show that the slopes and R^2 values for the isotherms are very close to unity, suggesting the application of the Langmuir isotherm to the adsorption of the amino acids (Eddy and Ebenso, 2010b). According to EddyOdoemelam (2009), the essential features of the Langmuir adsorption isotherm can be expressed in terms of dimensionless constant called separation factor or equilibrium parameter (K_L) which can be expressed according to the equation 4.19:

$$K_L = 1/(1 + K_{ads}C_0) \quad 4.19$$

where C_0 is the initial concentration of the adsorbate. The significance of equation 4.19 is that when $K_L > 1$, the adsorption is unfavourable; when $0 < K_L < 1$, the adsorption is favourable and when $K_L = 0$, the adsorption is irreversible. Values of K_L obtained in this study were within the range of 0 and unity showing that the adsorption of the inhibitors on the surface of mild steel is favourable.

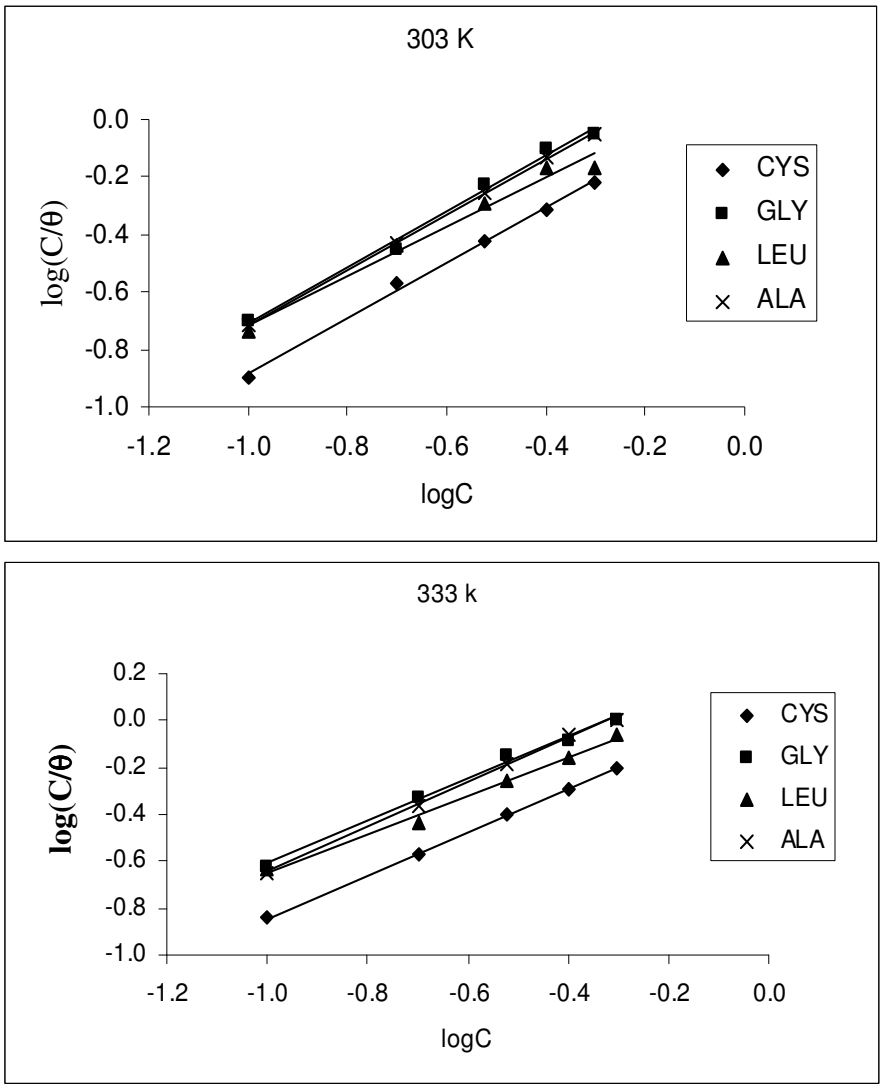


Fig. 4.5: Langmuir isotherm for the adsorption of some amino acids on mild steel surface at 303 and 333 K

Table 4.5: Langmuir parameters for the adsorption of some amino acids on mild steel surface at 303 and 333 K

T (K)		Slope	$logk_{ads}$	R^2	ΔG^0_{ads} (kJmol^{-1})
303 K	**CYS**	0.9585	0.0778	0.9968	-1.51
	GLY	0.9070	0.2612	0.9917	-1.75
	LEU	0.8523	0.1389	0.9793	-1.59
	ALA	0.9614	0.2448	0.9994	-1.73
333 K	**CYS**	0.9183	0.00739	0.9997	-1.55
	GLY	0.8937	0.2868	0.9938	-1.96
	LEU	0.8213	0.1695	0.9929	-1.79
	ALA	0.9475	0.3031	0.9999	-1.98

It is also significant to note that the value of the adsorption equilibrium constant (obtained from the intercept of the Langmuir adsorption isotherm) is related to the free energy of adsorption according to equation 4.20:

$$\Delta G^{0}_{ads} = -2.303RT\log(55.5K_{ads}) \quad 4.20$$

The free energies of adsorption calculated from equation 4.20 are also presented in Table 4.5. From the results obtained, the free energies are negatively less than the threshold value of-40 $kJmol^{-1}$, required if the mechanism is chemical adsorption. Therefore, the adsorption of the amino acids studied on mild steel surface is spontaneous and is consistent with the mechanism of physical adsorption (Eddy *et al*., 2009e).

4.1.6 IR study

IR analysis was carried out onthe corrosion product (in the absence and presence of the inhibitor) and the inhibitors. Fig. 4.6 shows the IR spectrum of the corrosion product from the corrosion of mild steel. From the spectrum, it can be seen that the corrosion product without the inhibitor is not IR active. Therefore there was no adsorption.

Fig. 4.7 shows the IR spectrum of CYS while Fig. 4.8 shows the IR spectrum of the corrosion product from the corrosion of mild steel when 0.5 g/l of CYS was used as an inhibitor. Frequencies and peaks of IR adsorption are presented in Table 4.6. From the results obtained, it is evident that in CYS, the N-H wag at 779.27, 846.78 and 873.78 cm^{-1} were shifted to 868.00 cm^{-1}, C-N stretch at 1194.94 cm^{-1}

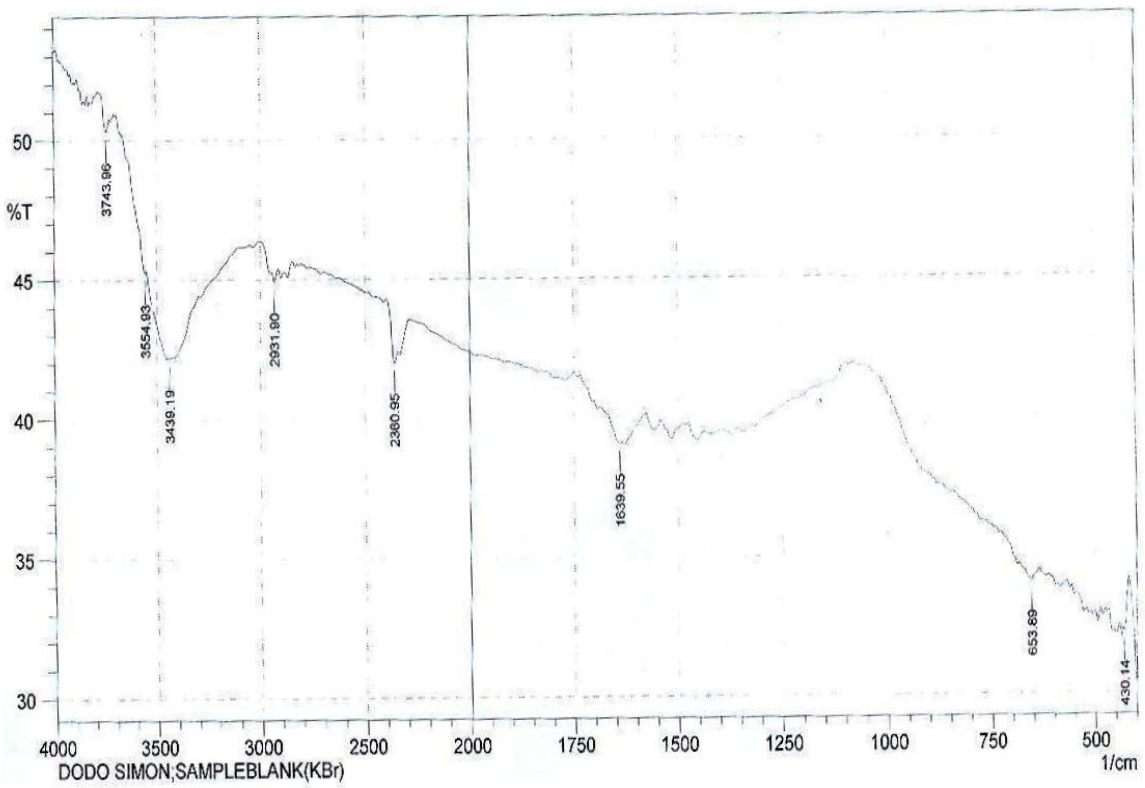


Fig. 4.6: FTIR spectrum of the corrosion product from the corrosion of mild steel in 0.1 M HCl

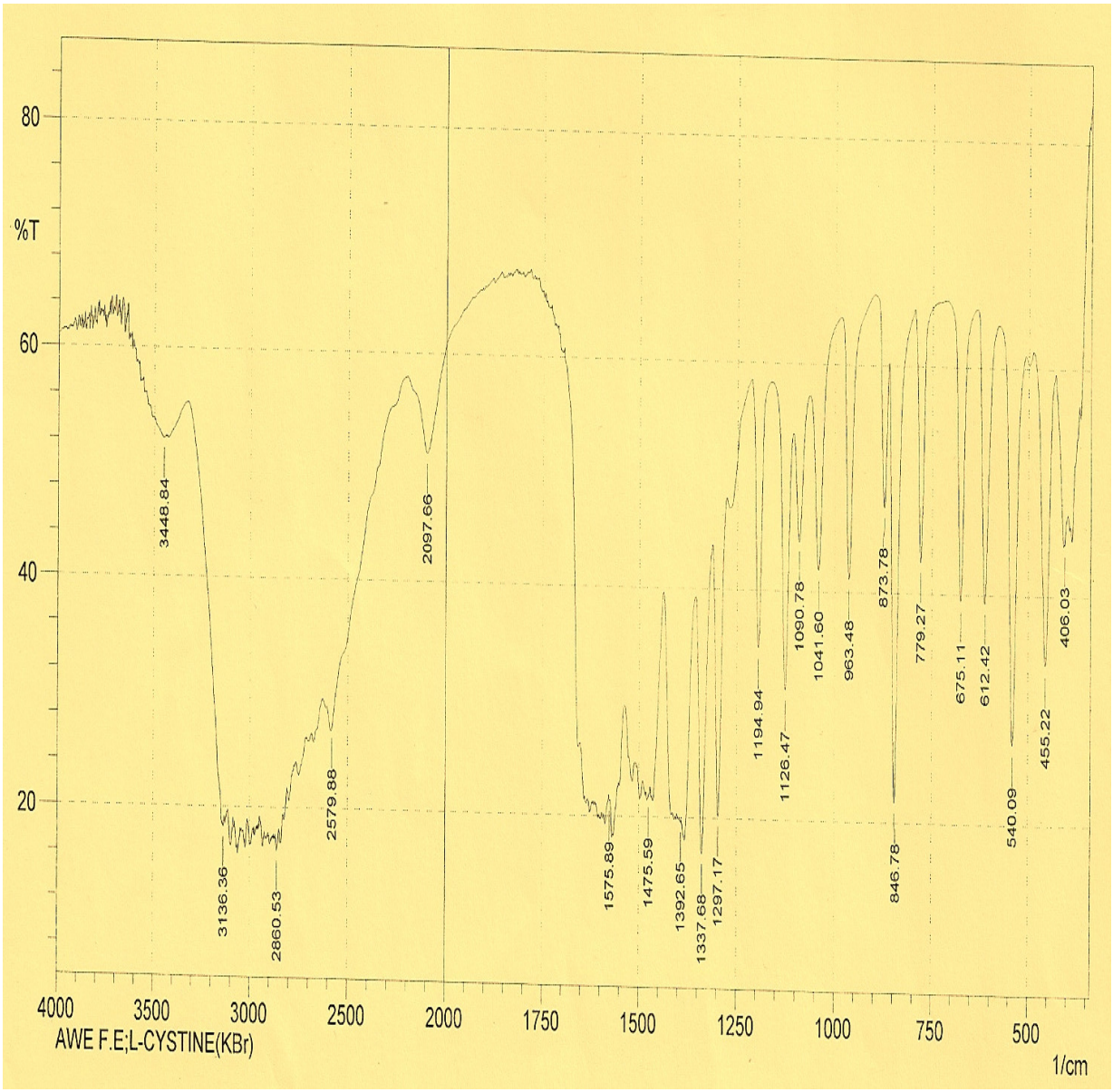


Fig. 4.7: IR spectrum of CYS

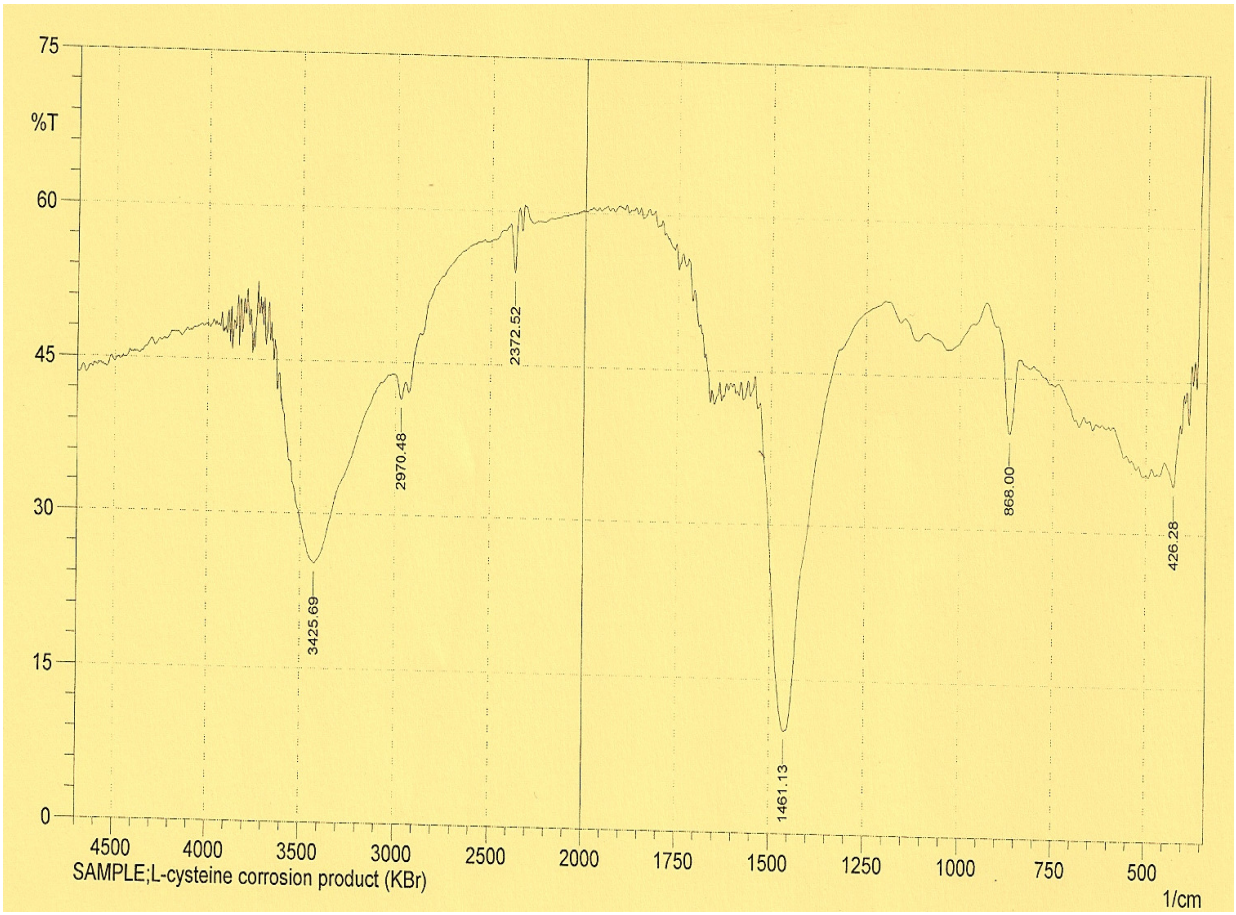


Fig. 4.8: IR spectrum of the corrosion product from the corrosion of mild steel when 0.5 g/l of CYS was used as an inhibitor

Table 4.6: Frequencies and peaks of IR adsorption by CYS and the corrosion product from the corrosion of mild steel (containing CYS)

Data for corrosion product when CYS is used as an inhibitor					
Peak	**Intensity**	**Base (H)**	**Base(L)**	**Area**	**Assignments**
868.00	39.55	901.75	840.03	21.64	N-H wag
1461.13	10.00	1528.64	1320.32	122.29	C-H bend
2372.52	53.97	2398.56	2352.27	11.28	C-N stretch
2970.48	41.45	3006.16	2947.33	21.77	O-H stretch
3425.69	25.19	3551.07	3114.18	217.37	O-H stretch
Data for CYS sample					
Peak	**Intensity**	**Base (H)**	**Base(L)**	**Area**	**Inferences**
779.27	42.79	796.63	730.08	15.06	N-H wag
846.78	21.78	862.21	796.63	20.52	N-H wag
873 .78	47.59	899.82	862.21	8.87	N-H wag
963.48	41.15	985.66	899.82	19.55	=C-H stretch
1041.60	41.88	1065.71	985.66	2.18	C-N stretch
1090.78	44.45	1107.18	1065.71	12.08	C-O stretch
1126.47	31.32	1163.11	1107.18	17.98	C-N stretch
1194.94	34.92	1213.27	1163.11	15.06	C-N stretch
1297.17	20.18	1312.60	1276.92	17.12	C-O stretch
1337.68	16.84	1355.04	1312.60	22.46	N-O stretch
1392.65	19.64	1395.54	1390.72	3.39	N-O stretch
1475.59	21.72	1476.56	1470.77	3.80	N-O asymmetric stretch
1575.89	21.29	1577.82	1574.93	1.93	N-H bend
2579.88	27.01	2581.51	2522.98	30.10	O-H stretch
3136.36	18.22	3140.22	3134.43	4.24	O-H stretch
3448.84	52.11	3459.45	3437.27	6.26	O-H stretch

was shifted to 2372.52 cm^{-1}, the O-H stretch at 2579.88 and 3136.36 cm^{-1} were shifted to 2970.48 cm^{-1} while the O-H stretch at 3448.84 cm^{-1} was shifted to 3425.69 cm^{-1} indicating that there is an interaction between the CYS and the mild steel surface. On the other hand, the C-N stretch at 1041.60 and 1126.47 and 1194.94 as well as the N-O asymmetric stretch at 1475.59 cm^{-1} were missing in the spectrum of the corrosion product indicating that these bonds might have been used for adsorption.

Figs. 4.9 and 4.10 respectively show the FTIR spectra of GLY and that of the corrosion product from mild steel corrosion when GLY was used as an inhibitor. Peak and frequencies of IR adsorption for both spectra are presented in Table 4.7. From the results obtained, it is also evident that the C-O stretch at 1042.56 cm^{-1} was shifted to 1028.09 cm^{-1}, the –C=C- stretch at 1674.27 cm^{-1} was shifted to 1656.91 cm^{-1}, the O-H stretch at 2906.82 cm^{-1} was shifted to 2924.18 cm^{-1} while the O-H stretch (H-bonded) was shifted from 3201.94 to 3430.51 cm^{-1}. These shifts in frequencies also indicate that there is an interaction between the inhibitor and the metal surface. It is also evident from the data obtained that the C-N stretch (at 1125.50 and 1247.99 cm^{-1}), the C-O stretch (at 1042.56 and 1730.21 cm^{-1}), the N-O symmetric stretch (at 1338.64 cm^{-1}) as well as N-H bend at 1590.36 cm^{-1} were missing in the spectrum of the corrosion product, suggesting that these bonds might have been used for adsorption of GLY on mild steel surface.

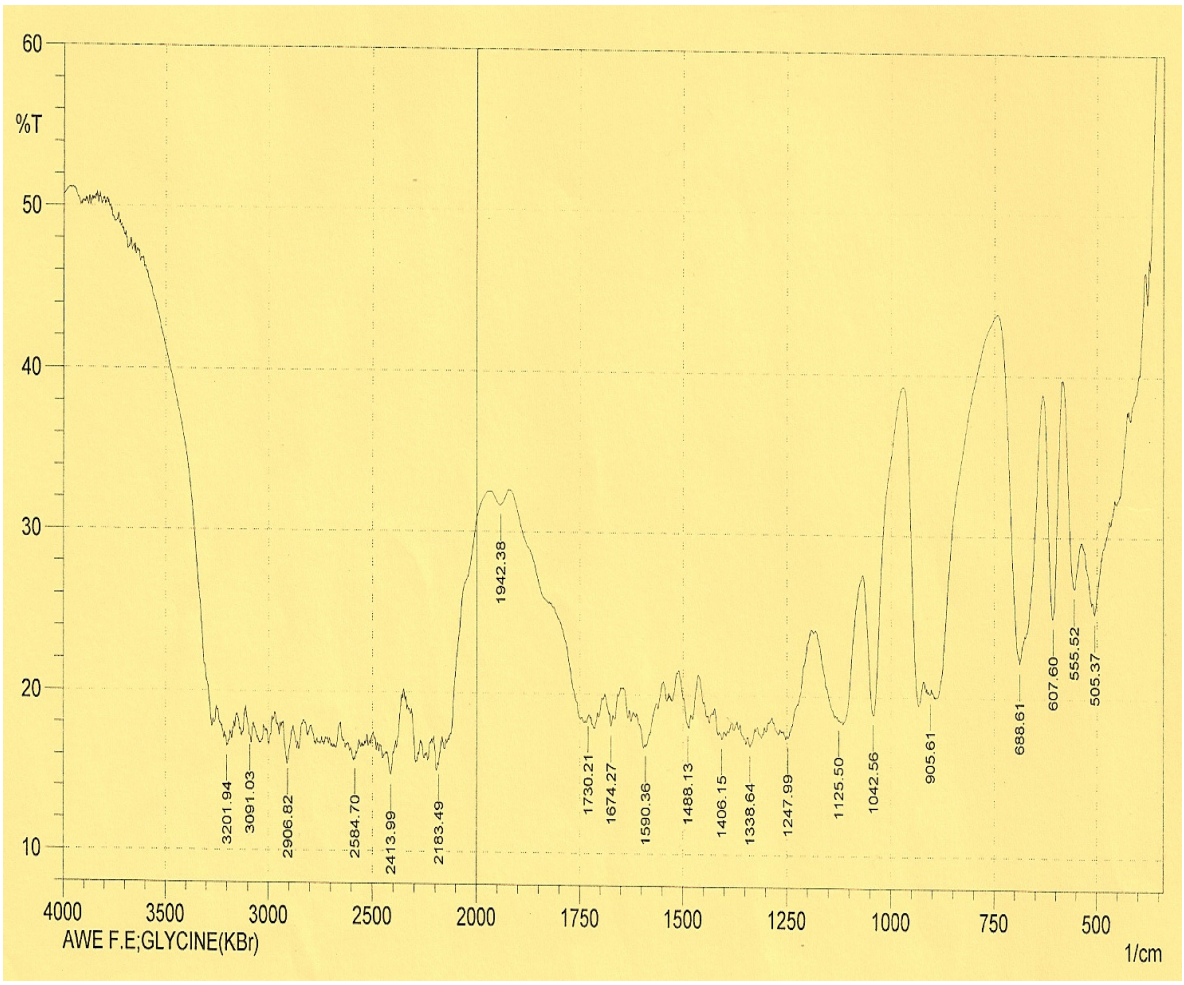


Fig. 4.9: IR spectrum of GLY

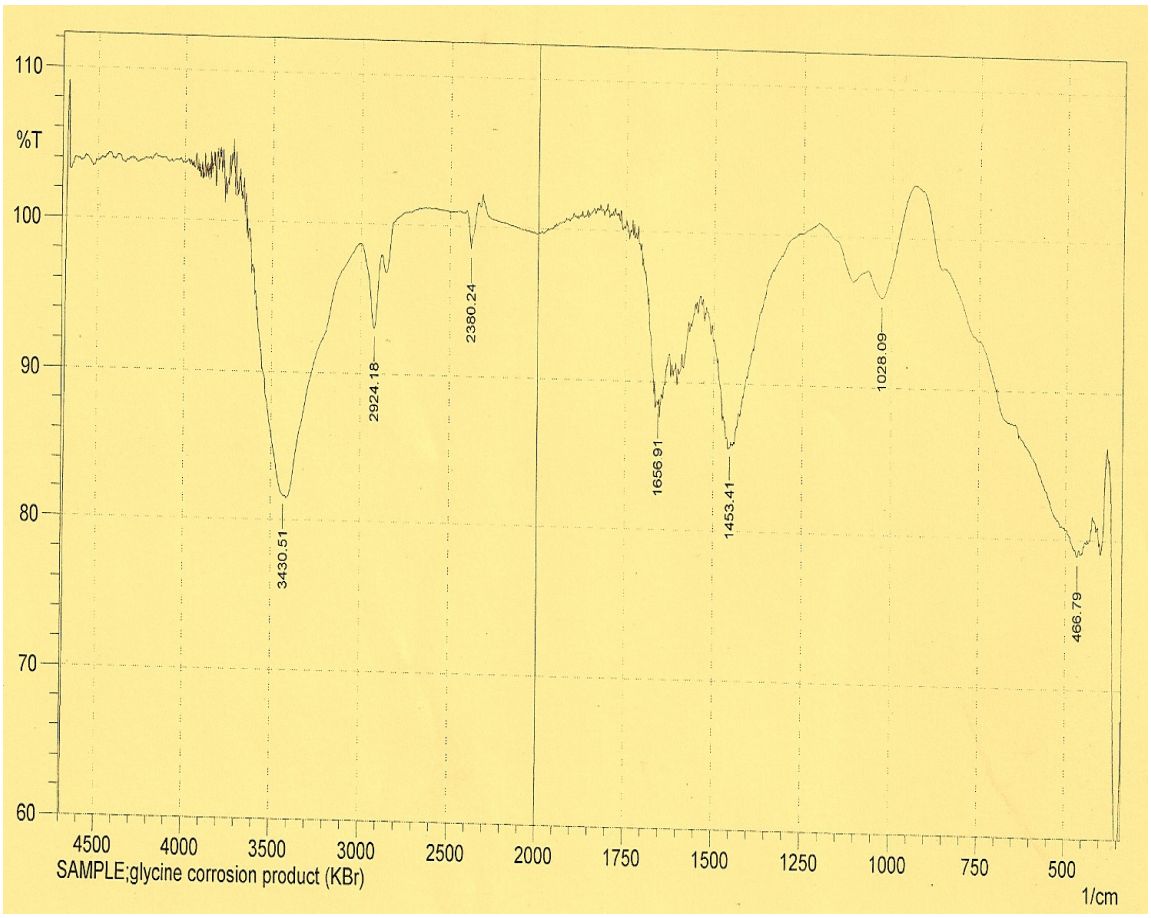


Fig. 4.10: IR spectrum of the corrosion product of mild steel when 0.5 g/l of GLY was used as an inhibitor

Table 4.7: Frequencies and peaks of IR adsorption by GLY and the corrosion product of mild steel (containing GLY)

Data for the corrosion product when GLY was used as an inhibitor					
Peak	**Intensity**	**Base (H)**	**Base (L)**	**Area**	**Assignments**
1028.09	95.959	1067.64	936.47	0.674	C-O stretch
1656.91	88.46	1659.8	1654.98	0.253	-C=C- stretch
2924.18	93.046	2997.28	2882.71	1.991	O-H stretch
3430.51	81.626	3519.24	3428.58	6.925	O-H stretch, H-bonded
Data for GLY sample					
Peak	**Intensity**	**Base(H)**	**BaseE(L)**	**Area**	**Assignments**
688.61	22.13	742.62	681.86	30.3	=C-H stretch
905.61	20.23	906.57	902.72	2.67	=C-H bend
1042.56	18.85	1067.64	972.16	51.92	C-O stretch
1125.50	18.49	1129.36	1124.54	3.52	C-N stretch
1247.99	17.35	1249.91	1243.16	5.12	C-N stretch
1338.64	16.79	1343.46	1336.71	5.2	N-O symmetric stretch
1590.36	16.73	1593.25	1589.4	2.99	N-H bend
1674.27	17.97	1678.13	1670.41	5.68	-C=C- stretch
1730.21	18.55	1731.17	1728.28	2.11	C=O stretch
2584.70	15.73	2587.59	2583.73	3.09	O-H stretch
2906.82	15.7	2907.79	2894.28	10.65	O-H stretch
3091.03	17.19	3098.75	3089.1	7.32	=C-H stretch
3201.94	16.5	3209.66	3200.98	6.7	O-H stretch, H bonded

Figures 4.11 and 4.12 respectively show the FTIR spectra of LEU sample and that of the corrosion product from mild steel corrosion when LEU was used as an inhibitor. Peaks and frequencies of adsorption, from the spectra are presented in Table 4.8. From the results obtained, it can be seen that theN-H wag at 669.32 and 770.59 cm^{-1} was shifted to 675.11 cm^{-1}, C-H bend at 842.92 was shifted to 867.03 cm^{-1}, the C-N stretches at 1084.03 and 1135.50 were shifted to 1032.92 and 114.89 cm^{-1} respectively, the O-H stretch at 2888.50 was shifted to 2927.08 cm^{-1} while the N-H stretch at 3125.75 cm^{-1} was shifted to 3437.26. These shifts in frequencies also confirm that there is an interaction due to the adsorption of LEU on mild steel surface. Also, the absence of C-N stretch, N-O asymmetric and symmetric stretches in the spectrum of the corrosion product suggests that some of these bonds were used for the adsorption of the inhibitor onto mild steel surface.

The FTIR spectra of ALA and that of the mild steel corrosion product when ALA was used as an inhibitor are presented in Figs. 4.13 and 4.14. The peaks and frequencies of IR adsorption, from the spectra are presented in Table 4.9. From the results obtained, it is evident that =C-H bend at 649.07 cm^{-1} was shifted to 673.18 cm^{-1}, the C-O stretch at 1017.48 cm^{-1} was shifted to 1030.02 cm^{-1}, the N-H bend at 1614.47 cm^{-1} was shifted to 1652.09 cm^{-1}, theO-H stretch at 2834.49 cm^{-1} and 3200.98 cm^{-1} were shifted to 2925.15 cm^{-1} and 3428.58 cm^{-1} respectively. In addition, C-H bend at 1448.59 cm^{-1} appeared in the spectrum of the corrosion product. The shifts in frequencies and the formation of a new bond indicate that there is an interaction between the mild steel surface and the inhibitor (i.e ALA). On the other hand, C-N stretches at 1113.93 cm^{-1} and at 1236.41 cm^{-1}, N-O symmetric and asymmetric stretches (at1301.03 cm^{-1} and 1515.14 cm^{-1}

respectively), C-H rock at 1365.65 cm^{-1} and O-H stretch at 2522.98 cm^{-1} were missing in the spectrum of the corrosion product of mild steel, indicating that some of these bonds might have been used for the adsorption of ALA onto mild steel surface.

4.2 Quantum Chemical Study

In this sub-section, semi-empirical and ab-initio studies are discussed. The semi-empirical parameters are used in the correlation of experimental and theoretical data while the ab-initio parameters are used in the projection of the sites for nucleophilic and electrophilic attacks.

4.2.1 Semi-empirical study

Table 4.10 presents values (obtained from gas phase calculations) for the frontier molecular orbital energies (i,e energies of the highest occupied molecular orbital, E_{HOMO} and that of the lowest unoccupied molecular orbital, E_{LUMO}), the energy gap, ΔE (i.e $E_{LUMO} - E_{HOMO}$), the electronic energy of the molecule (EE), the core core repulsion energy (CCR), the cosmo area (cosAr), the cosmo volume (cosVol), the dipole moment (μ) and the heat of formation (H_f). Table 4.11 presents similar parameters for the aqueous phase calculations.

According to the frontier molecular orbital theory, the formation of a transition state is due to an interaction between the frontier orbitals (HOMO and LUMO) of reacting species (Eddy and Ita, 2010a,b; Tanak and Yavuz, 2010). Therefore, the frontier molecular orbitals play significant roles in defining the reactivity of organic compounds. The energy of the highest occupied molecular orbital (E_{HOMO}) is related to the electron donating ability of the compound.

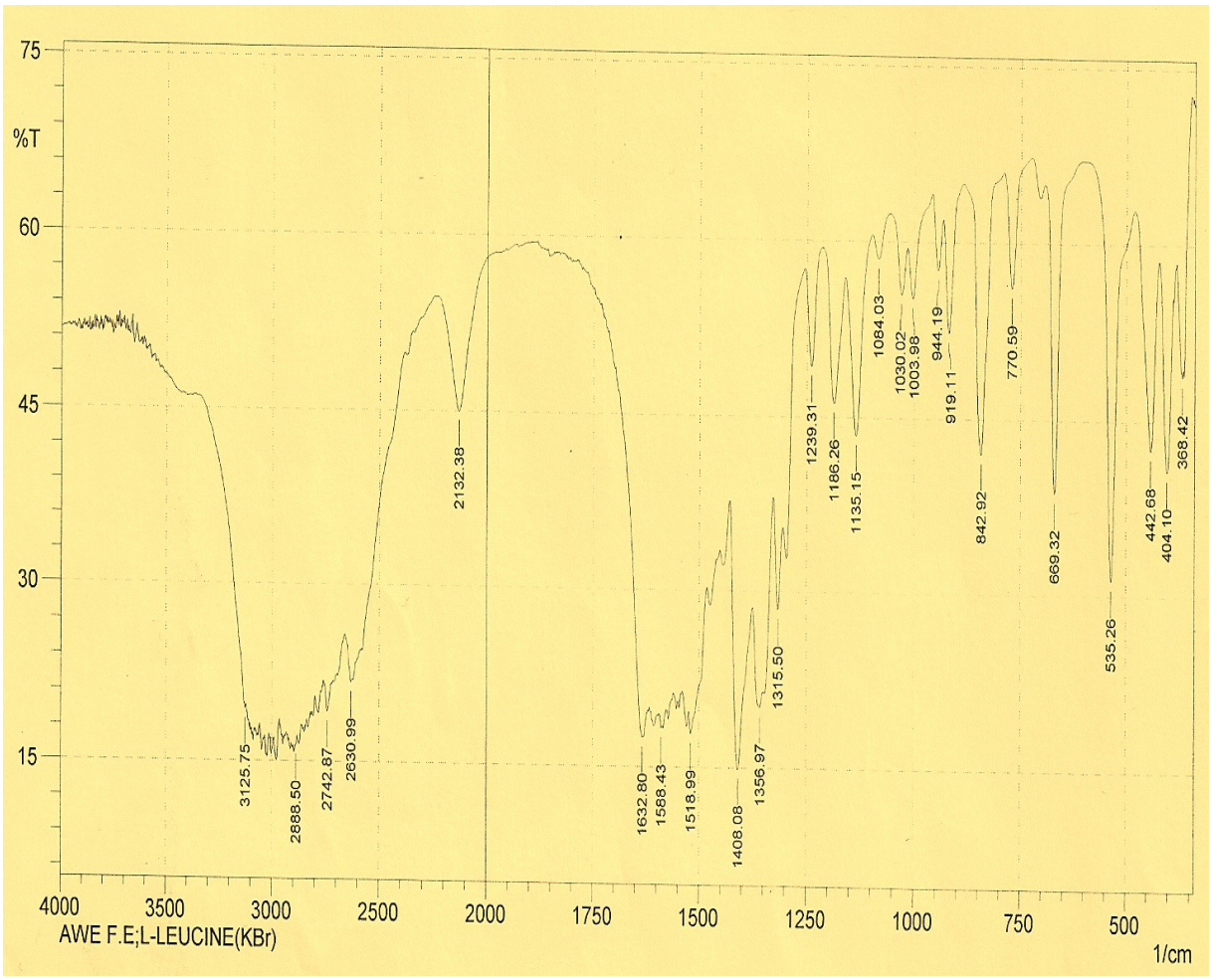


Fig. 4.11: IR spectrum of LEU

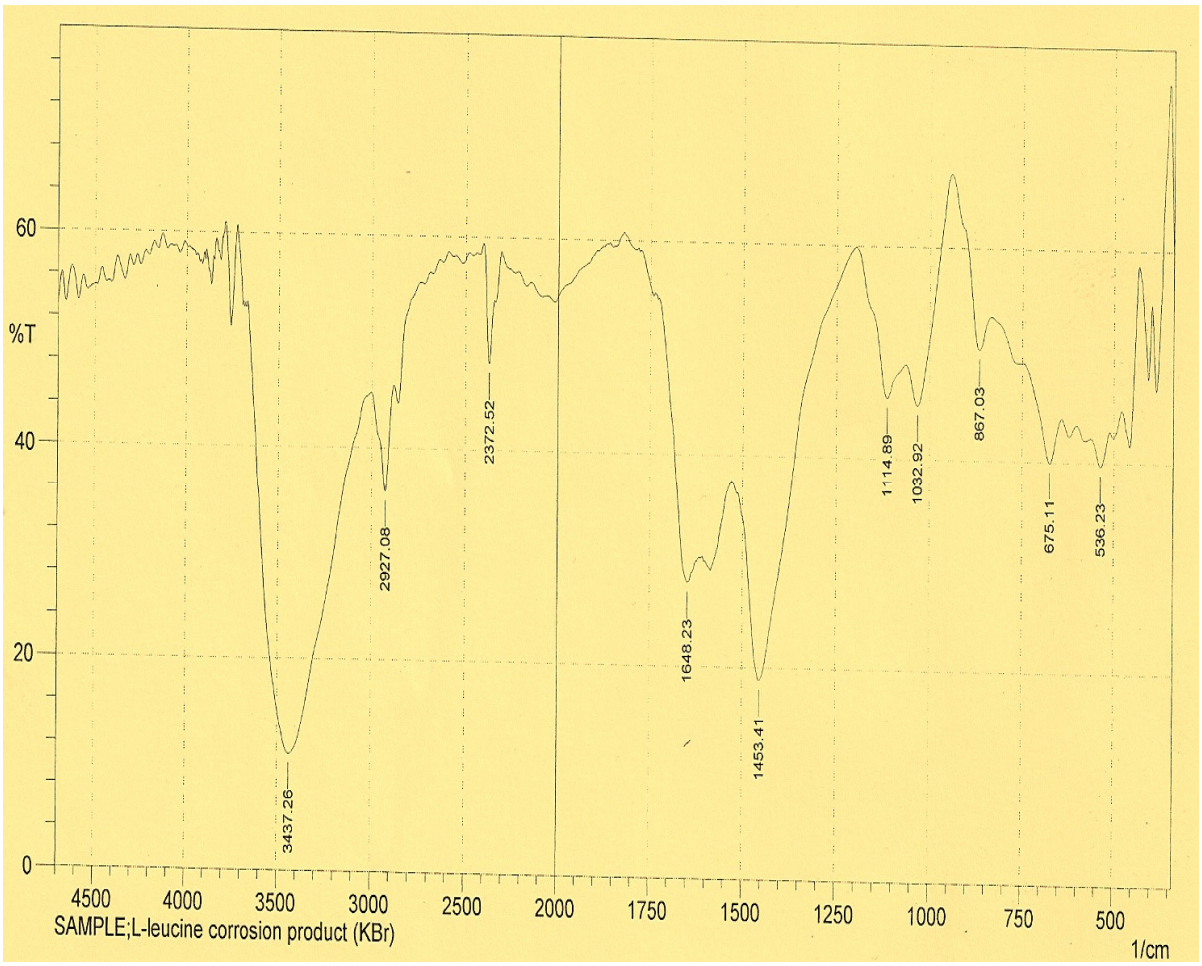


Fig. 4.12: IR spectrum of the corrosion product of mild steel when 0.5 g/l of LEU was used as an inhibitor

Table 4.8: Frequencies and peaks of IR adsorption by LEU and the corrosion product of mild steel (containing LEU)

Data for the corrosion product when LEU was used as an inhibitor					
Peak	**Intensity**	**Base (H)**	**Base (L)**	**Area**	**Assignments**
675.11	39.918	748.41	642.32	37.56	N-H wag
867.03	50.476	943.32	823.32	26.89	C-H bend
1032.92	45.122	1064.74	943.22	33.74	C-N stretch
1114.89	45.776	1198.8	1064.74	38.97	C-N stretch
1453.41	18.811	1413.21	1198.8	131.72	C-H bend
1648.23	27.873	1727.31	1616.4	4 8.37	N-H bend
2927.08	35.85	3004.23	2882.71	46.90	O-H stretch
3437.26	11.014	3667.77	3004.23	401.89	N-H stretch
		Data for LEU sample			
Peak	**Intensity**	**Base (H)**	**Base (L)**	**Area**	**Assignments**
669.32	38.78	693.43	605.67	19.93	N-H wag
770.59	56.13	790.84	724.29	13.07	N-H wag
842. 92	42.05	886.32	790.84	22.48	C-H bend
919.11	52.31	932.61	886.32	10.43	O-H bend
944.19	57.61	958.65	932.61	5.73	=C-H bend
1003.98	55.16	1017.48	958.65	12.99	=C-H bend
1030.02	55.52	1057.03	117…48	9.04	=C-H bend
1084.03	58.50	1098.5	1057.03	9.08	C-N stretch
1135.15	43.47	1160.22	1098.5	17.39	C-N stretch
1186.26	46.22	1214.23	1160.22	15.06	C-N stretch
1239.31	49.33	1254.74	1214.23	10.61	C-N stretch
1315.5	28.47	1327.07	1304.89	10.83	N-O symmetric stretch
1356.97	20.20	1358.90	1359.18	5.281	C-H rock
1518.99	17.86	1523.82	1513.21	7.75	N-O asymmetric stretch
1588.43	18.29	1591.33	1585.54	4.225	N-H bend
1632.8	17.50	1698.38	1631.83	31.66	N-H bend
2630.99	21.75	2660.89	2627.13	21.06	O-H stretch
2742.87	19.24	2753.48	2726.47	18.73	O-H stretch
2888.50	16.37	2889.46	2880.78	6.75	O-H stretch
3125.75	19.41	3129.61	312 2.86	4.77	N-H stretch

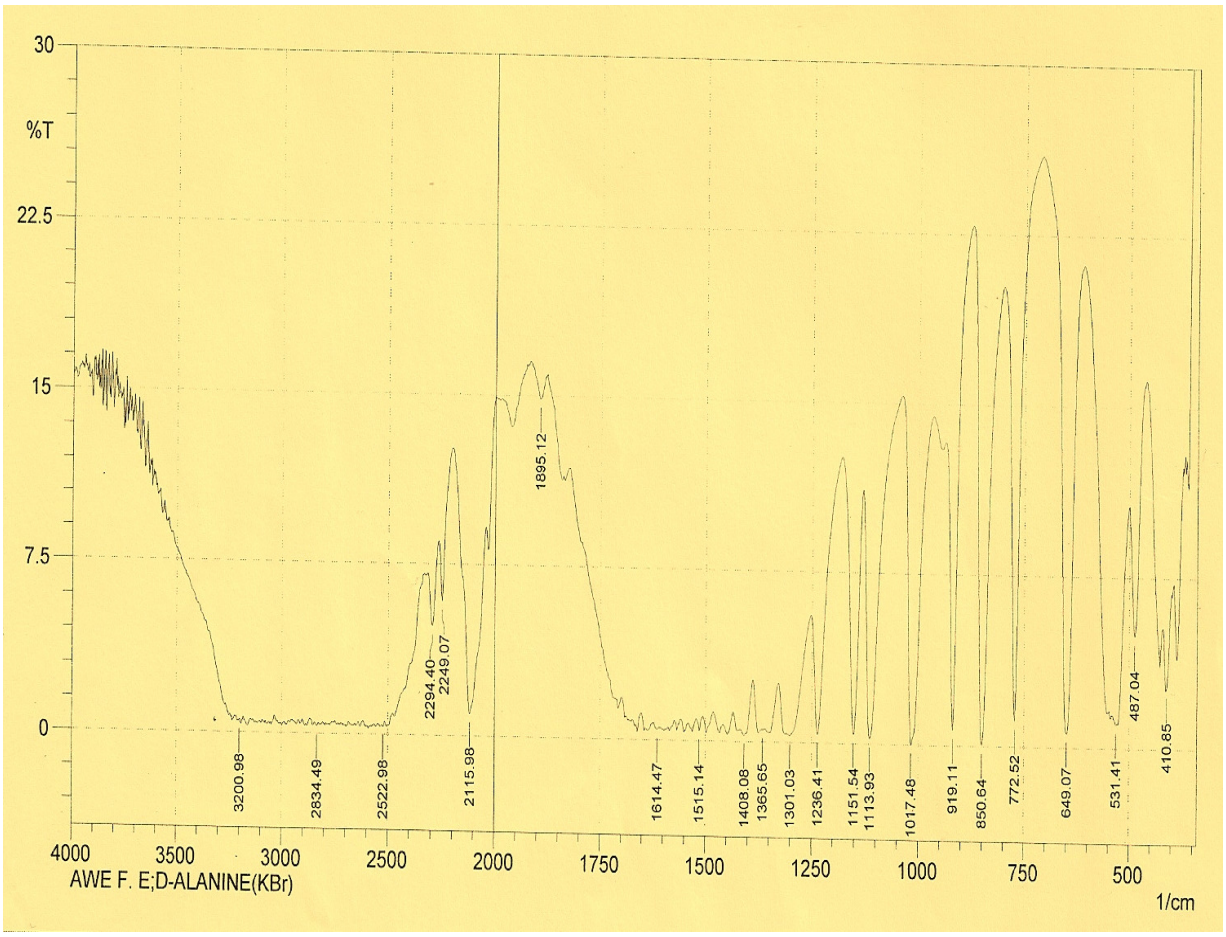


Fig. 4.13: IR spectrum of ALA

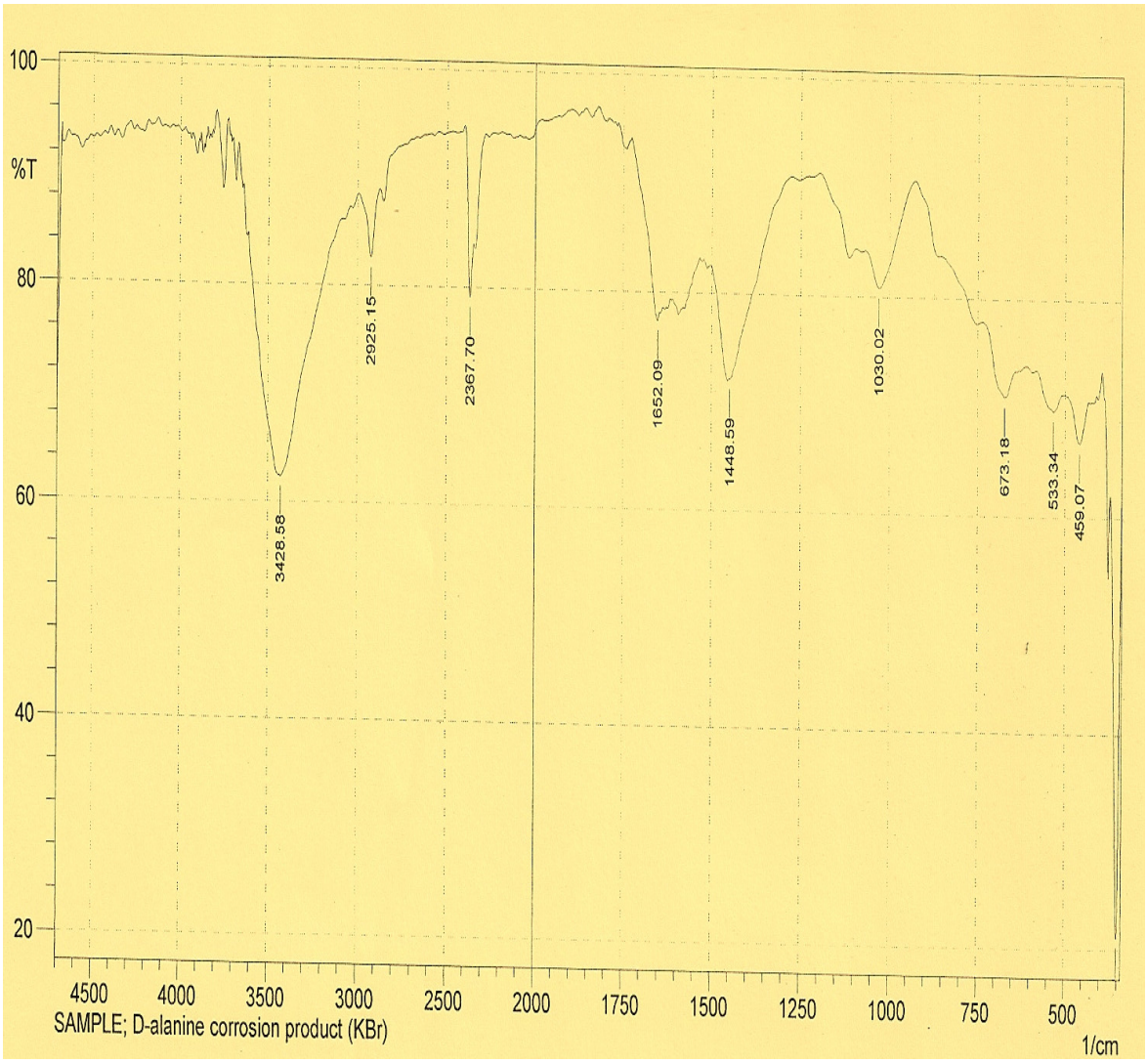


Fig. 4.14: IR spectrum of the corrosion product of mild steel when 0.5 g/l of ALA was used as an inhibitor

Table 4.9: Frequencies and peaks of IR adsorption by ALA and the corrosion product of mild steel (containing ALA)

Data for the corrosion product when ALA was used as an inhibitor					
Peak	**Intensity**	**Base (H)**	**Base (L)**	**Area**	**Assignments**
673.18	71.004	735.87	640.39	12.706	=C-H bend
1030.02	80.856	1069.56	929.72	9.93	C-O stretch
1448.59	72.154	1449.55	1275.95	14.448	C-H bend
1652.09	77.383	1728.28	1647.26	5.374	N-H bend
2925.15	82.628	2995.55	2876.92	7.548	O-H stretch
3428.58	62.352	3613.76	3086.21	71.331	O-H stretch, H-bonded
Data for ALA sample					
Peak	**Intensity**	**Base (H)**	**Base (L)**	**Area**	**Assignments**
649.07	0.63	711.76	611.45	92.69	=C-H bend
772.52	10.38	802.41	711.76	75.66	N-H wag
919.11	0.69	967.44	876.68	59.55	=C-H bend
1017.48	0.00	1039.67	967.33	97.82	C-O stretch
1113.93	0.24	1131.29	1040.63	109.06	C-N stretch
1236.41	0.38	1252.81	1180.47	94.21	C-N stretch
1301.03	0.28	1306.82	1298.14	21.56	N-O symmetric stretch
1365.65	0.53	1366.61	1358.90	17.43	C-H rock
1515.14	0.42	1521.89	1505.49	3 4.55	N-O asymmetric stretch
1614.47	0.46	1623.15	1609.65	30.53	N-H bend
2522.98	0.33	2526.83	2515.26	27.78	O-H stretch
2834.49	0.30	2843.17	2826.77	39.72	O-H stretch
3200.98	0.50	3201.94	3198.08	8.76	O-H stretch, H-bonded

Table 4.10: Gas phase quantum chemical parameters for some amino acids studied

	Models	E_{HOMO} (eV)	E_{LUMO} (eV)	ΔE (eV)	EE (eV)	CCR (eV)	CosAr (Å^2)	CosVol (Å^3)	μ (Debye)	H_f (eV)
CYS	PM6	-9.04	-0.10	8.94	-5537.62	4138.34	145.39	138.19	2.94	-3.01
	PM3	-8.98	-0.38	8.60	-5532.39	4133.75	145.39	138.19	3.04	-2.70
	AMI	-9.00	-0.02	8.98	-5708.11	4185.54	145.39	138.19	2.92	-3.02
	RMI	-9.32	0.17	9.50	-5706.71	4200.68	145.39	138.19	2.80	-3.16
	MNDO	-9.73	0.82	10.56	-5762.20	4199.46	145.39	138.19	2.72	-2.59
GLY	PM6	-8.92	0.46	9.38	-3422.63	2347.23	104.80	87.50	1.92	-3.37
	PM3	-8.64	1.05	9.69	-3428.71	2365.03	104.80	87.50	1.54	-3.38
	AMI	-9.32	1.23	10.55	-3557.46	2384.41	104.80	87.50	1.44	-3.65
	RMI	-9.23	1.17	10.4	-3550.36	2385.79	104.80	87.50	1.41	-3.68
	MNDO	-9.74	1.03	10.77	-3568.98	2390.56	104.80	87.50	1.28	-3.40
LEU	PM6	-8.88	0.53	9.41	-8307.24	6632.53	131.17	175.09	2.23	-4.18
	PM3	-8.64	1.09	9.73	-8229.87	6568.23	131.17	175.09	1.69	-4.11
	AMI	-9.24	1.30	10.54	-8408.40	6612.46	131.17	175.09	1.62	-4.38
	RMI	-9.19	1.24	10.43	-8434.65	6654.43	131.17	175.09	1.63	-4.45
	MNDO	-9.65	1.08	10.73	-8428.55	6625.27	131.17	175.09	1.42	-3.29
ALA	PM6	-9.97	0.49	10.46	-4537.73	3312.39	121.96	109.30	2.02	-3.69
	PM3	-8.68	1.07	9.75	-4525.53	3312.33	121.96	109.30	1.61	-3.59
	AMI	-9.31	1.27	10.58	-4667.48	3338.75	121.96	109.30	1.52	-3.79
	RMI	-9.27	1.21	10.48	-4667.34	3348.73	121.96	109.30	1.51	-4.00
	MNDO	-9.67	1.06	10.73	-4681.14	3346.46	121.96	109.30	1.37	-3.42

Table 4.11: Aqueous phase quantum chemical parameters for some amino acids

	Models	E_{HOMO} (eV)	E_{LUMO} (eV)	ΔE (eV)	EE (eV)	CCR (eV)	CosAr ($Å^2$)	CosVol ($Å^3$)	μ (Debye)	H_f (eV)	E_{dielec} (eV)
CYS	PM6	-9.30	-0.20	9.10	-1566.84	166.91	145.39	138.19	3.82	-3.66	-0.76
	PM3	-8.88	-0.33	8.56	-1561.41	162.32	145.39	138.19	3.83	-3.14	-0.52
	AMI	-9.28	0.05	9.33	-1737.16	214.11	145.39	138.19	3.72	-3.49	-0.54
	RMI	-9.44	0.21	9.65	-1735.73	229.25	145.39	138.19	3.64	-3.61	-0.52
	MNDO	-9.80	0.81	10.61	-1791.18	228.03	145.39	138.19	3.44	-3.00	-0.47
GLY	PM6	-9.05	0.24	9.29	-1081.09	5.26	104.50	87.50	2.78	-3.81	-0.50
	PM3	-8.63	0.96	9.59	-1087.01	23.05	104.50	87.50	2.16	-3.66	-0.32
	AMI	-9.34	1.11	10.45	-1215.80	42.43	104.50	87.50	1.98	-3.97	-0.36
	RMI	-9.25	1.06	10.31	-1208.71	43.81	104.50	87.50	1.96	-4.01	-0.37
	MNDO	-9.73	0.97	10.7	-1227.36	48.58	104.50	87.50	1.80	-3.70	-0.33
LEU	PM6	-9.05	0.22	9.27	-2302.68	627.55	172.96	175.09	3.00	-4.61	-0.49
	PM3	-8.70	0.94	9.64	-2225.15	563.24	172.96	175.09	2.26	-4.38	-0.31
	AMI	-9.31	1.11	10.42	-2403.72	607.47	172.96	175.09	2.12	-4.69	-0.35
	RMI	-9.28	1.06	10.34	-2429.97	649.45	172.96	175.09	2.14	-4.77	-0.35
	MNDO	-9.71	0.96	10.67	-2423.85	620.29	172.96	175.09	1.91	-3.57	-0.32
ALA	PM6	-9.10	0.22	9.32	-1392.55	166.79	121.96	109.30	2.80	-4.10	-0.47
	PM3	-8.71	0.94	9.65	-1380.20	166.73	121.96	109.30	2.20	-3.83	-0.31
	AMI	-9.34	1.11	10.45	-1522.19	193.16	121.96	109.30	2.06	-4.09	-0.35
	RMI	-9.32	1.05	10.37	-1522.06	203.13	121.96	109.30	2.04	-4.31	-0.35
	MNDO	-9.70	0.97	10.67	-1535.83	200.86	121.96	109.30	1.89	-3.71	-0.32

Higher value of E_{HOMO} indicates that the molecule has a higher tendency towards the donation of electron to appropriate acceptor molecules with low energy and empty molecular orbital. Based on the increasing value of E_{HOMO}, the variation of inhibition efficiencies of the studied inhibitors (using gas and aqueous phases data)is consistent with that obtained from experimental data (i.e CYS > LEU > ALA > GLY). However, results obtained for PM6 Hamiltonian using gas phase calculations, strongly deviate from this trend. This is due to the fact that all the semi empirical methods contain sets of parameters. Atomic and diatomic parameters exist in PM6, while MNDO, AM1, PM3, and MNDO-*d* use only single-atom parameters. Not all parameters are optimized for all methods for example, in MNDO and AM1 the two electron one center integrals are normally taken from atomic spectra. Therefore, atomic and diatomic parameters are significant in predicting the reactivity of the amino acids studied. On the other hand, the energy of the LUMO (E_{LUMO}) measures the tendency of a molecule to accept electron. Therefore a decreasing E_{LUMO} suggests better inhibition efficiency (Eddy and Ebenso, 2010a). From the results obtained, the expected trend for inhibition potentials of the amino acids studied is CYS > LEU > ALA > GLY. The observed trend is in agreement with experimental data. Another quantum chemical parameter that was found to have excellent correlation with experimental inhibition efficiency (IE_{exp}) is the energy gap, defined as the difference between E_{LUMO} and E_{HOMO} (Maltarollo *et al*., 2010). According to Eddy (2010), the energy gap is related to the hardness and softness of a molecule because a soft molecule has a low energy gap while a hard molecule has a large energy gap. Moreso, a soft molecule is more reactive than a hard molecule because the smaller the gap between the last occupied orbital and the first virtual orbital, the better is the ease

in which intermolecular electron transfer can proceed. Therefore, inhibition efficiency of the amino acids studied is expected to increase with decreasing value of ΔE. This assertion is supported by the experimental results. Figs. 4.15 and 4.16 show the variations of IE_{exp} with some quantum chemical parameters obtained from AM1 model for gas and aqueous phases respectively. From these figures, it can be seen that there is a strong correlation between IE_{exp} and the frontier molecular orbital energies (i.e E_{HOMO}, E_{LUMO} and ΔE). However, the plots only depict values obtained from AM1 model. Values of R^2 obtained for other Hamiltonians are presented in Table 4.12.

Tables 4.10 and 4.11 also contain electronic energies of the molecule (EE), core core repulsion energy (CCR), heat of formation (H_f), cosmo area (cosAr) and cosmo volume (cosVol). These parameters have been found to be useful in predicting the direction of a corrosion inhibition reaction for some systems (Eddy and Ebenso, 2010b). However, in this study, only the cosmo area was significant as can be seen by the low R^2 values between the respective quantum chemical parameters (except cosmo area) and the IE_{exp} (Table 4.12). The results obtained suggest that the inhibition potentials of the amino acids are not influenced by EE, cosVol and CCR.

The dipole moment (μ) is an index that can also be used for the prediction of the direction of a corrosion inhibition process. Dipole moment is the measure of polarity in a bond and is related to the distribution of electrons in a molecule (Arslan *et al*. 2009).

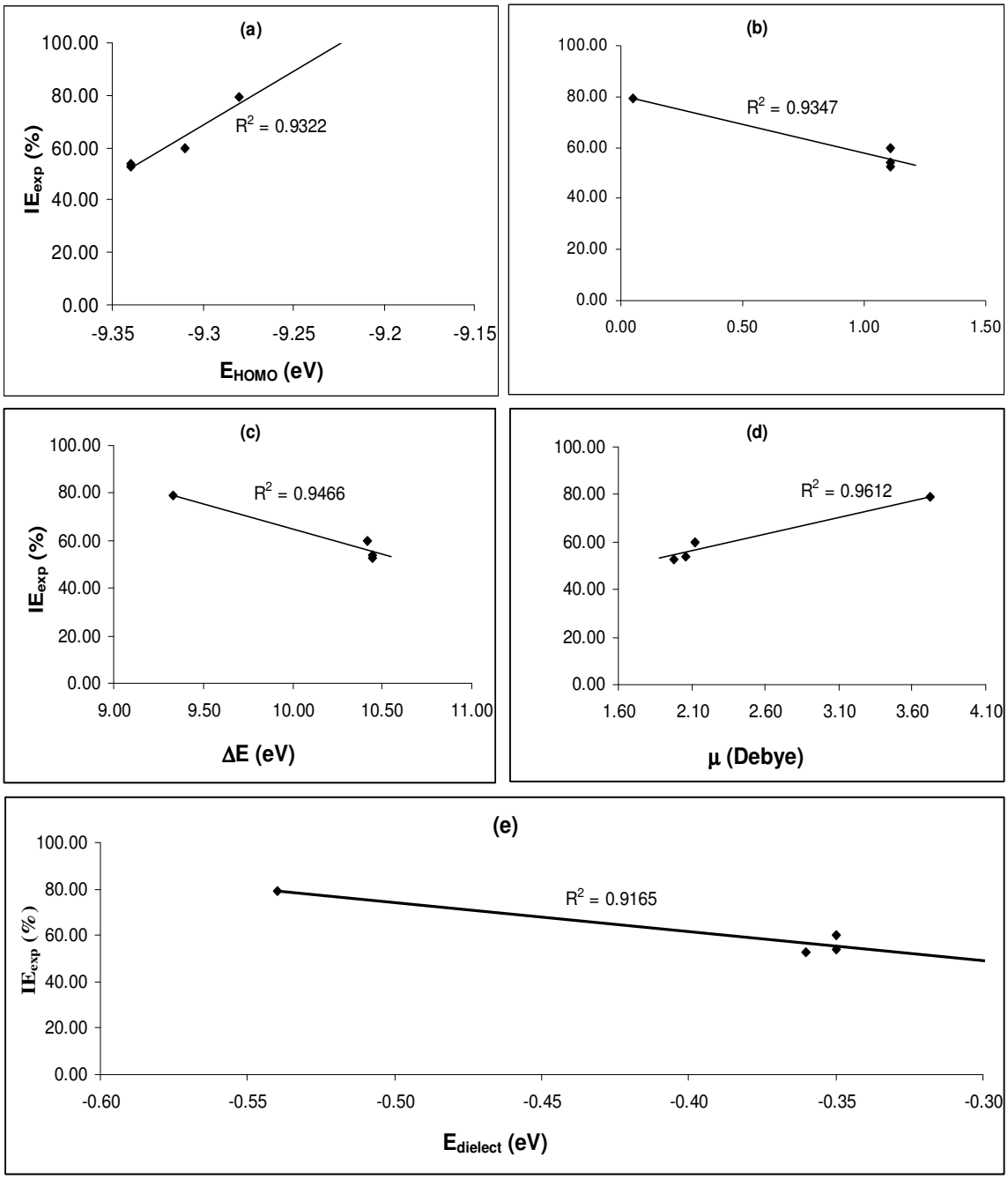


Fig. 4.15: Variation of experimental inhibition efficiency (IE_{exp}) with (a) the HOMO energy, E_{HOMO} (b) the LUMO energy, E_{LUMO} (c) the energy gap, ΔE (d) the dipole moment, μ and with (e) the dielectric energy, $E_{dielect}$ obtained for Aqueous phase calculations using AM1

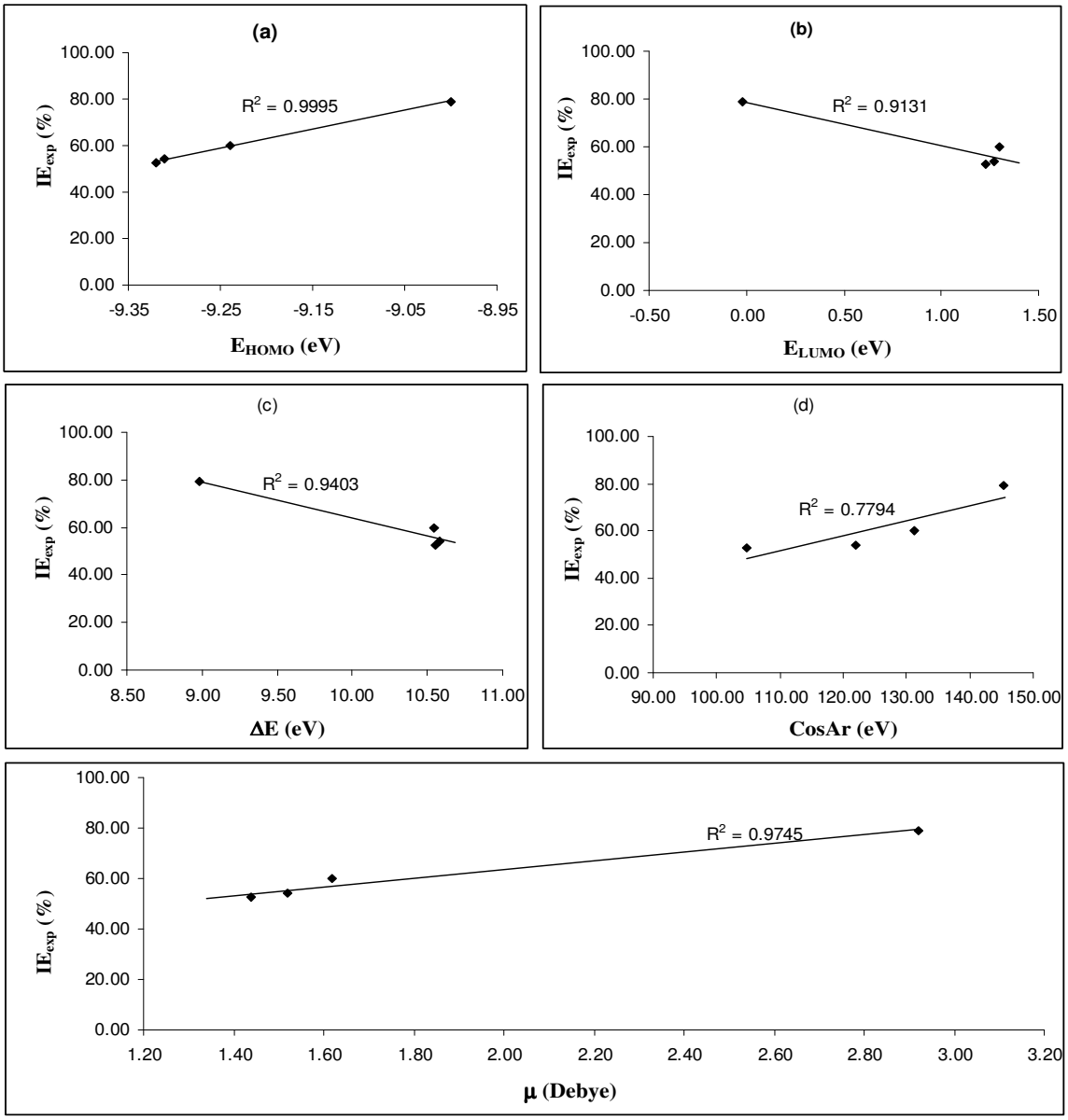


Fig. 4.16: Variation of experimental inhibition efficiency (IE_{exp}) with (a) the HOMO energy, E_{HOMO} (b) the LUMO energy, E_{LUMO} (c) the energy gap, ΔE (d) the cosmo area, cosAr and with (e) the dielectric energy, $E_{dielect}$ obtained for gas phase calculations using AM1

Table 4.12: Values of R^2 between experimental inhibition efficiencies and some semi-empirical parameters obtained from aqueous phase (gas phase) calculations for different Hamiltonians

	PM6	PM3	AM1	RM1	MNDO
E_{HOMO}	0.8651(0.0883)	0.917 (0.9029)	0.9322(0.995)	0.83819(0.4448)	0.8177(0.887)
E_{LUMO}	0.9469(0.881)	0.9392(0.9238)	0.9347(0.913)	0.9327(0.9073)	0.9608(0.8345)
ΔE	0.9651(0.4507)	0.9201(0.9251)	0.9466(0.9402)	0.9242(0.9291)	0.916(0.9601)
EE	0.0534(0.0794)	0.0635(0.0827)	0.0767(0.086)	0.0724(0.0848)	0.0982(0.0912)
CCR	0.005(0.0708)	0.0043(0.0725)	0.0139(0.0756)	0.0149(0.0751)	0.0168(0.0763)
cosAr	0.2013(0.7796)	0.2013(0.7796)	0.2013(0.7796)	0.2013(0.7796)	0.2013(0.7796)
cosVol	0.1864(0.1865)	0.1864(0.1865)	0.1864(0.1865)	0.1864(0.1865)	0.1864(0.1865)
μ	0.9967(0.9977)	0.5209(0.9683)	0.9612(0.9745)	0.9707(0.9827)	0.9542(0.9645)
H_f	0.1559(0.303)	0.3834(0.4741)	0.338(0.4249)	0.3426(0.4137)	0.992(0.9853)
E_{dielec}	0.928	0.9185	0.9165	0.8869	0.9108

Although the literature is inconsistent on the use of 'μ' as a predictor of the direction of a corrosion inhibition reaction, it is generally agreed that the adsorption of polar compounds possessing high dipole moments on the metal surface may lead to better inhibition efficiency. A comparison of the results obtained from quantum chemical calculations (for both gas and aqueous phases) with experimental inhibition efficiencies reveals that the % inhibition efficiencies of the inhibitors increase with increasing dipole moment. Excellent correlations were obtained between experimental inhibition efficiencies and calculated values of μ for all the Hamiltonians (except for aqueous phase PM3 model). Also, for all the amino acids studied, there is a significant difference between the dipole moments obtained from the gas and aqueous phases respectively.

Aqueous phase calculations also yielded dielectric energies of the molecules which also correlated excellently with experimental inhibition efficiency (Fig. 4.15 and Table 4.12).

4.2.2 Density functional theory (DFT)

DFT is one of the most powerful tools in quantum chemistry. It is the shooting star in theoretical modeling and that the development of ever better exchange-correlation functional has made it possible to calculate many molecular properties with accuracies. DFT is based on the principle that the energy of a molecule can be determined from the electron density instead of a wave function. The DFT based on the Hohnenberg-Kohn theorems has been found to be a strong tool for the modeling and development of conceptual issues on chemical reactivity (Eddy and Ita, 2010b). In corrosion study, DFT

has also been acknowledged as a powerful tool that can be used for the prediction of the sites for electrophilic and nucleophilic attacks (Eddy *et al*., 2009c)

According to Stoyanov *et al*. (2008), in DFT, the ground state energy of an atom or a molecule is expressed in terms of its electron density ρ(r) and that two chemical reactivity indices, namely chemical potential (ϒ) and global hardness (η) are defined as the first and second derivative of TE(ρ) with respect to the number of electrons, Thus,

$$\Upsilon = [\delta TE/\delta N]_v \quad 4.21$$

$$\eta = (\delta^2 TE/\delta N^2)_{V(r)} = \tfrac{1}{2}(\delta\Upsilon/\delta N)_{V(r)} \quad 4.22$$

where TE is the total energy, η is the global hardness and N is the number of electrons in the molecule. The global softness is the inverse of the global hardness and is defined as S = ½ η. From the application of the finite difference approximation, the global hardness and softness were evaluated using equations 4.23 and 4.24(Eddy and Ebenso, 2010a,b)

$$\eta = [(E_{(N-1)} - E_{(N)}) - (E_{(N)} - E_{(N+!)})] \quad 4.23$$

$$S = 1/[(E_{(N-1)} - E_{(N)}) - (E_{(N)} - E_{(N+!)})] \quad 4.24$$

where $E_{(N-1)}$, $E_{(N)}$ and $E_{(N+1)}$ are the ground state energies of the molecule with N-1, N and N+1 electrons respectively. Also, the ionization energy (IE) and the electron affinity (EA) of the molecules were calculated using the ground state energies of the respective systems using equations 4.25 and 4.26(Eddy and Ita, 2010c),

$$IE = E_{(N-1)} - E_{(N)} \quad 4.25$$

$$EA = E_{(N)} - E_{(N+!)} \quad 4.26$$

A Comparison of equations 4.23 and 4.24 with equations 4.25 and 4.26 showsthat the global softness and hardness can be expressed as equation 4.27 and 4.28

$$\eta = IE - EA \quad 4.27$$

$$S = 1/[(IE - EA)] \quad 4.28$$

Values of IE, EA, η and S calculated from equations 4.25 to 4.28 for aqueous and gas phases are presented in Tables 4.13 and 4.14 respectively. From the results obtained, it can be seen that the IE and the EA of the inhibitors decrease in the order similar to those obtained experimentally. It should be noted that the EA values for all the inhibitors (except that of CYS) were negative indicating the tendency of the molecule to be electrophilic. In Figure 4.17, the dependence of the calculated values of E_{HOMO} and E_{LUMO} on the IE and EA are presented. From the Figure, it is evident that there is a good linear relationship between the respective variables (i.e E_{HOMO} and IE and also E_{LUMO} and EA). Therefore the inhibitors have higher potentials toward the binding of electron-donating ligands.

The global softness and hardness of a molecule are DFT parameters that have been found to exhibit excellent relationship with the energy gap (E_L). As stated earlier, a soft molecule is more reactive than a hard molecule because a soft molecule has a lower energy gap. Therefore, as expected, the best inhibitor (CYS) is the inhibitor with the lowest global hardness but leastglobal softness deduced from both gas and aqueous phases calculations (Tables 4.13 and 4.14).

Table 4.13: Gas phase quantum chemical parameters for some amino acids

	Models	E_N (eV)	E_{N-1} (eV)	E_{N+1} (eV)	IE (eV)	EA (eV)	χ (eV)	S (/eV)	η (eV)	δ
CYS	**PM6**	-1399.28	-1390.88	-1400.25	8.40	0.97	4.68	0.13	7.43	0.16
	PM3	-1398.64	-1390.30	-1399.35	8.34	0.71	4.52	0.13	7.63	0.16
	AMI	-1522.57	-1513.90	-1523.02	8.67	0.45	4.56	0.12	8.22	0.15
	RMI	-1506.03	-1497.02	-1506.31	9.01	0.28	4.64	0.11	8.73	0.13
	MNDO	-1562.75	-1553.69	-1562.30	9.06	-0.45	4.30	0.11	9.51	0.14
GLY	**PM6**	-1075.40	-1066.99	-1074.86	8.41	-0.54	3.93	0.11	8.95	0.17
	PM3	-1063.68	-1055.52	-1062.47	8.16	-1.21	3.48	0.11	9.37	0.19
	AMI	-1173.05	-1164.40	-1171.86	8.65	-1.19	3.73	0.10	9.84	0.17
	RMI	-1164.57	-1156.11	-1163.35	8.46	-1.22	3.62	0.10	9.68	0.17
	MNDO	-1178.42	-1169.33	-1177.77	9.09	-0.65	4.22	0.10	9.74	0.14
LEU	**PM6**	-1674.71	-1666.50	-1674.69	8.21	-0.02	4.10	0.12	8.23	0.18
	PM3	-1661.64	-1653.62	-1660.95	8.02	-0.69	3.67	0.11	8.71	0.19
	AMI	-1795.93	-1787.51	-1794.84	8.42	-1.09	3.66	0.11	9.51	0.18
	RMI	-1780.22	-1771.95	-1779.49	8.27	-0.73	3.77	0.11	9.00	0.18
	MNDO	-1803.27	-1794.41	-1802.68	8.86	-0.59	4.13	0.11	9.45	0.15
ALA	**PM6**	-1225.30	-1216.97	-1225.30	8.43	-0.10	4.16	0.12	8.53	0.17
	PM3	-1213.20	-1205.07	-1212.48	8.13	-0.72	3.71	0.11	8.85	0.19
	AMI	-1328.73	-1320.17	-1327.92	8.56	-0.81	3.88	0.11	9.37	0.17
	RMI	-1318.61	-1310.20	-1317.86	8.41	-0.75	3.83	0.11	9.16	0.17
	MNDO	-1334.69	-1325.73	-1334.53	8.96	-0.16	4.40	0.11	9.12	0.14

Table 4.14: Aqueous phase quantum chemical descriptors for some amino acids

	Models	E_N (eV)	E_{N-1} (eV)	E_{N+1} (eV)	IE (eV)	EA (eV)	χ (eV)	S(/eV)	η (eV)	δ
CYS	**PM6**	-1399.93	-1394.13	-1403.79	5.80	3.86	4.83	0.52	1.94	0.56
	PM3	-1399.09	-1393.74	-1402.47	5.35	3.38	4.37	0.51	1.97	0.67
	AMI	-1523.04	-1516.97	-1526.06	6.07	3.02	4.54	0.33	3.05	0.40
	RMI	-1506.48	-1500.08	-1509.41	6.40	2.93	4.67	0.29	3.47	0.34
	MNDO	-1563.15	-1556.98	-1565.31	6.17	2.16	4.16	0.25	4.01	0.35
GLY	**PM6**	-1075.84	-1070.41	-1078.87	5.43	3.03	4.23	0.42	2.40	0.58
	PM3	-1063.96	-1058.97	-1066.18	4.99	2.22	3.61	0.36	2.77	0.61
	AMI	-1173.37	-1167.78	-1174.79	5.59	1.42	3.51	0.24	4.17	0.42
	RMI	-1164.90	-1159.47	-1167.10	5.43	2.20	3.81	0.31	3.23	0.49
	MNDO	-1178.72	-1172.73	-1180.99	5.99	2.27	4.13	0.27	3.72	0.39
LEU	**PM6**	-1175.14	-1669.53	-1678.12	5.61	2.98	4.29	0.38	2.63	0.51
	PM3	-1661.91	-1656.68	-1664.07	5.23	2.16	3.69	0.33	3.07	0.54
	AMI	-1796.24	-1790.48	-1798.31	5.76	2.07	3.91	0.27	3.69	0.42
	RMI	-1780.53	-1774.90	-1782.65	5.63	2.12	3.88	0.28	3.51	0.45
	MNDO	-1803.56	-1797.41	-1805.76	6.15	2.20	4.17	0.25	3.95	0.36
ALA	**PM6**	-1225.76	-1220.18	-1228.76	5.58	3.00	4.29	0.39	2.58	0.53
	PM3	-1213.47	-1208.30	-1215.64	5.17	2.17	3.67	0.33	3.00	0.55
	AMI	-1329.04	-1323.33	-1331.12	5.71	2.08	3.89	0.28	3.63	0.43
	RMI	-1318.92	-1313.34	-1321.06	5.58	2.14	3.86	0.29	3.44	0.46
	MNDO	-1334.97	-1328.92	-1337.19	6.05	2.22	4.13	0.26	3.83	0.37

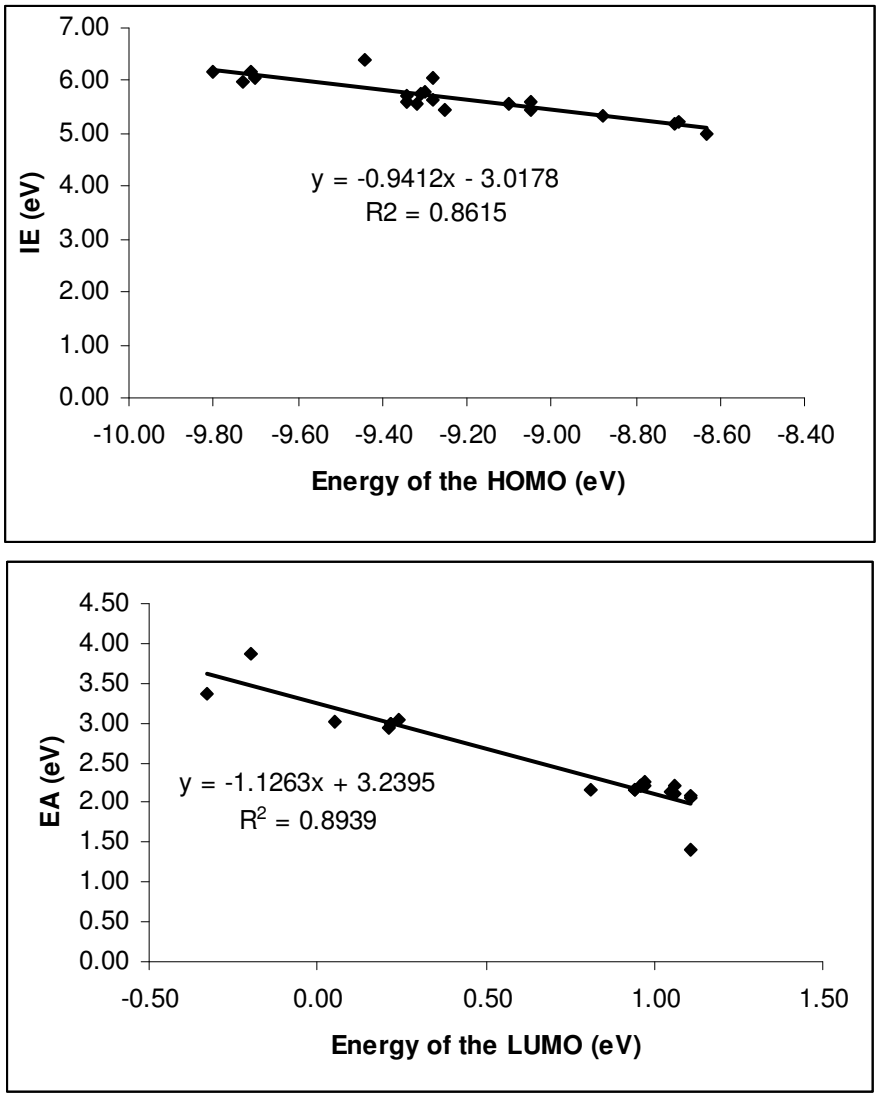


Fig. 4.17: Variation of IE with E_{HOMO} and EA with E_{LUMO} for the amino acid studied in aqueous phase

Electronegativity denotes the tendency of an atom in a molecule to attract the shared pair of electrons towards themselves. Calculated values for the electronegativity of the inhibitors studied for gas and aqueous phases are also presented in Tables 4.13 and 4.14 respectively. The results obtained indicate that the best inhibitor had the highest value of χ while the least value of χ was exhibited by the inhibitor that has the least IE_{exp}. It is significant thatχ is also related to IE and EA.

The fraction of electron transferred, δ was calculated using equation 4.29 (Eddy, 2010b),

$$\delta = (\chi_{Fe} - \chi_{inh})/2(\eta_{Fe} + \eta_{inh}) \quad 4.29$$

where χ_{Fe} and χ_{inh} are the electronegativity of Fe and the inhibitor respectively while η_{Fe} and η_{inh} are the global hardness of Fe and the inhibitor respectively. In this study, the theoretical values of χ_{Fe} = 7ev and η_{Fe} = 0 were used for the computation of δ values for the various Hamiltonians (Eddy, 2010). The results obtained from the gas and aqueous phases calculations ofδ show that for a given Hamiltonian, the fraction of the electron transferred is approximately similar indicating that the differences between the inhibition efficiencies of the amino acids studied can not be attributed to δ values alone.

4.2.2.1 Local selectivity

The merit behind the Fukui function is that it provides an avenue for analysing the local selectivity of a corrosion inhibitor (Eddy, 2010). The Fukui function can be defined according to equation 4.30:

$$f(r) = [(\delta\Upsilon/\delta\nu(r))]_N \quad 4.30$$

where $\nu(r)$ is the external potential, whose functional derivative must be taken at constant number of electrons. Assuming $[\delta TE/\delta N]_\nu$ and $[\delta TE/\delta \nu(r)]_N$ are exact differentials, then the Maxwell relations between the derivatives can be expressed as equation 4.31:

$$f(r) = [(\delta\rho(r)/\delta N)]_\nu \quad 4.31$$

According to Fuentealba *et al*. (2000), equation 4.31 is the most standard presentation of the Fukui function. However, owing to the discontinuity of the chemical potential at integer N, the derivative will be different if taken from the right or the left side. Therefore three different forms of Fukui functions (f^+,f^0 and f^-) are possible. These correspond to the situation when N increases from N to N+1(f^+) and when N decreases from N to N-1 (f^-). f^+ is associated with the LUMO and measures the reactivity towards a donor reagent while f^- is associated with the HOMO and measures the reactivity toward an acceptor reagent. However, the average of both (f^0) measures reactivity towards a radical. In this work, the finite difference approximation was used to calculate the electrophilic and nucleophilic Fukui function using equation 4.32 and 4.33:

$$f^+ = (\delta\rho(r)/\delta N)^+_\upsilon = q_{(N+1)} - q_{(N)} \quad 4.32$$

$$f^- = (\delta\rho(r)/\delta N)^-_\upsilon = q_{(N)} - q_{(N-1)} \quad 4.33$$

where ρ, $q_{(N+1)}$, $q_{(N)}$ and $q_{(N-1)}$ are the density of electron and the Muliken/Lowdin charge of the atom with N+1, N and N-1 electrons. Values of f^+ and f^- for CYS, GLY, LEU and ALA calculated from DFT-B3LYP (6-31G) and MP2 (STO-5G) models are presented in Tables 4.15 and 4.16 respectively. Since there is similarity between the Fukui function and the frontier molecular orbitals, it is expected that the site for nucleophilic attack is the site where the value of f^+ is maximum while the site for electrophilic attack is controlled by the values of f^-. From the results obtained for the inhibitors studied, the site for

electrophilic attack is on the amine bond (N2-C3) of the respective amino acids. On the other hand, the sites for nucleophilic attacks are on C3 atom of the respective amino acids. The observed similarity in the sites for electrophilic and nucleophilic attacks indicates that the amino acids studied inhibited the corrosion of mild steel through similar mechanism. It should be noted out that there is a close similarity between the Fukui function and electron density as can be seen in the Fukui function and electron density diagrams of the amino acids (Figs. 4.18 to 4.21). Figures 4.18 to 4.21 shows that the shapes of the respective molecule vary between states and therefore their reactivity is also expected to vary similarly. The Fukui function and the electron density are very useful descriptors for understanding the sites for electrophilic and nucleophilic reaction as well as hydrogen bonding interaction.

The local softness is defined as the product of the Fukui function and the global softness, S and can be expressed as equation 4.34 and 4.35 (Wang *et al*., 2007).

$$s^{+} = (f^{+})S \quad 4.34$$

$$s^{-} = (f^{-})S \quad 4.35$$

Calculated values of the local softness for the amino acids studied are also presented in Tables 4.15 and 4.16. Also, the relative nucleophilicity (s^{+}/s^{-}) and relative electrophilicity (s^{-}/s^{+}) are indices that are also related to the local softness

Table 4.15 : Fukui and softness functions for electrophilic and nucleophilic attacks on carbon and electronegative atoms in the some amino acids calculated from Muliken(Lowdin) charges using DFT-B3YLP (6-31G)

	Atom No	f^+	f^-	S^+	S^-
CYS	1 C	-0.1405(-0.1846)	-0.0323(0.0062)	-0.0169(-0.0222)	-0.0039(0.0007)
	2 N	-0.0120(-0.0187)	-0.2039(-0.2966)	-0.0014(-0.0022)	-0.0245(-0.0356)
	3 C	**0.0399(0.0126)**	**0.0781(0.0190)**	**0.0048(0.0015)**	**0.0094(0.0023)**
	4 C	0.0458(-0.0630)	**0.0663(**-0.0049)	0.0055(-0.0076)	0.0080(-0.0006)
	5 S	-0.1908(-0.1764)	-0.2980(-0.3130)	-0.0229(-0.0212)	-0.0358(-0.0376)
	6 O	-0.1563(-0.1639)	-0.0515(-0.0477)	-0.0188(-0.0197)	-0.0062(-0.0057)
	7 O	-0.0612(-0.0793)	-0.0046(-0.0124)	-0.0073(-0.0095)	-0.0006(-0.0015)
GLY	1 C	-0.4288(0.0379)	-0.0418(0.0010)	-0.0429(0.0038)	-0.0042(0.0001)
	2 N	**1.5359(1.0295)**	-0.3776(-0.5288)	0.1536(0.1030)	-0.0378(-0.0529)
	3 C	0.1369(0.2255)	0.1292(0.0212)	0.0137(0.0226)	0.0129(0.0021)
	4 O	1.0194(0.8084)	-0.0509(-0.0415)	0.1019(0.0808)	-0.0051(-0.0042)
	5 O	1.2327(0.7798)	-0.0439(-0.0519)	0.1233(0.0780)	-0.0044(-0.0052)
LEU	1 C	-0.1729(-0.2293)	-0.0458(0.0022)	-0.0173(-0.0229)	-0.0046(0.0002)
	2 N	-0.0066(-0.0140)	-0.3301(-0.4642)	-0.0007(-0.0014)	-0.0330(-0.0464)
	3 C	**0.0494(0.0087)**	0.1163(0.0193)	0.0049(0.0009)	0.0116(0.0019)
	4 C	0.0514(-0.0126)	0.0496(-0.0216)	0.0051(-0.0013)	0.0050(-0.0022)
	5 C	0.0285(-0.0022)	0.0235(-0.0019)	0.0029(-0.0002)	0.0024(-0.0002)
	6 C	0.0545(-0.0281)	0.0169(-0.0019)	0.0055(-0.0028)	0.0017(-0.0003)
	7 C	0.0295(-0.0144)	0.0093(-0.0080)	0.0030(-0.0014)	0.0009(-0.0008)
	8 O	-0.1724(-0.1878)	-0.0424(-0.0359)	-0.0172(-0.0188)	-0.0042(-0.0040)
	9 O	-0.0712(-0.0882)	-0.0287(-0.0359)	-0.0071(-0.0088)	-0.0029(-0.0036)
ALA	1 C	-0.1977(-0.2179)	-0.0481(0.0018)	-0.0198(-0.0218)	-0.0048(0.0002)
	2 N	**1.5181(1.0055)**	-0.3609(-0.5014)	0.1518(0.1006)	-0.0361(-0.0501)
	3 C	0.0746(0.0516)	0.1461(0.0280)	0.0075(0.0052)	0.0146(0.00280
	4 C	0.6893(0.6527)	0.0337(-0.0226)	0.0689(0.0653)	0.0034(-0.0023)
	5 O	1.0042(0.7850)	-0.0473(-0.0402)	0.1004(0.0785)	-0.0047(-0.0040)
	6 O	1.2276(0.7671)	-0.0345(-0.0430)	0.1228(0.0767)	-0.0035(0.0043)

Table 4.16 : Fukui and softness functions for electrophilic and nucleophilic attacks on carbon and electronegative atoms in some amino acids calculated from Muliken(Lowdin) charges using MP2 (STO-5G)

	Atom No	f^+	f^-	S^+	S^-
CYS	1 C	-0.3016(-0.3548)	0.0129(0.0245)	-0.0362(-0.0426)	0.0015(0.0029)
	2 N	-0.0061(-0.0068)	-0.0072(-0.0108)	-0.0007(-0.0008)	-0.0009(-0.0013)
	3 C	**0.0083(0.0103)**	-0.0008(-0.0013)	**0.0010(0.0012)**	**-0.0001(-0.0002)**
	4 C	**0.0110(0.0066)**	0.0005(-0.0175)	0.0013(0.0008)	0.0001(-0.0021)
	5 S	-0.0462(-0.0448)	-0.5635(-0.6231)	-0.0055(-0.0054)	-0.0676(-0.0748)
	6 O	-0.2267(-0.2316)	-0.0413(**-0.0453)**	-0.0272(-0.0278)	-0.0050(-0.0054)
	7 O	-0.0754(-0.0797)	**-0.0132(**-0.0142)	-0.0090(-0.0096)	-0.0016(-0.0017)
GLY	1 C	-0.3083(-0.3617)	0.0004(0.0185)	-0.0308(-0.0362)	0.00004(0.0019)
	2 N	-0.0074(-0.0087)	-0.3306(-0.4563)	-0.0007(-0.0009)	-0.0331(-0.0456)
	3 C	**0.0093(0.0082)**	**0.0256(0.0130)**	0.009(0.0008)	0.0026(0.0013)
	4 O	-0.2389(-0.2444)	-0.0549(-0.0568)	-0.0239(-0.0244)	-0.0055(-0.0057)
	5 O	-0.0779(-0.0818)	-0.0271(-0.0282)	-0.0078(-0.0082)	-0.0027(-0.0028)
LEU	1 C	-0.3048(-0.3588)	0.0008(0.0162)	-0.0305(-0.0359)	0.00009(0.0016)
	2 N	-0.0052(-0.0062)	-0.3253(-0.4481)	-0.0005(-0.0006)	-0.0325(-0.0448)
	3 C	**0.0067(0.0090)**	0.0261(0.0172)	0.0007(0.0009)	0.0026(0.0017)
	4 C	0.0006(-0.0056)	-0.0006(-0.0095)	0.00006(-0.0006)	-0.00006(-0.0001)
	5 C	0.0002(-0.0005)	0.0008(-0.0006)	0.00002(-0.0001)	0.00008(-0.00006)
	6 C	0.0022(0.0001)	0.0044(0.0025)	0.0002(0.00001)	0.0004(0.0003)
	7 C	0.0010(**-0.0012)**	0.0011(**-0.0016)**	0.0001(-0.0001)	0.0001(-0.0002)
	8 O	-0.2319(-0.2375)	-0.0461(-0.0475)	-0.0232(-0.0238)	-0.0046(-0.0048)
	9 O	**-0.0760(**-0.0799)	**-0.0228(**-0.0239)	-0.0076(-0.0080)	-0.0023(-0.0024)
ALA	1 C	-0.3063(-0.3598)	-0.0011(0.0142)	-0.0306(-0.0360)	-0.0001(0.0014)
	2 N	-0.0057(-0.0067)	-0.3277(-0.4513)	-0.0006(-0.0007)	-0.0328(-0.0451)
	3 C	**0.0084(0.0094)**	0.0280(0.0180)	0.0008(0.0009)	0.0028(0.0018)
	4 C	0.0039(-0.0051)	0.0037(-0.0083)	0.0004(-0.0005)	0.0004(-0.0008)
	5 O	**-0.2339(**-0.2395)	-0.0446(-0.0458)	-0.0234(-0.0240)	-0.0045(-0.0046)
	6 O	-0.0765(-0.0806)	-0.0250(-0.0256)	-0.0077(-0.0081)	-0.0025(0.0026)

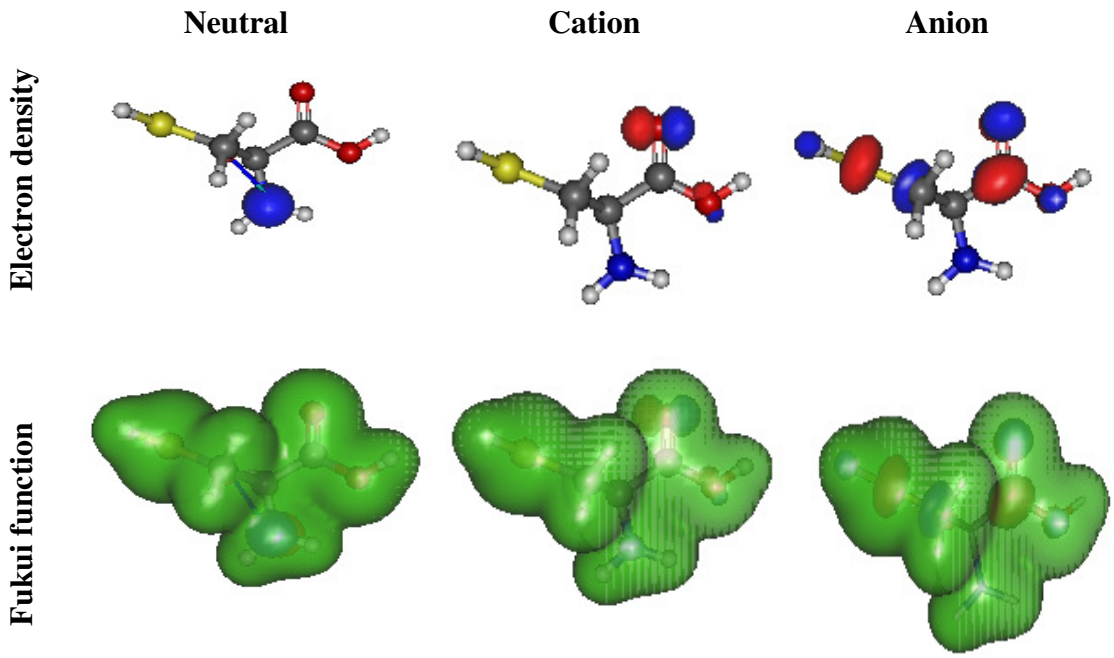


Fig. 4.18 Electron density and Fukui function diagrams for L cysteine radical, electrophile and nucleophile

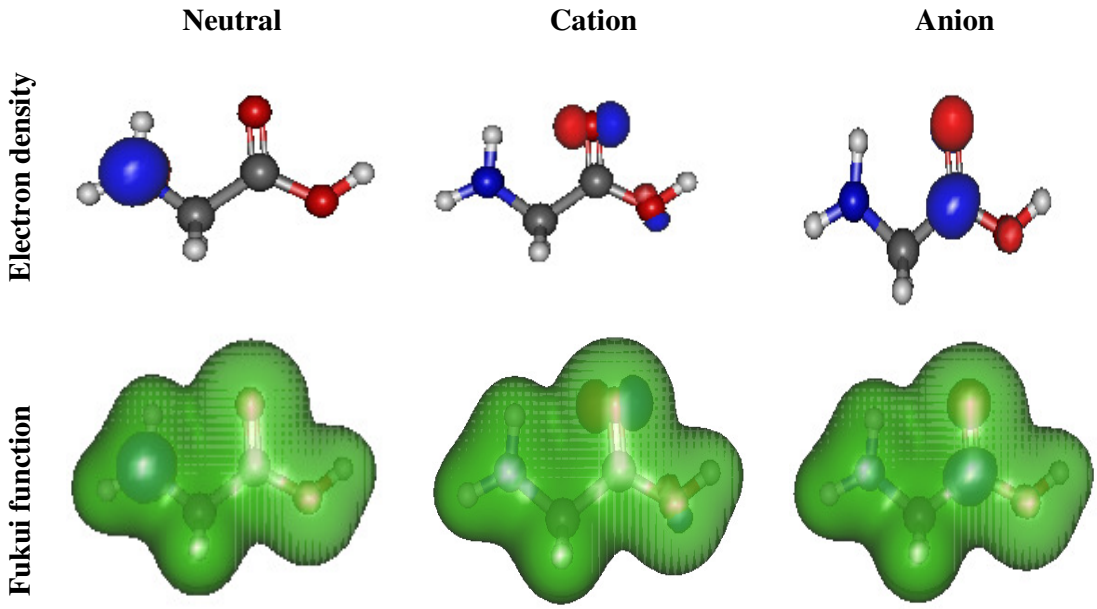


Fig. 4.19: Electron density and Fukui function diagrams for GLY radical, electrophile and nucleophile

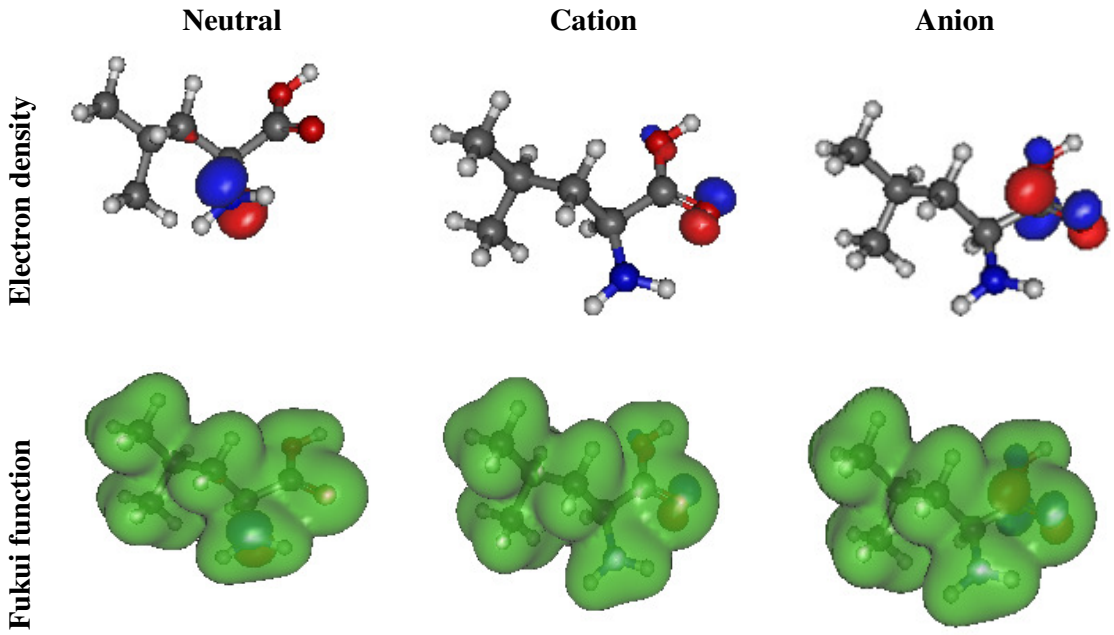


Fig. 4.20: Electron density and Fukui function diagrams for LEU radical, electrophile and nucleophile

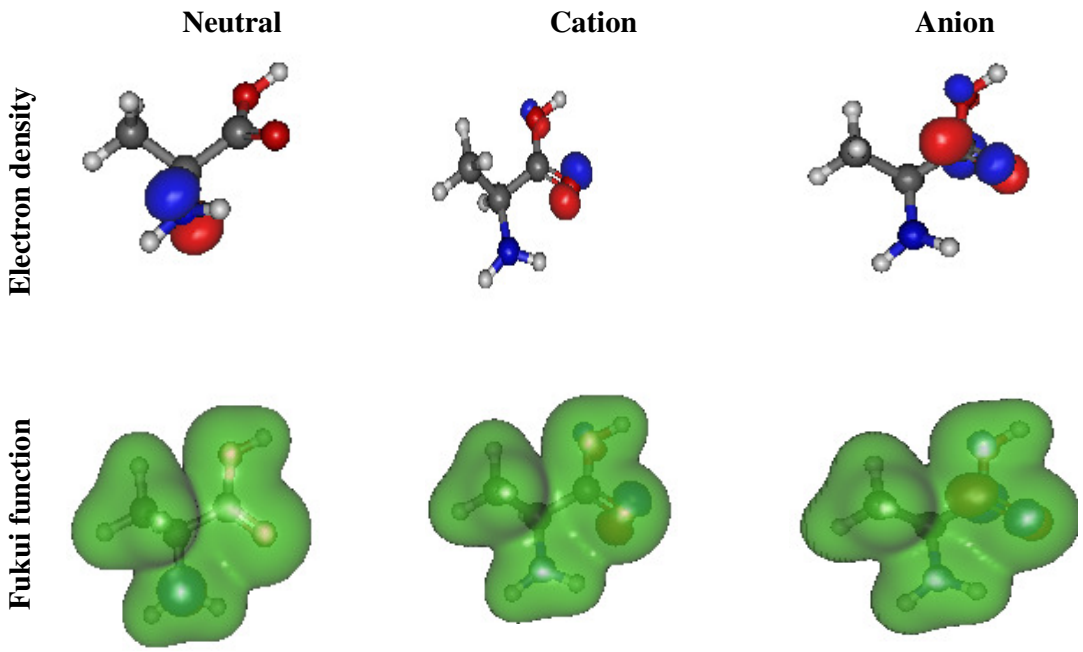


Fig. 4.21 : Electron density and Fukui function diagrams for ALA radical, electrophile and nucleophile

and can be applied for the prediction of the sites for nucleophilic and electrophilic attacks. Although the values of the relative nucleophilicity and relative electrophilicity are not recorded, it was observed that both approaches gave results that are similar to those obtained from the Fukui function calculations.

Figure 4.22 present the molecular orbitals of the amino acids used for the HOMO and LUMO .In the orbital (green represents positive while red represents negative), it can be seen that the sites for electrophilic and nucleophilic attack obtained from Fukui calculations are consistent with what is represented in the Figure 4.22.

Table 4.17 presents Huckel charges on carbon and electronegative elements in the amino acids. The Huckel charges on atoms in the molecules have been reported by Eddy and Ita (2010b) to be significant parameters that can be used to analyse the mechanism of corrosion inhibition. The results obtained reveal that the most negative charge in the amino acids is on the oxygen nitrogen atoms. However, nitrogen is more electronegative than oxygen, therefore the likely site for electrophilic attack is on the nitrogen atom of the respective inhibitor. This finding is consistent with those obtained from Fukui functions. It was also found that there is a strong correlation between experimental inhibition efficiencies and the total negative charge (TNC) on the electronegative atoms of the amino acids. The TNC was found to decrease in the following trend CYS (-1.0578) >LEU (-1.052) > ALA (-1,0434) > GLY(-1.0249) and is consistent with the trend obtained from experimental results.

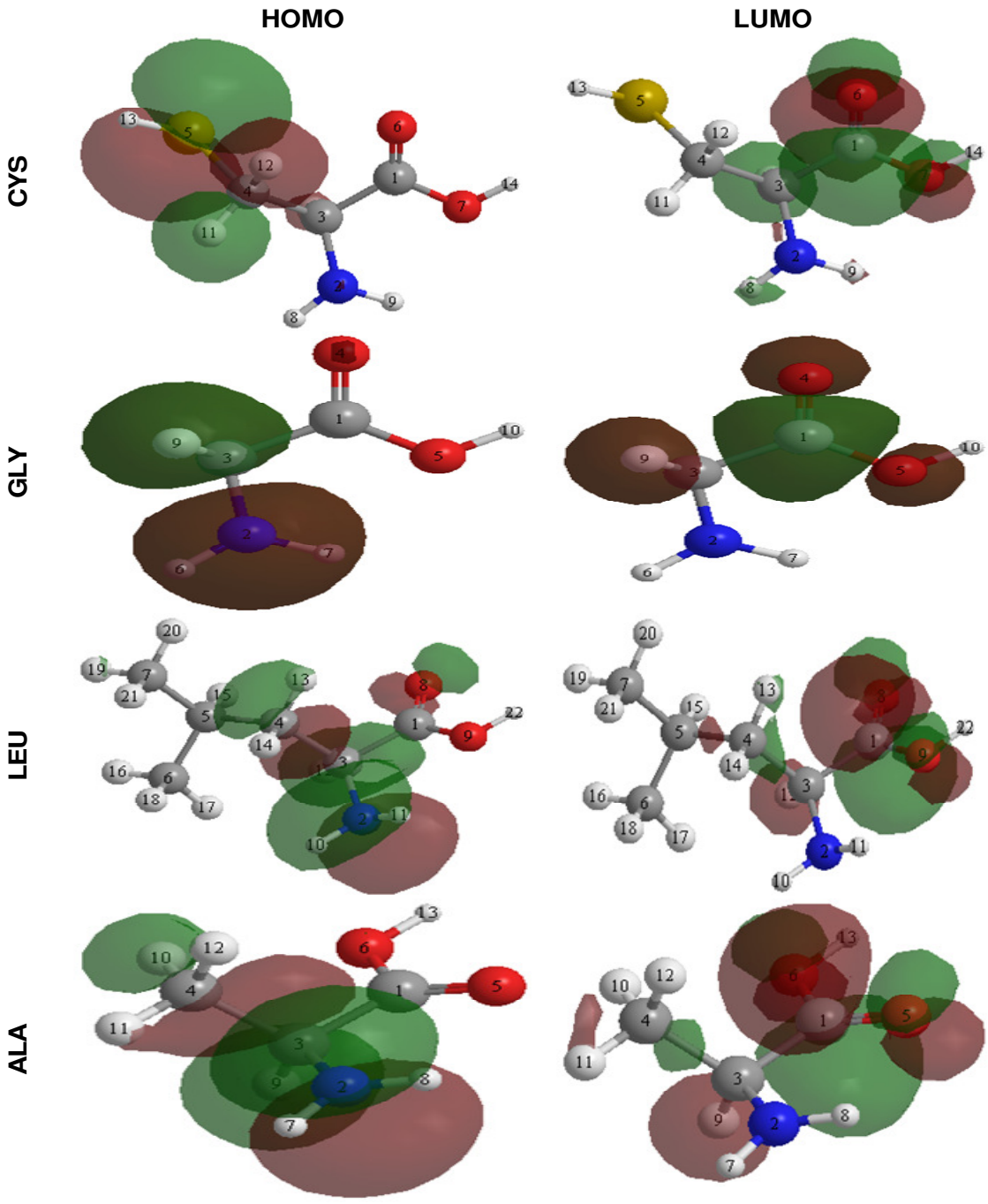


Fig. 4.22: Extended Huckel Molecular orbital of some amino acids showing the HOMO and the LUMO

Table 4.17: Huckel charges on carbon and electronegative atoms in some amino acids

CYS		GLY		LEU		ALA	
Atom	**charge**	**Atom**	**charge**	**Atom**	**charge**	**Atom**	**Charge**
C(1)	0.5881	C(1)	0.5846	C(1)	0.5842	C(1)	0.58103
N(2)	-0.2506	N(2)	-0.2412	N(2)	-0.2504	N(2)	-0.2487
C(3)	0.0432	C(3)	-0.0232	C(3)	0.0348	C(3)	0.05596
C(4)	-0.0600	O(4)	-0.6574	C(4)	-0.0538	C(4)	-0.1184
S(5)	-0.0093	O(5)	-0.1263	C(5)	0.0379	O(5)	-0.6632
O(6)	-0.6751			C(6)	-0.1408	O(6)	-0.1314
O(7)	-0.1228			C(7)	-0.1342		
				O(8)	-0.6666		
				O(9)	-0.1352		

4.2.2.2 Quantitative structure activity relation (QSAR) study

QSAR gives the relationship between descriptors characterizing the structural properties of chemicals on quantitative basis (Bentiss *et al*., 2007b). In corrosion study, the subject of QSAR has been given wider attention and considerations (Karelson and Lobanov, 1996)

From the present study, it has been established that the mechanism of inhibition involves the donation of electron to vacant d- orbital ofFe in mild steel. However, it has also been found that the inhibitor can not only donate electrons to the metal but can also accept electron from the lone pair of electron, leading to the formation of a feed back bond (Fang and Li, 2002). The formation of a feed back bond was analysed by theestablishment of a quantitative relationship between the E_{HOMO}, E_{LUMO} and the experimental inhibition efficiency. These considerations led to the derivation of equations 4.36 to 4.40 for PM6, PM3, AM1, RM1 and MNDO Hamiltonians respectively.

$$IE_{exp} = 2.73E_{HOMO} - 37.43E_{LUMO} + 99.53 \quad (4.36)$$

$$IE_{exp} = 23.55E_{HOMO} - 21.45E_{LUMO} + 282.33 \quad (4.37)$$

$$IE_{exp} = 86.77E_{HOMO} - 1.25E_{LUMO} + 860.04 \quad (4.38)$$

$$IE_{exp} = 78.36E_{HOMO} - 29.26E_{LUMO} + 814.18 \quad (4.39)$$

$$IE_{exp} = 125.80E_{HOMO} - 121.83E_{LUMO} + 1402.96 \quad (4.40)$$

From the above equations, it is apparent that the coefficients of the E_{HOMO} are positive while those of E_{LUMO} are negative indicating that the formation of a feed back bond is favoured by increasing value of E_{HOMO} but with decreasing value of E_{LUMO}. Correlations between the above equation and the experimental inhibition efficiencies were good (R^2 ranges from 0.8923 to 0.9357). However, when all the calculated quantum chemical

parameters were used for development of suitable models for the different Hamiltonians (through multiple regression), it was not possible to obtained simple equations such as those given by equations 4.36 to 4.40. This indicates that the corrosion inhibition process is a composite function of some quantum chemical descriptors.

According to Eddy *et al*. (2010a), the linear model approximates corrosion inhibition potentials according to equation 4.41:

$$IE_{Theor} = Ax_iC_i + B \qquad 4.41$$

where A and B are the regression coefficients determined through regression analysis, x_i is a quantum chemical index characteristic of the molecule i, C_i is the experimental concentration of the inhibitor. However, the linear model expressed by equation 4.41 did not give a good relationship between the experimental and theoretical inhibition efficiencies. Therefore, a non linear model (equation 4.42), which was first proposed by Lukovitis *et al*. (2003) for the study of interaction of corrosion inhibitors with metal surface in acidic solutions was used. This non linear model is based on the Langmuir adsorption isotherm and can be written as follows,

$$IE_{Theor}(\%) = \frac{(Ax_j + B)C_i}{1 + (Ax_j + B)C_i} \times 100 \qquad 4.42$$

where IE_{Theor} is the theoretical inhibition efficiency, A is a regression coefficient, B is a regression constant, C_i is the experimental concentration of the inhibitor and x_i is a quantum chemical index of the molecule, i. Application of equation 4.42 to the presence systems yielded equations 4.43 to 4.47 for gas phase PM6, PM3, AM1, RM1 and MNDO Hamiltonians respectively.

$$IE_{Theor} = \frac{(1.4999E_{HOMO} + 0.984E_{LUMO} + 1.0276\Delta E + \mu + 20.8235)*C \times 100}{(1+(1.4999E_{HOMO} + 0.984E_{LUMO} + 1.0276\Delta E + \mu + 20.8235)*C} \qquad 4.43$$

$$IE_{Theor} = \frac{(2.150E_{HOMO} + 0.409E_{LUMO} + 3.322\Delta E + \mu)*C \times 100}{(1+(2.150E_{HOMO} + 0.409E_{LUMO} + 3.322\Delta E + \mu)*C} \quad \textbf{4.44}$$

$$IE_{Theor} = \frac{(1.085E_{HOMO} + 1.114E_{LUMO} + \Delta E + 4.128\mu)*C \times 100}{(1+(1.085E_{HOMO} + 1.114E_{LUMO} + \Delta E + 4.128\mu)*C} \quad 4.45$$

$$IE_{Theor} = \frac{(1.53E_{HOMO} + 0.549E_{LUMO} + 2.072\Delta E + \mu)*C \times 100}{(1+(1.53E_{HOMO} + 0.549E_{LUMO} + 2.072\Delta E + \mu)*C} \quad 4.46$$

$$IE_{Theor} = \frac{(3.2296*E_{HOMO}+E_{LUMO}+3.7704\Delta E + 0.0245*\mu+5.4307 \times 10^{-18}) \times C \times 100}{(1+(3.2296*E_{HOMO}+E_{LUMO}+3.7704\Delta E + 0.0245*\mu+5.4307 \times 10^{-18})*C} \quad 4.47$$

Table 4.18presents theoretical inhibition efficiencies computed for gas phase models. Also, Figures 4.23, 4.24, 4.25 and 4.26 show the variation of experimental inhibition efficiencies with gas phase theoretical inhibition efficiencies for CYS, GLY, LEU and ALA respectively. From these Figures, it is evident that R^2 values approximate unity for the various inhibitors and Hamiltonians indicating that there is a strong correlation between experimental and theoretical inhibition efficiencies. This also indicates that gas phase models can be used for the modeling of the inhibitive behaviour of amino acids in HCl solutions.

Table 4.18: Theoretical inhibition efficiencies (IE_{Theor}) of some amino acids from gas phase calculations

Inhibitor	C (g/l)	Inhibition efficiency (%)				
		PM6	PM3	AM1	RM1	MNDO
CYS	0.1	65.86	54.85	53.11	45.29	48.13
	0.2	79.42	70.84	69.38	62.35	64.98
	0.3	85.27	78.47	77.26	71.29	73.57
	0.4	88.53	82.93	81.92	76.81	78.77
	0.5	90.53	85.87	84.99	80.54	82.27
GLY	0.1	66.05	60.92	49.32	48.56	50.53
	0.2	79.56	75.71	66.06	65.37	67.13
	0.3	85.37	82.38	74.49	73.9	75.39
	0.4	88.61	86.18	79.56	79.06	80.33
	0.5	90.88	88.63	82.95	82.52	83.62
LEU	0.1	66.58	61.37	52.75	49.55	50.99
	0.2	79.94	76.06	69.07	66.27	67.54
	0.3	85.67	82.66	77.01	74.66	75.74
	0.4	88.85	86.4	81.71	79.71	80.63
	0.5	90.68	88.82	84.81	83.08	83.88
ALA	0.1	65.66	61.21	50.57	49.15	50.79
	0.2	79.27	75.94	67.17	65.91	67.36
	0.3	85.15	82.56	75.42	74.36	75.56
	0.4	88.44	86.32	80.36	79.45	80.5
	0.5	90.61	88.75	83.65	82.86	83.77

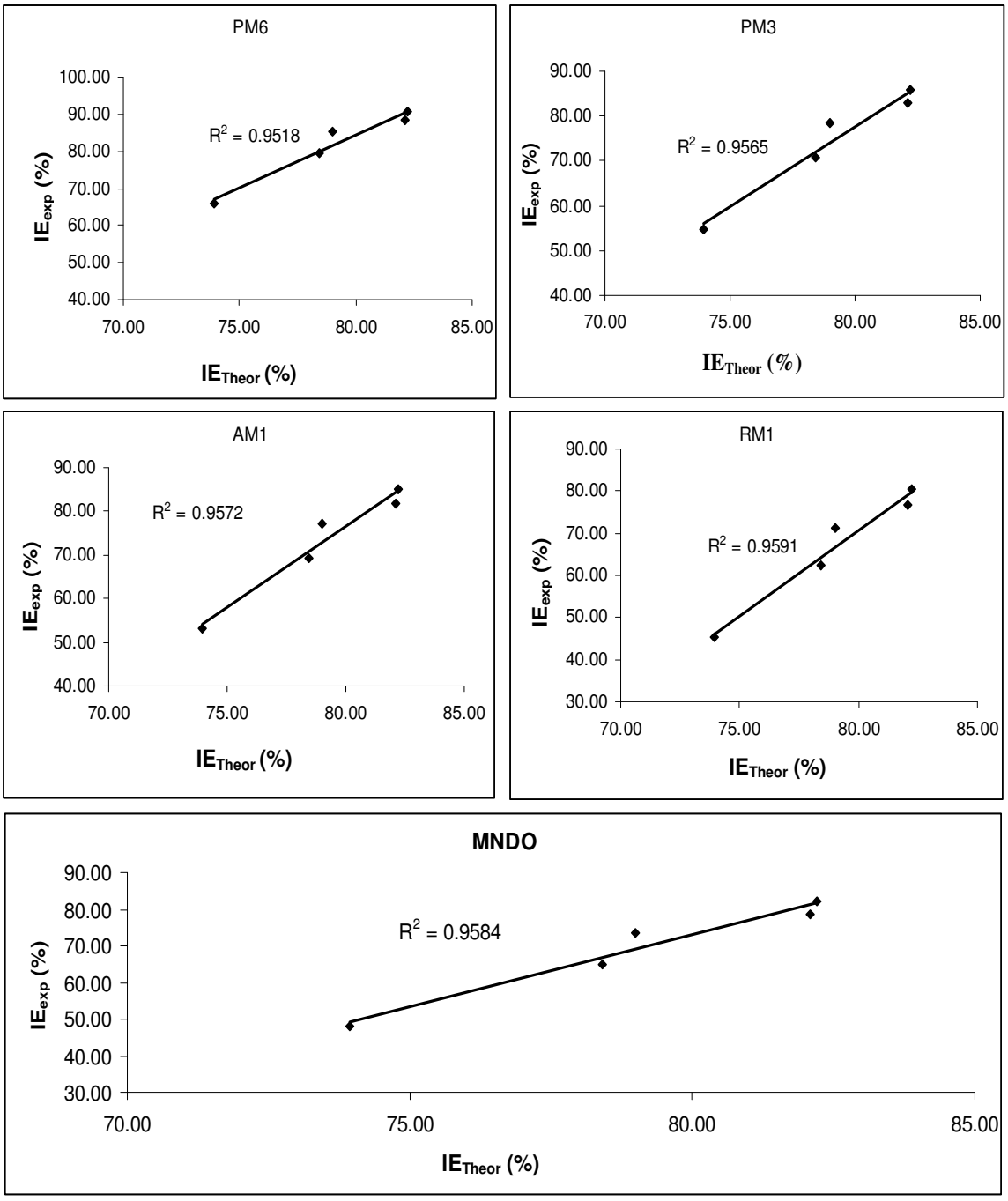


Fig. 4.23: Variation of experimental with theoretical inhibition efficiencies of CYS in gas phase for the various Hamiltonians

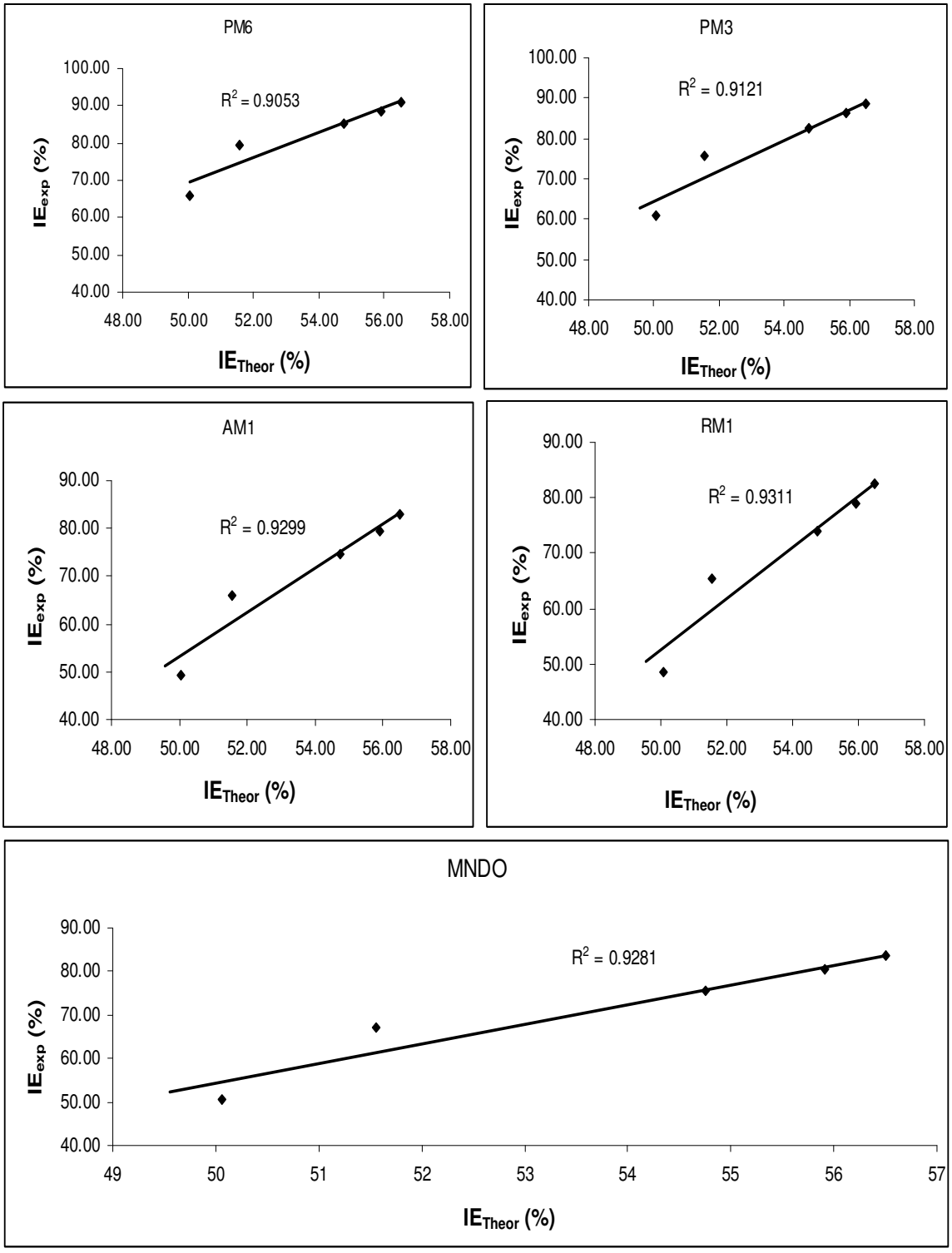


Fig. 4.24: Variation of experimental with theoretical inhibition efficiencies of GLY in gas phase for the various Hamiltonians

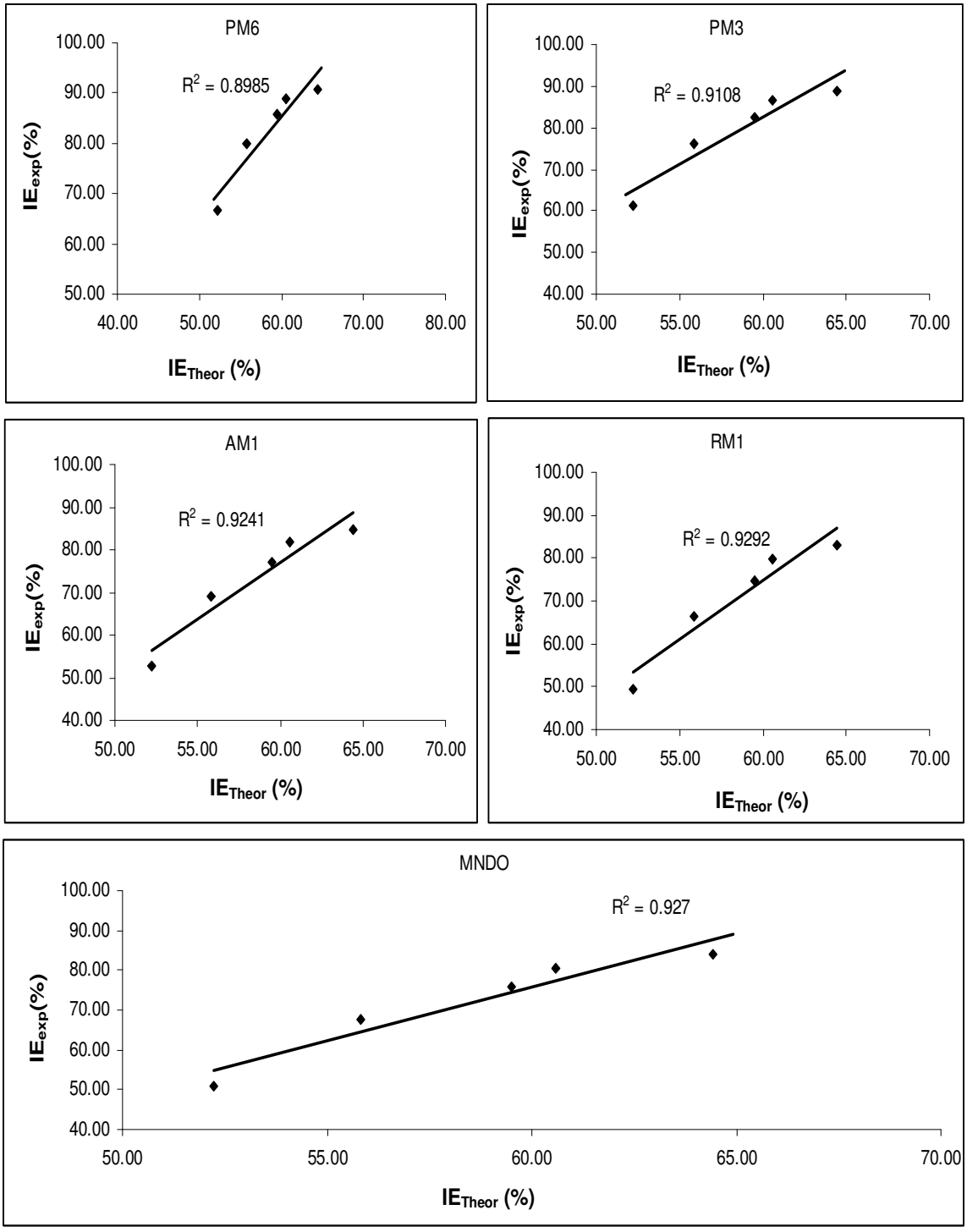


Fig. 4.25: Variation of experimental with theoretical inhibition efficiencies of LEU in gas phase for the various Hamiltonians

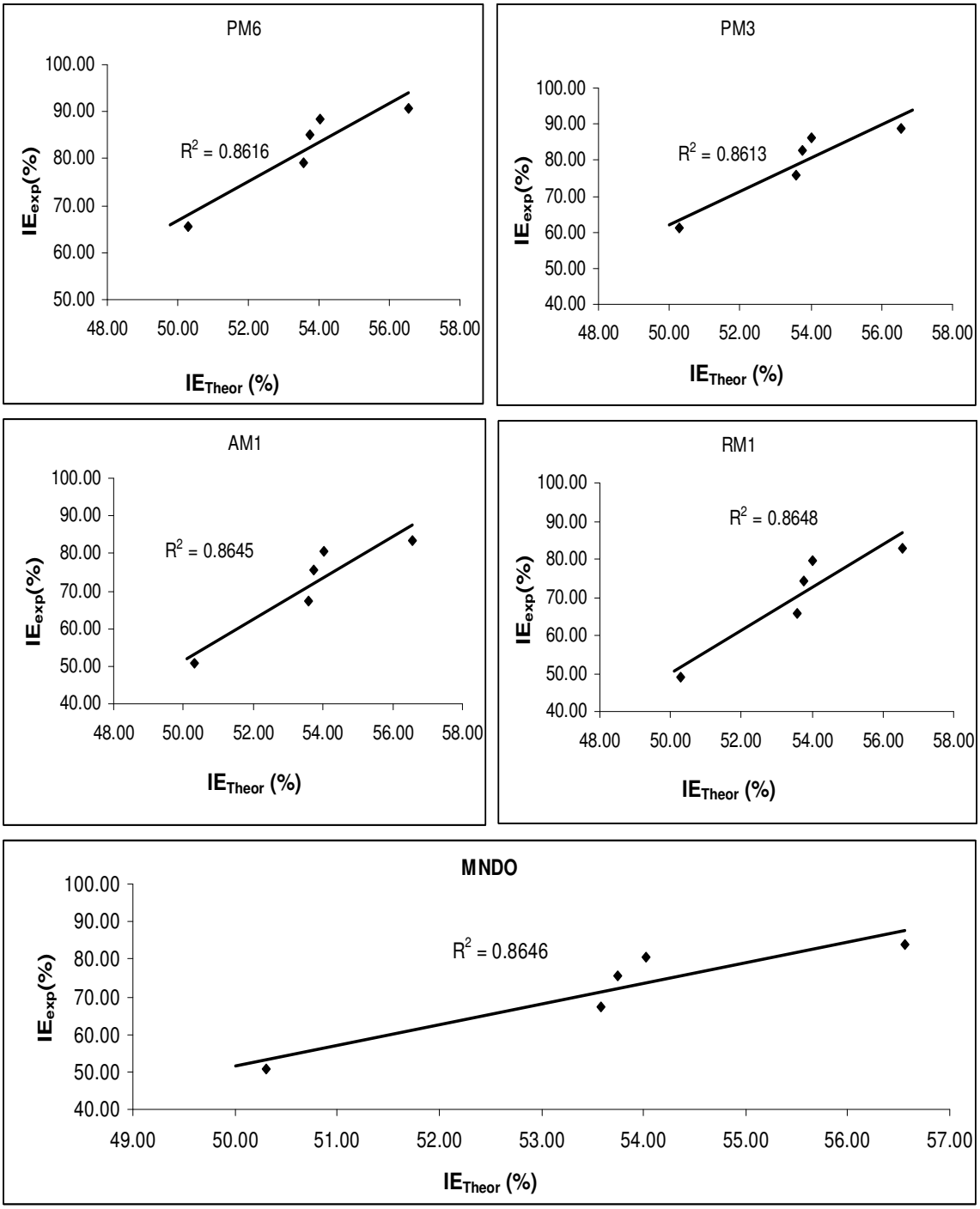


Fig. 4.26: Variation of experimental with theoretical inhibition efficiencies of ALA in gas phase for the various Hamiltonians

It was also necessary to predict the inhibitive potentials of the amino acids studied using data obtained from aqueous phase calculations. In light of the above, the application of equation 4.42 to aqueous phase medium yielded equations 4.48 to 4.52 for PM6, PM3, AM1, RM1 and MNDO Hamiltonians respectively.

$$IE_{Theor}(\%) = \frac{(0.950E_{HOMO} + 1.4785E_{LUMO} + \Delta E + \mu + 0.97498E_{diel} + 11.6321)*C \times 100}{(1+((0.950E_{HOMO} + 1.4785E_{LUMO} + \Delta E + \mu + 0.97498E_{diel} + 11.6321)*C} \quad 4.48$$

$$IE_{Theor}(\%) = \frac{(0.860E_{HOMO} + 1.37E_{LUMO} + \Delta E + \mu + 1.193E_{diel} + 1.193 + 70.79)*C \times 100}{(1+(0.860E_{HOMO} + 1.37E_{LUMO} + \Delta E + \mu + 1.193E_{diel} + 1.193 + 70.79)*C} \quad 4.49$$

$$IE = \frac{(0.862E_{HOMO} + 1.08E_{LUMO} + 0.7356\Delta E + \mu + E_{diel} + 11.24)*C \times 100}{(1+(0.862E_{HOMO} + 1.08E_{LUMO} + 0.7356\Delta E + \mu + E_{diel} + 11.24)*C} \quad 4.50$$

$$IE = \frac{(0.896E_{HOMO} + 1.38E_{LUMO} + \Delta E + \mu + 1.649E_{diel} + 18.38)*C \times 100}{(1+(0.896E_{HOMO} + 1.38E_{LUMO} + \Delta E + \mu + 1.649E_{diel} + 18.38)*C} \quad 4.51$$

$$IE_{Theor}(\%) = \frac{(1.301E_{HOMO} + 0.946E_{LUMO} + \Delta E + \mu + 3.467E_{diel} + 22.28)*C \times 100}{(1+(1.301E_{HOMO} + 0.946E_{LUMO} + \Delta E + \mu + 3.467E_{diel} + 22.28)*C} \quad 4.52$$

The theoretical inhibition efficiencies computed from equations 4.48 to 4.52 are recorded in Table 4.19. In Figs. 4.27, 4.28, 4.29 and 4.30, Plots of the variation of experimentalinhibition efficiencies with theoretical inhibition efficiencies from aqueous phase calculations are presented in figs 4.27, 4.28, 4.29 and 4.30. From the Figures, it is evident that R^2 values for the various inhibitors and Hamiltonians are also close to unity. Consequently, therefore, it can be reasonably assumed that the aqueous phase calculations can adequately be used as model for the inhibitive behaviour of amino acids in HCl solutions.

Table 4.19: Theoretical inhibition efficiencies (IE_{Theor}) of some amino acids from aqueous phase calculations

Inhibitor	C (g/l)	Inhibition efficiency (%)				
		PM6	PM3	AM1	RM1	MNDO
CYS	0.1	87.70	50.96	63.71	63.71	58.24
	0.2	93.45	67.51	77.83	77.83	73.61
	0.3	95.54	75.71	84.04	84.04	80.71
	0.4	96.61	80.61	87.53	87.53	84.7
	0.5	97.27	83.86	89.77	89.77	87.46
GLY	0.1	87.81	50.22	63.26	63.26	50.53
	0.2	93.51	66.86	77.5	77.50	67.14
	0.3	95.58	75.16	83.78	83.78	75.39
	0.4	96.65	80.14	87.32	87.32	80.34
	0.5	97.3	83.45	89.59	89.59	83.63
LEU	0.1	87.69	48.74	61.76	61.76	51.83
	0.2	93.44	65.54	76.36	76.36	68.28
	0.3	95.53	74.05	82.89	82.89	76.35
	0.4	96.61	79.18	86.59	86.59	81.15
	0.5	97.27	82.62	88.98	88.98	84.33
ALA	0.1	87.78	50.12	62.67	62.67	50.69
	0.2	93.49	66.77	77.05	77.05	67.27
	0.3	95.57	75.09	83.44	83.44	75.51
	0.4	96.64	80.07	87.04	87.04	80.44
	0.5	97.29	83.4	89.35	89.35	83.71

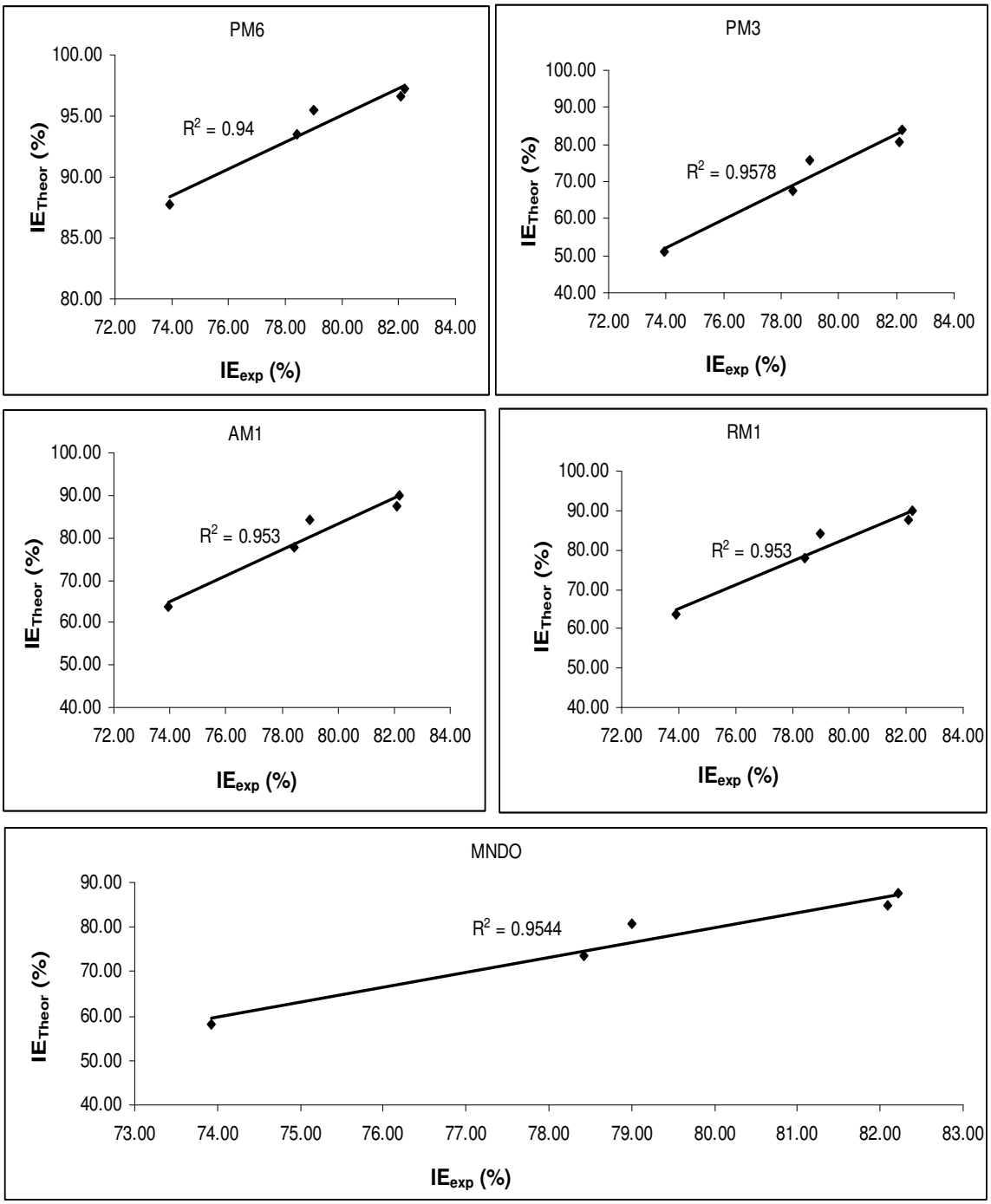


Fig. 4.27: Variation of experimental with theoretical inhibition efficiencies of CYS in aqueous phase for the various Hamiltonians

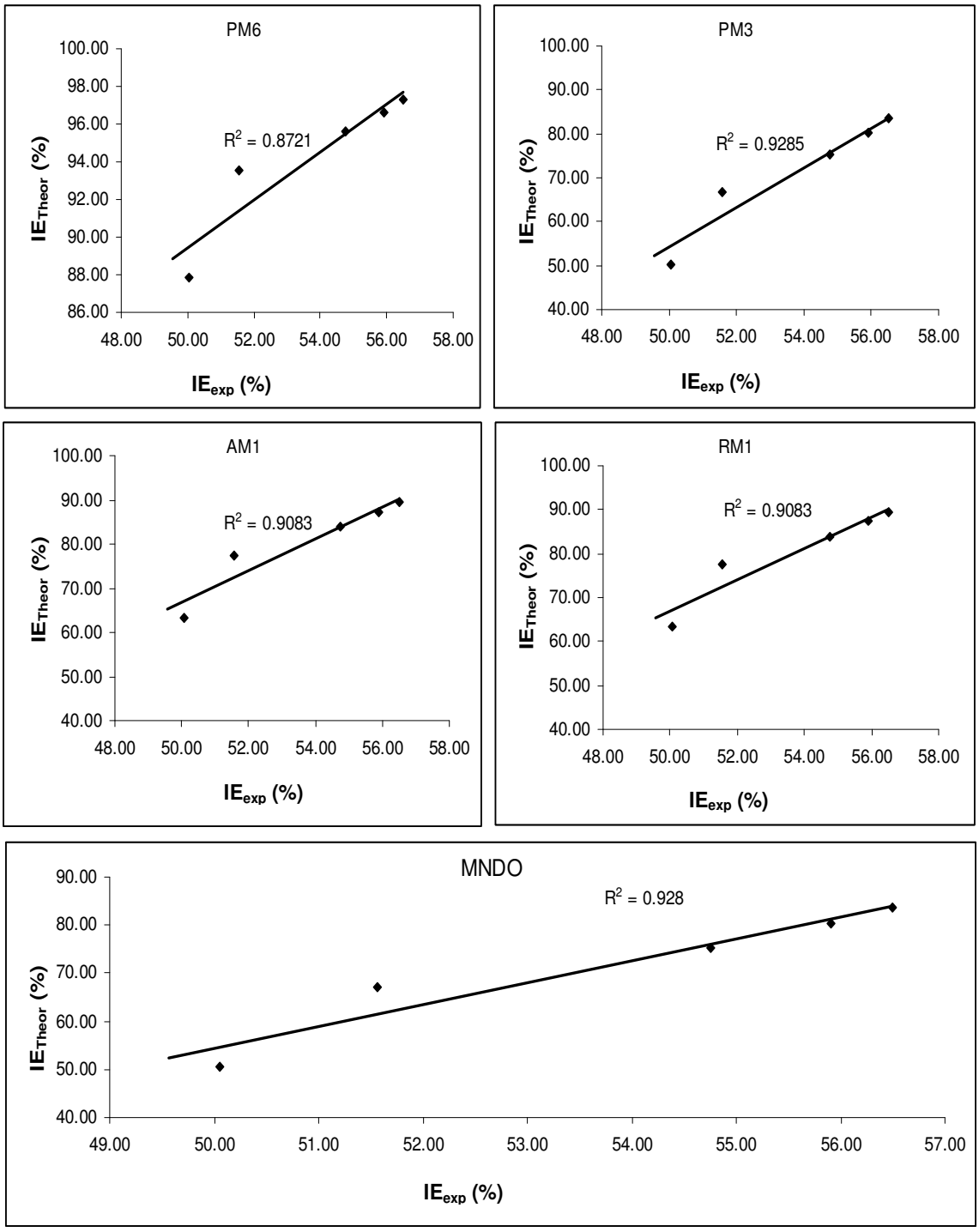


Fig. 4.28: Variation of experimental with theoretical inhibition efficiencies of GLY in aqueous phase for the various Hamiltonians

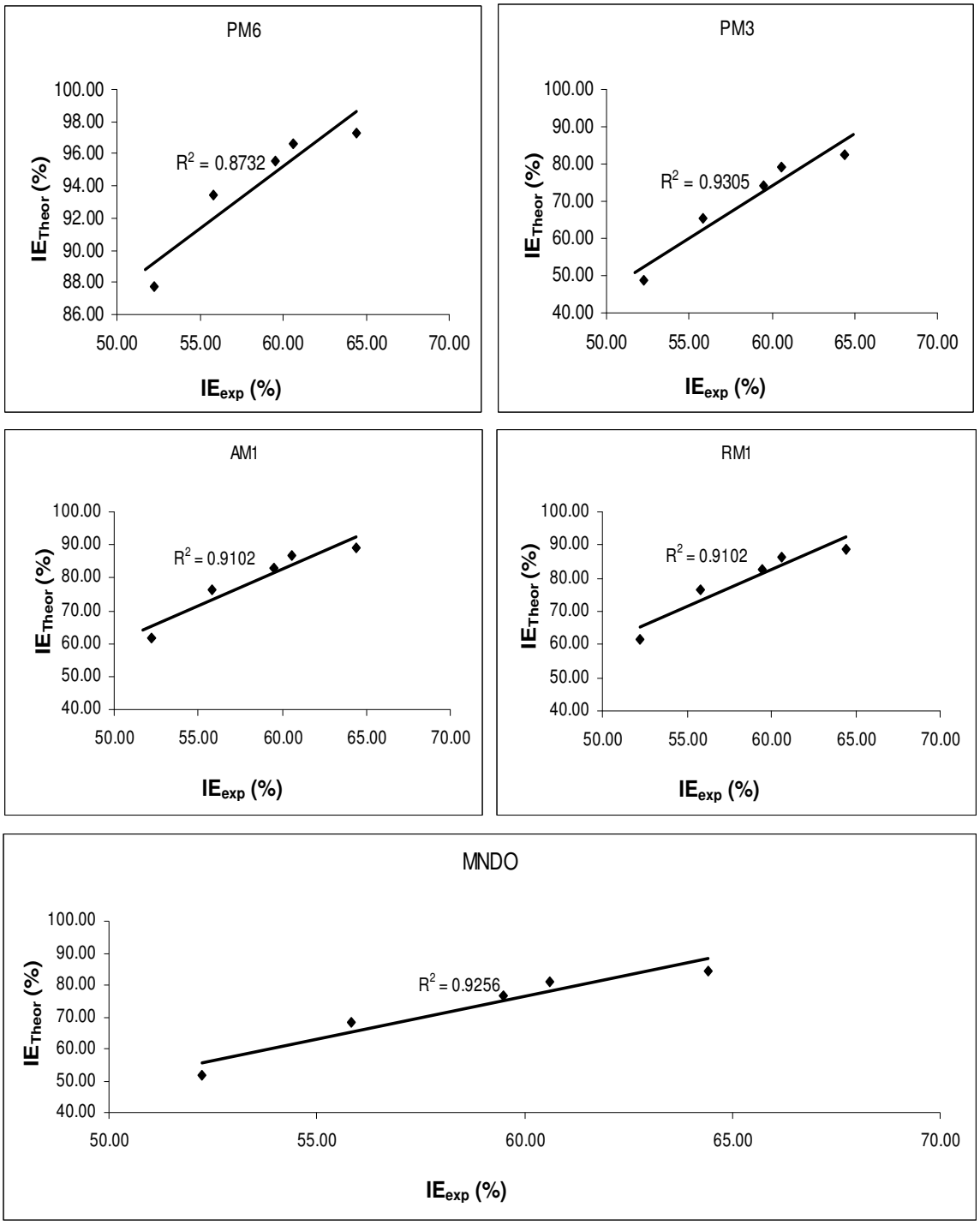


Fig. 4.29: Variation of experimental with theoretical inhibition efficiencies of LEU in aqueous phase for the various Hamiltonians

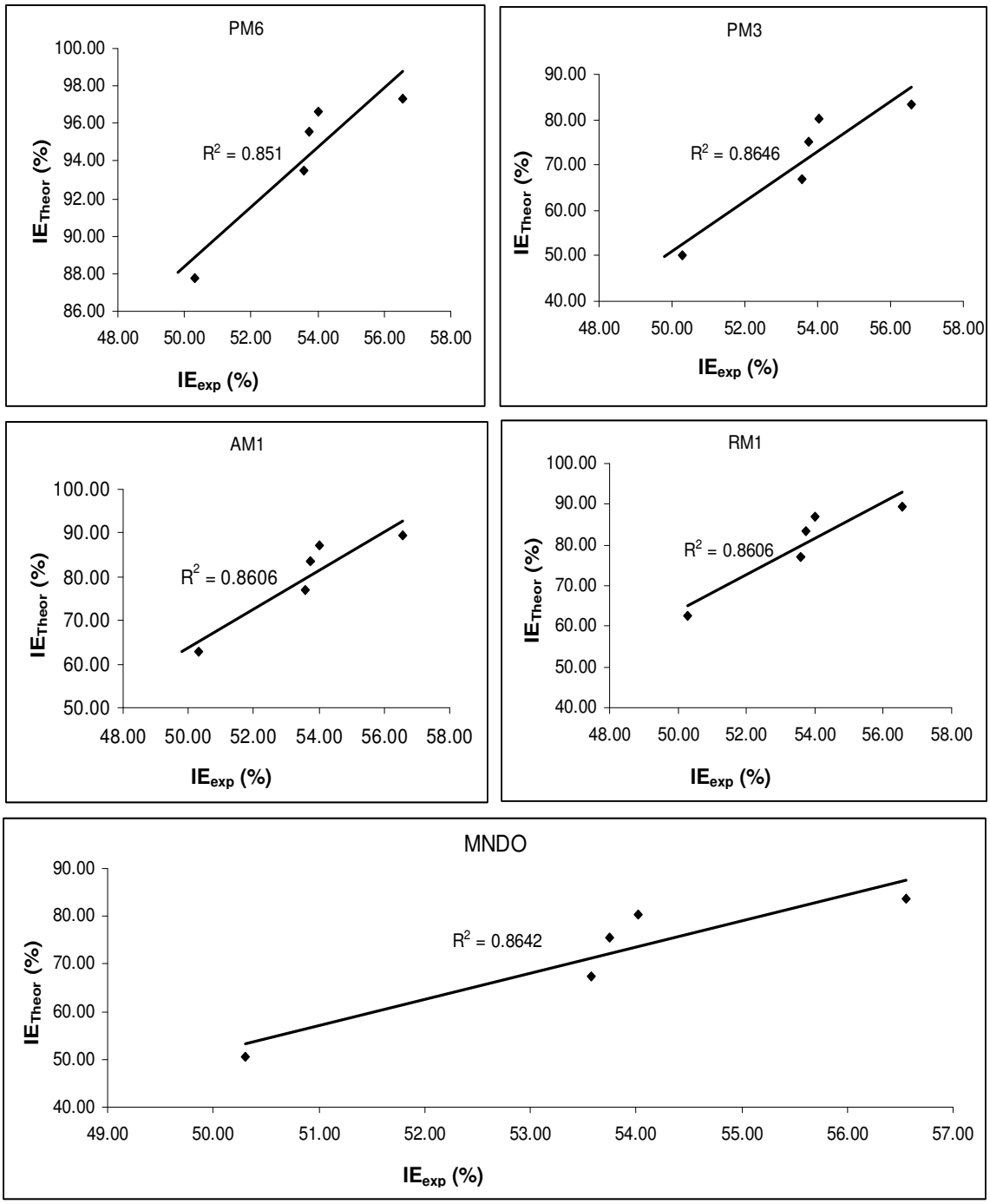


Fig. 4.30: Variation of experimental with theoretical inhibition efficiencies of ALA in aqueous phase for the various Hamiltonians

4.2.2.3 Mechanism of inhibition

The mechanism of inhibition of mild steel corrosion by the amino acids probably involves the blockage of mild steel surface by the inhibitor molecules via physical adsorption (Eddy and Ita, 2010a). However, it is worth nothing that after physical adsorption, the mechanism of chemical adsorption is certain. In acidic medium, the amino acids may be protonated (fig 4.31a, b). The protonated form of the amino acids may accept two electrons from iron in mild steel leading a lone pair of electrons in the amino nitrogen. After protonation, it is assumed that the double bond in the carbonxylic functional group of the amino acids may be broken (Fig. 4.31 c, d). This implies that a negative charge may be present in the amino acids (F4.31e). The overall mechanism therefore probably involves the adsorption of two molecules of the charged amino acids on Fe2+ in mild steel. In this case, it is assumed that Zwitter ion forms may contribute significantly to the actual state of the molecules leading their adsorption. However, if it is assumed that Zwitter ion forms of the molecules do not contribute to their respective adsorption, then both functional groups may be adsorbed on the cathodic sites of the corroding metal as shown in Fig. 4.31f. From the above, it is evident that the adsorption of the amino acids may be governed by,

(1) Ion-pair adsorption between charged inhibitor's molecule and charged metal surface

(2) Interaction between the lone pair of electrons on oxygen and nitrogen atom with the vacant d orbital of metal atom.

Therefore, in the present case, primary attachment between the mild steel surface and the amino acids may be through ion-pair mechanism and dπ-pπ

interaction with the lone pair of electron on oxygen atom of carboxyl group (of amino acid)

Chapter 5

CONCLUSIONS AND RECOMMENDATIONS

From the results and findings of the study, the following conclusions are made,

(i) CYS, GLY, LEU and ALA inhibited the corrosion of mild steel through the mechanism of physical adsorption. The adsorption of the inhibitor on mild steel surface is exothermic (values of ΔH_{ads} were negative) spontaneous (values of ΔG_{ads} were negative) and supports the Langmuir adsorption model.

(ii) The corrosion of mild steel in HCl containing various concentrations of CYS, GLY, LEU and ALA follows a first order reaction. Also the studied amino acids increase the half life of mild steel in HCl solutions.

(iii) The activation energies for the inhibited corrosion reaction of mild steel are higher than those calculated for the blank. Therefore, the studied amino acids retarded the corrosion of mild steel in HCl solutions.

(iv) Experimental inhibition efficiencies of the studied amino acids correlated excellently with E_{LUMO}, E_{HOMO}, ΔE, $E_{dielect}$ and with μ for both gas and aqueous phases. Correlations between theoretical inhibition efficiencies obtained from QSAR calculations were also excellent.

(v) From FTIR data, Fukui function calculations, consideration of Huckel charges on the atoms, it is indicative that the site for electrophilic attack on the studied amino acids is at the amino nitrogen atom.

From the above, the use of the studied amino acids as inhibitors for the corrosion of mild steel is advocated in this work. Extension of quantum chemical studies to other amino acids is recommended for future study.

REFERENCES

Abdallah, M. (2004a). Guar gum as corrosion inhibitor for carbon steel in sulphuric acid solutions. *Portugaliae Electrochimica Acta*, **22:**161-175.

Abdallah, M. (2004b). Antibacterial drugs as corrosion inhibitors for aluminium in HCl solution. *Corrosion Science,***46:** 1981-1996.

Abiola K.O., Oforka, N. C, Ebenso, E.E. and Nwinuka, N.M. (2007). Ecofriendly corrosion inhibitors: Inhibitive action of Delonix regia extract for the corrosion of aluminium in acidic medium. *Anti-Corrosion Methods and Materials,***54(4):** 219-224.

Acharya, S. and Upadhyay, S.N. (2004). The inhibition of corrosion of mild steel by some flouroquinolones in sodiumchloride solution. *Transaction of the Indian Institute of Metals,***57(3):**297-306.

Affrossman, S.,Daviot J.,Holmes D,Pethrick R.A. andWilson, M. (2001). Molecular design for inhibition of titanium corrosion in resist cleaner systems. *Corrosion Science,***43 :**939–950.

Ajayi, E.O. (2003). Predictive model for evaluating corrosion rate of mild steel in six environments. LAUTECH, *Journal of Engineering and Technology,***1:**75-81.

Akpan, I.A. (1994). Kinetic study of corrosion of aluminium and steel in acidic medium and their inhibition by thiosemicarbozone derivatives M.Sc. Thesis. University of Calabar. Calabar.

Aksot, A. A. and Bilgic, S. (1992). *The effect of amino acids on the corrosion of nickel in H_2SO_4.Corrosion Science,***33:**379-387.

Allam, N.K. (2007). Thermodynamic and quantum chemistry characterization of the adsorption of triazole derivatives during Muntz corrosion in acidic and neutral solutions. *Journal of Applied surface science* **253 :** 4570–4577.

Armstrong D.R.,Ferrari, E.S.,Roberts, K.J and Adams, D.(1998) An examination of the reactivity of zinc di-alkyl-di-thiophosphate in relation to its use as an anti-wear and anti-corrosion additive in lubricating oils Wear, **217 :**276–287.

Armstrong, D. R.,Ferrari, E. S.,Roberts, K.J and Adams D.(1997) An investigation into the molecular stability of zinc di-alkyl-di-thiophosphates (ZDDPs) in relation to their use as anti-wear and anti-corrosion additives in lubricating oils Wear 208:138–146.

Arora, P., Kumar, S., Sharma,M.K. and Mathur, S.P. (2007). Corrosion inhibition by capparis deciduas in acidic media. *Electronic Journal of chemistry***4(4):**450-456.

Arshadi, M.R.,Lashgari, M. and Parsafar, G.A. (2004). Cluster approach to corrosion inhibition problems: interaction studies. *Materials Chemistry and Physics***86 :** 311– 314.

Arslan, T., Kandemirli, F., Ebenso, E. E., Love, I and Alemu, H. (2009). Quantum chemical studies on the corrosion inhibition of some sulphonamides on mild steel in acidic medium. *Corrosion Science***51:** 35-47.

Ashassi-Sorkhabi, H.,Shaabani, B. And Seifzadeh, D. (2005b). Effect of some pyrimidinic Schiff bases on the corrosion of mild steel in hydrochloric acid solution. *Electrochimica Acta,***50:**3446–3452.

Ashassi-Sorkhabi, H.,Shabani, B.,Aligholipour, B.,Seifzadeh, D. (2006). The effect of some Schiff bases on the corrosion of aluminium in hydrochloric acid solution. *AppliedSurface Science***252:**4039–4047.

Ashassi-Sorkhabi, H.,Shabani, B.andSeifzadeh, D. (2005b). Corrosion inhibition of mild steel by some Schiff base compounds in hydrochloric acid. *Applied surface science***239 :**154–164.

Ashassi-Sorkhabi, H., Ghasemi, Z. and Seifzadeh, D. (2005a). The inhibition effect of some amino acids towards the corrosion of aluminium in 1 M HCl + 1 M H_2SO_4 solution. *Applied Surface Science***249:**408-418.

Ashassi-Sorkhabi, H., Majidi, M. R. and Seyyedi, K. (2004). Investigation of inhibition effect of some amino acids against steel corrosion in HCl solution. *Applied Surface Scienc,***225:**176–185.

Atkins, P. (2002). *Physical Chemistry*, 7th edition. Oxford: Oxford press.

Attar, M.M. and Scantlebury, J.D.(2005). Polyaniline as a possible inhibitor for the corrosion of mild steel. *Journal of Corrosion and Engineering***8(1):**97-99.

Awad, M.K. (2004). Semiempirical investigation of the inhibition efficiency of thiourea derivatives as corrosion inhibitors*Journal of elctroanalytical chemistry,***567:**219–225.

Babic´-Samardzˇija, K. and Hackerman, N. (2006). Iron corrosion inhibition with dihydrobis - and hydrotris-(1-pyrazolyl)borates. *Anti-corrosion Method and Material,***53 :** 19– 29.

Babic´-Samardzˇija, K.,Khaled, K.F. and Hackerman, N. (2005a). Investigation of the inhibiting action of O-, S- and N-dithiocarbamato(1,4,8,11-tetraazacyclotetradecane)cobalt(III) complexes on the corrosion of iron in $HClO_4$ acid *Applied Surface Science***240 :** 327–340.

Babic´-Samardz˘ija, K.,Khaled, K.F. and Hackerman, N. (2005b). N-heterocyclic amines and derivatives as corrosion inhibitors for iron in perchloric acid. *Anti-corrosion Method and Materials***52 :**11–21.

Badawy, W. A., Ismail, K. M., Ahlam, H. and Fathi, M. (2006). Corrosion control of Cu–Ni alloys in neutral chloride solutions by amino acids. *Electrochimica Acta***51:**4182–4189

Barouni, K., Bazzi, L., Salghi, R., Mihit, M., Hammouti, B., Albourine, A. and El Issami, S. (2008). *Some amino acids as corrosion inhibitors for copper in nitric acid solution*. *Materials Letters***62:**3325–3327.

Bartley, J.,Huynh, N.,Bottle, S.E.,Flit, H.,Notoya, T. and Schweinberg, D.P. (2003). Computer simulation of the corrosion inhibition of copper in acidic solution by alkyl esters of 5-carboxybenzotriazole. *Corrosion Science***45:** 81–96.

Benabdellah, M.,Touzani, R.,Aouniti, A.,Dafali, A.,El Kadiri, S.,Hammouti, B. and Benkaddour, M. (2007). Inhibitive action of some bipyrazolic compounds on the corrosion of steel in 1 M HCl Part I: electrochemical study. *material Chemistry and Physics***105:**373–379.

Benali, O.,Larabi, L.,Traisnel, M.,Gengembre, L. and Harek, Y. (2007). Electrochemical, theoretical and XPS studies of 2-mercapto-1-methylimidazole adsorption on carbon steel in 1 M $HClO_4$.*Applied Surface Science***253 :** 6130–6139.

Bendahou, M.A., Benadellah, M. B. E. and Hammouti, B. B. (2006). A study of rosemary oil as a green corrosion inhibitor for steel in 2M H_3PO_4. *Pigment and Resin Technology***35(2):**95-10.

Bentiss, F.,Bouanis, M.,Mernari, B.,Traisnel, M.,Vezin, H. and Lagrenée, M. (2007a). Understanding the adsorption of 4H-1,2,4-triazole derivatives on mild steel surface in molar hydrochloric acid. *Applied Surface Science,***253 :**3696–3704.

Bentiss, F.,Lebrini, M.,Lagrenée, M.,Traisnel, M.,Elfarouk, A. and Vezin, H. (2007b). The influence of some new 2,5-disubstituted 1,3,4-thiadiazoles on the corrosion behaviour of mild steel in 1 M HCl solution: AC impedance study and theoretical approach. *Electrochimica Acta***52:** 6865–6872.

Bentiss, F.,Lebrini, M.,Vezin, H. and Lagrenée, M. (2004a). Experimental and theoretical study of 3-pyridyl-substituted 1,2,4-thiadiazole and 1,3,4- thiadiazole as corrosion inhibitors of mild steel in acidic media. *Materia Chemistry and Physic*s**87 :**18–23.

Bentiss, F.,Traisnel, M.,Chaibi, N.,Mernari, B.,Vezin, H. and Lagrenée, M. (2002). 2,5-Bis(nmethoxyphenyl)- 1,3,4-oxadiazoles used as corrosion inhibitors in acidic media: correlation between inhibition efficiency and chemical structure. *Corrosion Science***44 :** 2271–2289.

Bentiss, F.,Traisnel, M.,Vezin, H. and Lagrenée, M. (2003). Linear resistance model of the inhibition mechanism of steel in HCl by triazole and oxadiazole derivatives: structure–activity correlations. *Corrosion Science***45:**371–380.

Bentiss, F.,Traisnel, M.,Vezin, H.,Hildebrand, H.F. and Lagrenée, M. (2004). 2,5-Bis(4-dimethylaminophenyl)-1,3,4-oxadiazole and 2,5-bis(4- dimethylaminophenyl)-1,3,4-thiadiazole as corrosion inhibitors for mild steel in acidic media. *Corrosion Science***46:**2781–2792.

Bereket, G.,Güleç, M. and Yurt, A. (2006). Inhibition efficiencies of some organic compounds on the corrosion of zinc in alkaline media. *Anti-corrosion Method and materials***53 :**52–56.

Bereket, G.,Hür, E. and Öğretir, C. (2002). Quantum chemical studies on some imidazole derivatives as corrosion inhibitors for iron in acidic medium. *Journal of Molecular Structure* (THEOCHEM) **578 :**79–88.

Bereket, G.,Öğretir, C. and Özs_ahin, C. (2003a). Quantum chemical studies on the inhibition efficiencies of some piperazine derivatives for the corrosion of steel in acidic medium. *Journal of Molecular Structure* (THEOCHEM) **663 :**39–46.

Bereket, G.,Öğretir, C. and Yurt, A. (2001). Quantum mechanical calculations on some 4- methyl-5-substituted imidazole derivatives as acidic corrosion inhibitor for zinc. *Journal of Molecular Structure* (THEOCHEM),**571:**139–145.

Bhrara, K. and Singh, G. (2006). The inhibition of corrosion of mild steel in 0.5 M sulphuric acid solution in the presence of benzyl triphenyl phosphonium bromide. *Applied Surface Science***253:** 846–853.

Bereket, G., Öğretir, C., Yaman, M. and Hür, E. (2003b). Tautomeric studies on 2-mercapto pyrimidines and their significance in corrosion process. *Journal of Molecular Structure* (THEOCHEM) **625:**31–38.

Bilgic, L. and Caliskan, N. (2001). An investigation of some Schiff bases as corrosion inhibitors for austenite chromium-nikel steel in H_2SO_4. *Journal of Applied Electrochemistry***31:**79-83.

Blajiev, O. and Hubin, A. (2004). Inhibition of copper corrosion in chloride solutions by amino-mercapto-thiadiazole and methyl-mercapto-thiadiazole: an impedance spectroscopy and a quantum chemical investigation. *Electrochimica Acta,***49:** 2761–2770.

Bouayed, M.,Rabaa, H.,Srhiri, A.,Saillard, J.Y. and Ben Bachir, A. (1999). Experimental and theoretical study of organic corrosion inhibitors on iron in acidic medium. *Corrosion Science***41:**501–517.

Bouklah, M.,Hammouti, B.,Benkaddour, M.,Attayibat, A. and Radi, S. (2005). Corrosion inhibition of steel in hydrochloric acid solution by new bipyrazole derivatives. *Pigment Resin Technology***34:**197–202.

Bouyanzer, A and Hammouti, B. (2004). A study of anti-corrosion effects of Artemisia oil on steel. *Pigment and Resin Technology***33(5):**287-292.

Cardoso, S.P., Hollauer, E., Borges, L.E.P. and Gomes, J.A.C.P. (2006). QSPR prediction analysis of corrosion inhibitors in hydrochloric acid on 22%-Cr stainless steel. *Journal of Brazilian Chemical Society***17:** 1241-1249.

Cardoso, S.P.,Gomes, J.A.C.P.,Borges, L.E.P. and Hollauer, E. (2007). Predictive QSPR analysis of corrosion inhibitors for super 13% Cr steel in hydrochloric acid. *Brazilain Journal of ChemicalEngineering***24 :** 547–559.

Chakrabarti, A. (1984). Quantum chemical study of the corrosion inhibition of mild steel in 6 percent (wt/wt) HCl by means of cyanoguanidine derivatives. *Brazil Corrosion Journal***19:**124–126.

Cheng, J.X. and Zhou, J.M.(1993). Control of corrosion by inhibitors in drilling muds containing high concentration of H_2S. *Corrosion Science Sectariate* (NACE),**49:** 170–174.

Chetounani, A., Hammouti, B. and Benkaddour, M. (2004). Corrosion inhibition of iron in hydrochloric acid solution by jojoba oil. *Pigment and Resin Technology,***33(1):**26-31.

Chittendon, F. (1951). RHS Dictionary of Plants Plus Supplement, OxfordUniversity Press.

Clark, D.S. and Varney, W.R. (1987). Physical Metallurgy for Engineers. Canada: Van Nostrand Reinhold ltd.

Costa, J.M. and Lluch, J.M. (1984). The use of quantum mechanics calculations for the study of corrosion inhibitors. *Corrosion Science***11/12:** 929–933.

Dewar, M.J.S. and Thiel, W. (1977). Ground states of molecules.38. The MNDO method Approximations and parameters. *Journal of American Chemical Society***99:**4899–4907.

Dewar, M.J.S., Zoebisch, E.G., Healy, E.F. and Stewart, J.J.P. (1985). Development and use of quantum mechanical molecular models.76.AM1: a new general purpose

quantum mechanical molecular model. *Journal of American Chemical Society***107:** 3902– 3909.

Domenicano, A. and Hargittai,I.(1992). Accurate molecular structures, their determination and importance, Oxford University Press, New York.

Ebenso, E. E., Eddy, N. O. and Odiongenyi, A. O. (2008a). Corrosion inhibitive properties and adsorption behaviour of ethanol extract of Piper guinensis as a green corrosion inhibitor for mild steel in H_2SO_4. *African Journal of Pure & Applied Chemistry,***4(11):** 107-115.

Ebenso, E.E. (2003a). Effect of halide on the corrosion inhibition of steel in H_2SO_4 using methyl red-Part1. *Bulettin of Electrochemistry,***19(5):** 209-216.

Ebenso, E.E. (2003b). Synergistic effect of halides ions on the corrosion inhibition of aluminium in H_2SO_4 using 2-acetylphenothiazine. *Material Chemistry& Physics*,**79:** 58-70.

Ebenso, E.E. (2004). Effect of methyl red and halide ions on the corrosion of aluminium in H_2SO_4. Part 2. *Bullettin of Electrochemistry* **12:**551-559.

Ebenso, E.E. and Ekpe, U.J. (1996). Kinetic study of corrosion and corrosion inhibition of mild steel in H_2SO_4 using Carica papaya leaves extract. *West African Journal of Boilogical Applied Chemistry***41:**21-27.

Ebenso, E.E., Ekpe, U.J. and Ibok, U.J. (1998). Studies on the inhibition of mild steel corrosion by some plant extracts in acidic medium. *Discovery and Innovation***10:**52-59.

Ebenso, E.E., Ekpe, U.J., Umoren, S.A., Jackson, E., Abiola, O. K. and Oforka, N.C. (2005). Synergistic effect of halides ions on the corrosion inhibition of aluminium in acidic medium by some polymers. *Journal of Applied Polymer Science***100:**2889-2894.

Ebenso, E.E., Ibok, U.J., Ekpe, U.J., Umoren, S., Ekarete Jackson, Abiola, O.K., Oforka, N.C., and Martinez S. (2004a). Corrosion inhibition studies of some plant extracts on aluminiumin acidic medium. *Transaction Of SAEST*, **39(4):**117-123.

Ebenso, E.E., Okafor, P.C., Ibok, U.J., Ekpe, U.J. and Onuchukwu, A.I. (2004b). The joint effect of halide ions and methylene blue on the corrosion inhibition of aluminium and mild steel in acid corrodent. *Journal of Chemical Society of Nigeria***29(2):**15-25.

Eddy, N. O. (2008). Inhibition of the corrosion of mild steel in H_2SO_4 by some antibiotics. Ph. D Thesis, University of Calabar, Calabar.

Eddy, N. O. (2009a). Ethanol extract of *Phyllanthus amarus* as a green inhibitor for the corrosion of mild Steel in H_2SO_4. *Portugaliae Electrochimica Acta***27(5):**579-589.

Eddy, N. O. (2009b). Inhibitive and adsorption properties of ethanol extract of *Colocasia esculenta* leaves for the corrosion of mild steel in H_2SO_4. *International Journal of Physical Science***4(3):** 1-7.

Eddy, N. O. and Ebenso, E. E. (2008). Adsorption and inhibitive properties of ethanol extract of *Musa sapientum* peels as a green corrosion inhibitor for mild steel in H_2SO_4. *African Journal of Pure and Applied Chem*istry **2(6):** 1-9.

Eddy, N. O. and Ebenso, E. E. (2010a). Quantum chemical studies on the inhibition potentials of some penicillin compounds for the corrosion of mild steel in 0.1 M HCl. *Journal of Molecular Modeling***16:**1291-1306

Eddy, N. O. and Ebenso, E. E. (2010b). Corrosion inhibition and adsorption properties of ethanol extract of Gongronema latifolium on mild steel in H_2SO_4. *Pigment and Resin Technology***42(7):** 1029-1032.

Eddy, N. O. (2010). Theoretical study on some amino acids and their potential activity as corrosion inhibitors for mild steel in HCl. *Molecular Simulation.* **35(5)**:354-363.

Eddy, N. O. and Odoemelam, S. A. (2009). Inhibition of the corrosion of mild steel in H_2SO_4 by ethanol extract of *Aloe vera. Resin and Pigment Technology***38(2):** 111-115.

Eddy, N. O., Ekwumengbo, P. A. and Mamza, P. A. P. (2009a). Ethanol extract of *Terminalia catappa* as a green inhibitor for the corrosion of mild steel in H_2SO_4. *Green Chemistry Letters and Review,***2(4):** 223-231.

Eddy, N. O., Ibok, U. J. and Ebenso, E. E. (2009b). Adsorption, synergistic inhibitive effect and quantum chemical studies on ampicillin and halides for the corrosion of mild Steel, *Journal of Applied Electrochemistry***DOI:** 10.1007/s10800-009-0015-z

Eddy, N. O., Ibok, U. J., Ebenso, E. E., Ahmed, El Nemr, and El Sayed, H.El Ashry (2009c). Quantum chemical study of the inhibition of the corrosion of mild steel in H_2SO_4 by some antibiotics. *Journal of Molecular Modeling,***15(9):** 1085-1092.

Eddy, N. O., Odoemelam, S. A. and Ibiam. (2009d). Adsorption and inhibitive properties of ethanol extract of *Costus afer* on the inhibition of the corrosion of mild steel in H_2SO_4. *Journal Surface Science Technol*ogy,**25 (3-4):**1-14.

Eddy, N. O., Odoemelam, S. A. and Odiongenyi, A. O. (2008b). Ethanol extract of Musa acuminate peel as an eco-friendly inhibitor for the corrosion of mild steel in H_2SO_4. *Advances in natural and Applied Sciences***2(1):**35-42.

Eddy, N. O., Odoemelam, S. A. and Odiongenyi, A. O. (2009f). Inhibitive, adsorption and synergistic studies on ethanol extract of Gnetum africana as green corrosion inhibitor for mild steel in H_2SO_4. *Green Chemistry Letters & Review,***2 (2):**111-119.

Eddy, N. O., Odoemelam, S. A. and Odiongenyi, A. O. (2009g). Joint effect of halides and ethanol extract of Lasianthera Africana on the inhibition of the corrosion of mild steel in H_2SO_4. *Jounal of Applied Electrochemistry*,**39(6):** 849 – 857.

Eddy, N.O. and Odoemelam,S.A. (2008a). Effect of pyridoxal hydrochloride-2,4-dinitrophenyl hydrazone on the corrosion of mild steel in HCl. *Journal of Surface Science Technology***24(1-2):** 1-14.

Eddy, N. O., Ekop, A. S. and Odiongenyi, A. O. (2008a). Effect of 2-dichloro-N-[ar,br]-b-hydroxy-a-hydroxymethyl-4-nitrophenethyl]-acetamide on the corrosion of mild steel: Kinetics, thermodynamics and adsorption studies. *Journal of Organic Chemistry***4(2):** 17-30.

Eddy, N.O. and Odoemelam,S.A. (2008b). Norfloxacin and sparfloaxin as corrosion inhibitors for zinc. Effect of concentrations and temperature. *Journal of Material Science,***4:**87.

Eddy, N. O**.** and Ita, B. I. (2010a). QSAR, DFT and Quantum chemical studies on the inhibition potentials of some carbozones for the corrosion of mild steel in HCl. Journal of Molecular Modeling,**DOI:** 10.1007/s00894-010-0731-7.

Eddy, N. O. and Ita, B. I. (2010b). Experimental and theoretical studies on the inhibition potentials of some derivatives of cyclopenta-1,3-diene. *International Journal of Quantum Chemistry* **DOI:** 104152/pea.200904443.

Eddy, N. O. and Mamza, P. A. P. (2009). Inhibitive and adsorption properties of ethanol extract of seeds and leaves of *Azadirachta indica*. *Portugaliae Electrochimica Acta***27(2):** 20-28.

Eddy, N. O., Ibok, U. J. and Ebenso, E. E. (2010a). Adsorption, synergistic inhibitive effect and quantum chemical studies on ampicillin and halides for the corrosion of

mild Steel, *Journal of Applied. Electrochemistry,* **40:**445-456.DOI: 10.1007/s10800-009-0015-z (Published by Springer Journals, Germany).

Eddy, N. O., Odoemelam S. A. and Odiongenyi, A. O. (2009h). Joint effect of halides and ethanol extract of Lasianthera Africana on the inhibition of the corrosion of mild steel in H_2SO_4. *Journal of Applied Electrochemistry*,**39(6):** 849 – 857.

Eddy, N. O., Odoemelam, S. A. and Ibiam (2009e). Adsorption and inhibitive properties of ethanol extract of Costus afer on the inhibition of the corrosion of mild steel in H_2SO_4. *Journal of Surface Science Technology*, **25 (3-4):**1-14.

Eddy, N. O., Odoemelam, S. A. and Ibiam, E. (2010b). Ethanol extract of Occimium gratissimum as a green corrosion inhibitor for mild steel in H_2SO_4. *Green Chemistry Letters and Review***DOI:** 10.1080/17518251003636428.

Edwards, A., Osborne, C., Klenerman, D., Joseph, M., Ostovar, P. and Doyle, M. (1994). Mechanistic studies of the corrosion inhibitor oleic imidazoline. *Corrosion Science***36:**313–325.

Ehteshanmzade, M., Shahrabi, T. and Hosseni, M.G. (2006). Inhibition of copper corrosion by self assembled films of new Schiff bases and their modification with alkanethiols in aqueous medium. *Applied Surface Science***252:**2949-2959.

Ekpe, U.J., Ebenso, E.E. and Ibok, U.J. (1994). Inhibitory action of Azadiracchta indica leaves extract on the corrosion of mild steel in H_2SO_4. *Journal of West African Science Association***37:**13-30.

El Ashry, E.H., El Nemr, A., Essawy, S.A. and Ragab, S. (2008). Corrosion inhibitors partV: QSAR of benzimidazole and 2-substituted derivatives as corrosion inhibitors by using the quantum chemical parameters. Prog. Org. Coat.,**61:** 11–20.

El Ashry, E.H., El Nemr, A., Essawy, S.A. and Ragab, S.(2006b). Corrosion inhibitors partIII : quantum chemical studies on the efficiencies of some aromatic hydrazides and Schiff bases as corrosion inhibitors of steel in acidic medium. ARKIVOC **11:**205–220.

El Ashry, E.H.,El Nemr, A.,Essawy, S.A. and Ragab, S. (2006a). Corrosion inhibitors PartII: quantum chemical studies on the corrosion inhibitions of steel in acidic medium by some triazole, oxadiazole and thiadiazole derivatives. *Electrochimica Acta***51:**3957–3968.

El Ashry, H.E., El Nemr, A., Esawy, S. A. and Ragab, S. (2006C). Corrosion inhibitors Part IV: Quantum chemical studies on the corrosion inhibition of steel in acidic medium by some aniline derivatives. *Journal of Physical Chemistry***1:**41-55.

El Issami, S., Hammouti, B., Kertitm, S., Ait Addi, E. and Salghi, R. (2007). Triazolic compounds as corrosion inhibitors for copper in hydrochloric acid. *Pigment and Resin Technology* **36:**161–168.

Elayyoubi, S.B., Hammouti, S., Kertit, H.O. and Maarouf, E.B. (2004). Corrosion inhibition of mild steel in hydrochloric acid solutions by malonitrile compounds. *Rev. Met. Paris*,**2:**153-157.

El-Etre, A.Y. (1998). Natural honey as corrosion inhibitor for metals and alloy: Copper in neutral aqueous solution. *Corrosion Science,* **40(11):**1845-1850.

El-Etre, A.Y. and Abdallah, M. (2002). Natural honey as corrosion inhibitor for metals and alloys II C-steel in high saline water. *Corrosion Science***42:** 731-738.

El-Etre, A.Y. (2003). Inhibition of aluminum corrosion using Opuntia extract. **45:**2485-2495.

El-Etre, A.Y. (2006). Khillah extract as inhibitor for acid corrosion of SX 326 steel. *Applied Surface Science,* **252:**8521-8525.

El-Rabiee, M.M., Helal, N.H., Abd El-Hafez, G.M. and Badawy, G.A. (2008). Corrosion control of vanadium in aqueous solutions by amino acids.*Journal of Alloys and Compounds***459:** 466–471.

Emregul, K.C. and Hayvali, M. (2006). Studies on the effect of a newly synthesized Schiff base compound from phenazone and vanillin on the corrosion of steel in 2M HCl. *Corrosion Science* **48:** 797-812.

Emregul, K.C., Kurtaran, R. and Atakol, O. (2003). An investigation of chloride-substituted Schiff bases as corrosion inhibitors for steel. *Journal of Corrosion Science***45:**2803-2817.

Evans, U.R. (1981). Introduction to metallic corrosion. London: Edward Arnold.

Fang, J. and Li, J. (2002). Quantum chemistry study on the relationship between molecular structure and corrosion inhibition efficiency of amides. *Journal of Molecular Structure* (THEOCHEM) **593:**179–185.

Feng, Y., Chen, S., Guo, W., Zhang, Y. and Liu, G. (2007). Inhibition of iron corrosion by5,10,15,20-tetraphenylporphyrin and 5,10,15,20-tetra-(4-chlorophenyl)porphyrin adlayers in 0.5 M H_2SO_4 solutions. *Journal of Electroanalytical Chemistry***602 :** 115–122.

Feng, Y., Chen, S., Zhang, H., Li, P., Wu, L., Guo, W. (2006). Characterization of iron surface modified by 2-mercaptobenzothiazole self-assembled monolayers. *Applied Surface Science***253 :** 2812–2819.

Francis, P.E. and Mercer, A.D. (1990). Chemical inhibition for corrosion control. B.G. Clubly edited. England: Royal society of Chemistry.

Fuentealba, P. Perez, P. and Contreras, R. (2000). On the condensed Fukui function *Journal of Chemistry and Physics*,**113 (7):** 2544-2551.

Fukui, K. (1975). Theory of Orientation and Stereoselection, Springer-Verlag, New York.

GadAllah, A.G. and Moustafa, H. (1992). Quantum mechanical calculations of amino pyrazole derivatives as corrosion inhibitors for zinc, copper and α-brass in acid chloride solution. *Journal of Applied Electrochemistry***22:**644–648.

Gao, G. and Liang, C. (2007). Electrochemical and DFT studies of β-amino alcohols as corrosion inhibitors for brass. *Electrochimica Acta***52:** 4554-4559.

Ghasemi, Z. and Tizpar, A. (2006). *The inhibition effect of some amino acids towards Pb–Sb–Se–As alloy corrosion in sulphuric acid solution*. *Applied Surface Science***252:** 3667–3672.

Grüber, C. and Buss, V. (1989). Quantum-mechanically calculated properties for the development of quantitative structure-activity relationships (QSAR'S). pKAvalues of phenols and aromatic and aliphatic carboxylic acids. *Chemosphere***19:**1595–1609.

Hammett, L.P. (1940). Physical Organic Chemistry, New York: McGraw-Hill.,

Hansch, C. and Leo, A. (1979). Substituent constants for correlation analysis in chemistry and biology. New York: Wile

Hasanov, R.,Sadıkogˇlu, M. and Bilgiç, S.(2007). Electrochemical and quantum chemical studies of some Schiff bases on the corrosion of steel in H_2SO_4 solution. *Applied Surface Science***253 :**3913–3921.

He, Y. C., Wang, J.and Huang, B.G. (1997). The corrosion and scaling inhibition by imidazoline derivatives. *Oilfield Chemistry***14:**336–339.

Henríquez-Román, J.H., Padilla-Campos, L., Páez, M.A., Zagal, J.H., Rubio, M.A., Rangel, C.M., Costamagna, J. and Cárdenas-Jirón, G. (2005). The influence of aniline and its derivatives on the corrosion behaviour of copper in acid solution: a theoretical approach. *Journal of Molecular Structure* (THEOCHEM) **757:** 1–7.

Hinchliffe, A. (1994). Modelling Molecular Structures. John Wiley & Sons, New York.

Hinchliffe A. (1999). Chemical Modelling From Atoms to Liquids, John Wiley & Sons, New York.

Hohenberg, P. and Kohn, W. (1964). Inhomogeneous electron gas. Phys. Rev. **136:**864–871.

Hosseini, M.,Mertens, S.F.L.,Ghorbani, M., andArshadi, M.R. (2003). Asymmetrical Schiff bases as inhibitors of mild steel corrosion in sulphuric acid media.*Material Chemistry and Physics***78:** 800–808.

Hosseini, S. M. A., Eftekhar, S. and Amiri, M. (2007). Polarization behavior of stainless steel type 302 in HCl solution of benzotriazole. *Asian Journal of Chemistry*,**19(4):**2574-2580.

Ita, B.I. (2004a). 4-Formylmorpholine hydrazone and 4-formymorpholine: New corrosion inhibitors for mild steel in 0.1M hydrochloric acid solution. *Proccurement Of the Chemical Society Of Nigeria*(Suppl. to the J. of the Chem.)

Ita, B.I. (2004b). A study of corrosion inhibition of mild steel in 0.1M hydrochloric acid by O-vanilin hydrazone. *Bulletine of Electrochemistry*,**20(8):**363-370.

Ita, B.I. (2005). Inhibition of mild steel corrosion in hydrochloric acid by anisaldehyde and anisaldehyde glycine. *Bulletine of electrochemistry***21(7):** 219-323.

Ita, I.B. and Offiong, O.E. (1997). The inhibition of mild steel corrosion in hydrochloric acid by $2,2^{1}$-pyridil and ∞-pyridon. *Materials Chemistry and Physics,***51:**203-210.

Jensen, F. (2007). Introduction to Computational Chemistry. John Wiley & Sons, Chichester.

Jiang, J.Y. and Geng, D.S. (1998). Anti-inflammatory effects of berberine *Chin. Pharmacol. Bulletin***14 :**434–437.

Jones, D.A. (1982). Forms of corrosion, recognition and prevention Dillon, C.P. edited. NACE, Houston. Reprinted by permission of the National Association of Corrosion Engineers.

Ju, H.,n Kai, Z.P.andLi, Y. (2008). Aminic nitrogen-bearing polydentate Schiff base compounds as corrosion inhibitors for iron in acidic media: a quantum chemical calculation.*Corrosion Science***50:** 865–871.

Kalman, E., Felhosi, I., Karman, F.H., Lukovits, I., Telgdi, J. and Palinkas, G. (2000). Environmentally friendly corrosion inhibitors, in Corrosion and Environmental Degradation. Vol. 1 (Scutze, M., edt.). Wiley-VCH, Weinhem, Germany (Series of Materials Sciences and Technology. A Comprehensive treatment).

Kandemirli, F. and Sagdinc, S. (2007). Theoretical study of corrosion inhibition of amides and thiosemicarbazones.*Corrosion Science*,**49 :** 2118–2130.

Kanojia, R. and Singh, G. (2005). An interesting and efficient organic corrosion inhibitor for mild steel in acidic medium, *Surface Engineering,***21:**180–186.

Karelson, M., and Lobanov, V. (1996). Quantum chemical descriptors in QSAR/QSPR studies. *Chemical Review***96:** 1027–1043.

Kelly, L.G., Scully, J.R., Shoessmith, D.W and Buchheit, R.G. (2003). Electrochemical techniques in corrosion science. NewYork. Morcell Dekker.

Khaled, K.F. (2006). Experimental and theoretical study for corrosion inhibition of mild steel in hydrochloric acid solution by some new hydrazine carbodithioic acid derivatives, *Applied Surface Science***252 :**4120–4128.

Khaled, K.F. (2008). Molecular simulation, quantum chemical calculations and electrochemical studies for inhibition of mild steel by triazoles.*Electrochimica Acta***53 :** 3484–3492.

Khaled, K.F.,Babic´-Samardzˇija, K.,Hackerman, N. (2005). Theoretical study of the structural effects of polymethylene amines on corrosion inhibition of iron in acid solutions.*Electrochimica Acta***50:**2515–2520.

Khaled, K.F.,Babic´-Samardzˇija, K.,Hackerman, N. (2006). Cobalt(III) complexes of macrocyclic-bidentate type as a new group of corrosion inhibitors for iron in perchloric acid.*Corrosion Science,***48 :** 3014–3034.

Khalil, N. (2003). Quantum chemical approach of corrosion inhibition.*Electrochimica Acta***48 :** 2635–2640.

Khavasfar, A. and Iran, M. (2006). Study of organic corrosion inhibition on CO_2 corrosion of mild steel by electrochemical measurements. Paper presented at the 5th Internal surface engineering congress. Seattle, Washington. May 16, 2006.

Kiani, M. A. Mousavi, M. F., Ghasemi, S. Shamsipur, M. and Kazemi, S. H. (2008). Inhibitory effect of some amino acids on corrosion of Pb–Ca–Sn alloy in sulphuric acid solution.*Corrosion Science***50:**1035–1045.

Kikuchi, O. (1987). Systematic QSAR procedures with quantum chemical descriptors.*Quant. Struct.-Act. Relat*.,**6:**179–184.

Kliskic, M., Radoservic, J., Gudic, S. and Katalinic, V. (2000). Aqueous extract of Rosmmarius officinalis L. as inhibitor of Al-Mg alloy corrosion in chloride solution. *Journal of Applied Electrochemistry***30:**823-830.

Kouznetsov, D.L.,Podkopeva, O.Y.,Shevchenko, S.M.,Chizhov, Y.V andAltsybeeva, A.I. (2000). Relationship between the inhibition effect and electron structure of phenyl-N,N-dimorpholinemethanes in: Proceedings of the 9th European Symposium on Corrosion Inhibitors (9 SEIC). Ann. Univ. Ferrara, N.S., Sez. V, Suppl. N. **11:**1075-1086.

Krajewka, D., Dabrowska, M., Jackonny, P. and Rozonski, A. (2002). Purole analysis of chloramphenicle: Synthesis and antimicrobial activity. *Acta Pol. Pharm.***59:**127-132.

Kraka, E., and Cremer, D. (2000). Computer design of anticancer drugs. *Journal of American Chemical Society***122 :**8245–8264.

Kumar, A. (2008). Corrosion inhibition of mild steel in hydrochloric acid by sodium laury sulphate. *Electronic Journal of Chemistry***5(2):** 275-280.

Kutsán, G.,Rauscher, A.,Dömötör, G.,Bundula, R andKörtvélyesi, T. (2000). Correlation between structural parameters and inhibitor efficiency of thiocarbamide derivatives in: Proceedings of the 9th European Symposium on Corrosion Inhibitors (9 SEIC). Ann. Univ. Ferrara, N.S., Sez. V, Suppl. N. **11:**761-769.

Lagrenée, M.,Mernari, B.,Chaibi, N.,Traisnel, M.,Vezin, H andBentiss, F. (2001). Investigation of the inhibitive effect of substituted oxadiazoles on the corrosion of mild steel in HCl medium. *Corrosion Science***43:**951–962.

Lashgari, M.,Arshadi, M.R andParsafar, G.A. (2005). A simple and fast method for comparison of corrosion inhibition powers between pairs of pyridine derivative molecules. *Corros. Sci. Sect.* (NACE)**61:** 778–783.

Lashgari, M.,Arshadi, M.R.,Parsafar, G.A andSastri, V.S. (2006). Cluster/polarized continuum models for density functional theory investigations of benzimidazole corrosion inhibitors at metal–solution interface. *Corros. Sci. Sect.* (NACE) **62:** 199–206.

Lashkari, M. and Arshadi, M.R. (2004). DFT studies of pyridine corrosion inhibitors in electrical double layer: solvent, substrate, and electric field effects. *Chem. Phys.* **299 :** 131–137.

Lazarova, E.,Kalcheva, S.,Neykov, G.,Yankova, T andStoyanov, N. (2000). Electrochemical investigation of the adsorption behaviour of anhydrides and imides on iron in acid medium. *Journal of Applied Electrochemistry***30 :** 561–570.

Lazarova, E.,Yankova, T andAleksiev, B. (1995). Adsorption of maleimide and its derivatives on an iron electrode in acidic and neutral media. *Langmuir***11 :**2231–2236.

Lebrini, M.,Bentiss, F.,Vezin, H andLagrenée, M. (2006). The inhibition of mild steel corrosion in acidic solutions by 2,5-bis(4-pyridyl)-1,3,4-thiadiazole: structure-activity correlation. *Corrosion Science***48 :** 1279–1291.

Lebrini, M.,Lagrenée, M.,Traisnel, M.,Gengembre, L.,Vezin, H., and Bentiss F. (2007b). Enhanced corrosion resistance of mild steel in normal sulphuric acid medium by 2,5-bis(n-thienyl)-1,3,4-thiadizoles: electrochemical, X-ray photoelectron spectroscopy and theoretical studies. *Applied Surface Science***253 :** 9267–9276.

Lebrini, M.,Lagrenée, M.,Vezin, H.Gengembre, L. and Bentiss, F. (2005). Electrochemical and quantum chemical studies of new thiadiazole derivatives adsorption on mild steel in normal hydrochloric acid medium. *Corrosion Scien,***47:** 485– 505.

Lebrini, M.,Lagrenée, M.,Vezin, H.,Traisnel, M. and Bentiss, F. (2007a). Experimental and theoretical study for corrosion inhibition of mild steel in normal hydrochloric acid solution by some new macrocyclic polyether compounds. *Corrosion Science***49 :**2254–2269.

Lebrini, M.,Traisnel, M.,Lagrenée, M.,Mernari, B. and Bentiss, F. (2008). Inhibitive properties, adsorption and a theoretical study of 3,5-bis(n-pyridyl)-4- amino-1,2,4- triazoles as corrosion inhibitors for mild steel in perchloric acid. *Corrosion Science***50 :** 473–479.

Lendvay-Györik, G.,Mészáros, G.,Lengyel, B andLendvay, G. (2003). Electrochemical and quantum chemical studies on the formation of protective films by alkynols on iron. *Corrosion Science***45 :** 1685–1702.

Levine, I.N. (1991). Quantum Chemistry. Prentice Hall, New Jersey.

Lewis, D.F.V.,Ioannides, C andParke, D.V. (1994). Interaction of a series of nitriles with the alcohol-inducible isoform of P450:Computer analysis of structure–activity relationships. *Xenobiotica***24:**401–408.

Li, S.L.,Wang, Y.G.,Chen, S.H.,Yu, R.,Lei, S.B.,Ma, H.Y.,Liu, D.X. (1999b). Some aspects of quantum chemical calculations for the study of Schiff base corrosion inhibitors on copper in NaCl solutions. *Corrosion Science***41:**1769–1782.

Li, W.,He, Q.,Pei, C.,Hou, B. (2007). Experimental and theoretical investigation of the adsorption behaviour of new triazole derivatives as inhibitors of mild steel corrosion in acid media. *Electrochimica Acta***52 :** 6386–6394.

Li, Y.,Zhao, P.,Liang, Q andHou, B. (2005). Berberine as a natural source inhibitor for mild steel in 1 M H_2SO_4. *Applied Surface Science***252:**1245–1253.

Li, S.L., Wang, Y.G., Chen, S.H., Yu, R., Lei, S.B., Ma,H.Y., and Liu,D.X. (1999a). Investigation of some Schiff bases as HCl corrosion inhibitors for Cu. *Corrosion Science***41:** 1273-1287.

Lukovits, I., Bakó, I., Shaban, A., and Kálmán, E. (1998). Polynomial model of the inhibition mechanism of thiourea derivatives. *Electrochimica Acta***43:** 131–136.

Lukovits, L., Shaban, A., Kalman, E. (2003). Corrosion inhibitor, quantitative structural activity relationships. *Rusian Journal of Electrochemistry***19(2):** 177-181.

Ma, H.,Chen, S.,Liu, Z andSun, Y. (2006). Theoretical elucidation on the inhibition mechanism of pyridine-pyrazole compound: a Hartree–Fock study. *Journal of Molecular Structure* (THEOCHEM) **774 :**19–22.

Ma, H.,Song, T.,Sun, H andLin, X. (2008). Experimental and theoretical elucidation on the inhibition mechanism of 1-methyl-5-mercapto-1,2,3,4-tetrazole selfassembled films on corrosion of iron in 0.5 M H_2SO_4 solutions. *Thin Solid Films* **516 :** 1020–1024.

Maltarollo, V. G., Homem-de-Mello, P. and Honorio, K. M. (2010). Theoretical study on the molecular and electronic properties of some substances used for diabetes mellitus treatment. *Journal of Molecular Modelling***16:** 799-804

Mansfeld, F. (1987). Corrosion mechanisms. New York: Dekker M.

Martinez, S. (2002). Inhibitory mechanism of mimosa tannin using molecular modeling and substitutional adsorption isotherms. *Material Chemistry and Physics***9288 :**1–6.

Martinez, S. and Štagljar,I. (2003). Correlation between the molecular structure and the corrosion inhibition efficiency of chestnut tannin in acidic solutions. *Journal of Molecular Structure*(THEOCHEM) **640:**167–174.

Mercer,A.P. (1990). Chemical inhibitors for corrosion control. Glubley edited. London: *Royal Society Of Chemistry.*

Monika, W.A., Dubey, A. and Arwind, D. (2005). Inhibiting effect of N-acetyl N,N,N-trimethylammonium bromide on corrosion of mild steel in acidic medium. *PortugalliseElectrochemica Acta***23(4):**445-455.

Moniz, B. J. (1986). Process industries corrosion Moniz, B.J. and Pollock edited. NACE. Houston. Reprinted by permission of the National Association of Corrosion Engineers.

Moore, J.J. (1996). Chemical metallurgy. 2nd edition. London. Butterworths.

Moretti, G, Guidi, F. and Grion, G. (2004). Tryptamine as a green iron corrosion inhibitor in 0.5 M deaerated sulphuric acid. *Corrosion Science***46:**387–403.

Morgan, W.M. (1984) .Outline of paint technology. England: Charles Griffins Ltd.

Muralidharan, S., Chandrasekar, R. and Iyer, S.V.K. (2000). Effect of piperidones on hydrogen permeation and inhibition of mild steel in acidic solutions. *Proccurement of Indian Academy of Science***112(2):** 127-136.

Murrell, J.N.,Kettle, S.F andTedder, J.M. (1985). The Chemical Bond. John Wiley & Sons, Chichester.

Mutombo, P. and Hackerman, N. (1998). The effect of some organophosphorus compounds on the corrosion behaviour of iron in 6 M HCl. *Anti-corrosion Method* **45 :**413–418.

Noor, E. A. (2009). Potential of aqueous extract of Hibiscus sabdariffa leaves for inhibiting the corrosion of aluminium in alkaline solutions. *Journal of Applied Electrochemistry***39:** 1465-1475.

Odiongenyi, A. O., Odoemelam, S. A. and Eddy, N. O. (2009). Corrosion inhibition and adsorption properties of ethanol extract of Vernonia Amygdalina for the corrosion of mild steel in H_2SO_4. *Portugaliae Electrochimica Acta***27(1):** 33-45.(http://www.peacta.org/)

Ögˇretir, C.,Çalıs_, S.,Bereket, G andBerber, H. (2003). A theoretical search on metal–ligand interaction mechanism in corrosion of some imidazoline derivatives. *Journal of Molecular Structure* (THEOCHEM) **626:**179–186.

Ögˇretir, C.,Mihçi, B.,Bereket, G. (1999). Quantum chemical studies of some pyridine derivatives as corrosion inhibitors. *Journal of Molecular Structure* (THEOCHEM) **488:** 223–231.

Oguzie, E. E. (2008). Corrosion inhibitive effect and adsorption behaviour of Hibiscus Sabdariffaextract on mild steel in acidic media. *Portugaliae Electrochimica Acta* **26:** 303-314.

Oguzie, E.E. (2005). Inhibition of acid corrosion of mild steel by Telfaria occidentalis extract. *Pigment and Resin Technology,***34(6):** 321-326.

Oguzie, E.E. (2006a). Studies on the inhibition effect of Occinum vivridis extract on acid corrosion of mild steel. *Material Chemistry and Physics,***99(2-3):**441-446.

Oguzie, E.E. (2006b). Adsorption and corrosion inhibitive properties of Azadirachta indica in acid solutions. *Pigment and Resin Technology*, **35(6):** 334-340.

Oguzie, E.E. (2007). Corrosion inhibition of aluminum in acidic and alkaline media on Sanseviera triasciata extract. *Corrosion Science*,**49:** 1527-1539.

Oguzie, E. E., Onuoha, G. N. and Ejike, E. N. (2007).Effect of Gongronema latifolium extract on aluminium corrosion in acidic and alkaline media. *Pigment and Resin Technolgy* 36(1):44 - 49.

Oguzie, E.E., Onuchukwu, A.I., Okafor, P.C. and Ebenso, E.E. (2006). Corrosion inhibition and adsorption behavior of Occimum basiclicum extract on aluminum. *Pigment and Resin technology*, **35(2):**63-70.

Okafor, P.C. (2004). Investigation and modeling of carbon (IV) oxide corrosion of carbon steel in the presence of acetic acid.Ph.D thesis. University of Calabar. Calabar.

Okafor, P.C. and Ebenso, E.E. (2007). Inhibitive action of Carica papaya extracts on the corrosion of mild steel in acidic media and their adsorption characteristics. *Pigment and Resin Technology***36(3):**134-140.

Okafor, P.C., Ekpe, U.J., Ebenso, E.E., Umoren, E. S. and Leizou, K.E. (2005). Inhibition of mild steel corrosion in acidic medium of sativum.*Bulletin of Electrochemistry***21(8):**347-352.

Okafor, P.C., Ikpi, M.I., Uwah, I.E., Ebenso, E.E., Ekpe, U.J. and Umoren, S.A. (2008). Inhibitory action of Phyllanthus amarus on the corrosion of mild steel in acidic medium. *Corrosion Science* doi:10.1016/j.corros.sci.2008.05.009.

Okafor, P.C., Osabor, V. and Ebenso, E.E. (2007). Eco friendly corrosion inhibitors: Inhibitive action of ethanol extracts of Garcinia Kola for the corrosion of aluminium in acidic medium. *Pigment and Resin Technology*, **36(5):**299-305.

Olivares-Xometl, O., Likhanova, N. V., Dom´ınguez-Aguilar, M. A., Arce, E., Dorantesc, H. and Arellanes-Lozada, P. (2008). Synthesis and corrosion inhibition of amino acids alkylamides for mild steel in acidic environment. *Materials Chemistry and Physics* **110:** 344-351.

Özcan, M. and Dehri,I. (2004). Electrochemical and quantum chemical studies of some sulphur-containing organic compounds as inhibitors for the acid corrosion of mild steel. *Progr. Org. Coat*.,**51:** 181–187.

Özcan, M.,Dehri, I andErbil, M. (2004). Organic sulphur-containing compounds as corrosion inhibitors for mild steel in acidic media: correlation between inhibition efficiency and chemical structure. *Applied Surface Science***236 :** 155– 164.

Özcan, M.,Karadag˘, F and Dehri, I. (2008). Investigation of adsorption characteristics of methionine at mild steel/sulphuric acid interface: an experimental and theoretical study. *Coll. Surf. A:Physicochem. Eng. Aspects***316 :** 55– 61.

Parr, R.G.,Craig, D.P and Ross, I.G. (1950). Molecular orbital calculations of the lower excited electronic levels of benzene, configuration interaction included. *Journal of Chemistry and Physics***18 :**1561–1563. G. Gece / Corrosion Science 50 (2008) 2981–2992 2991

Paurbaix, J.L. (1981). Atias of electrochemical equilibrium in aqueous solution. NACE, London.

Pearson, R.G. (1989). Absolute electronegativity and hardness: applications to organic chemistry. *Journal of Organic Chemistry***54:**1423–1430.

Pokhmurs'kyi, V.I.,Khoma, M.S.,Kopylets', V.I andKornii, S.A. (2003). Investigation of the initial stage of selective dissolution of zinc–aluminium alloys in chloridecontaining media. *Material Science***39:** 394–399.

Popova, A.,Christov, M andZwetanova, A. (2007). Effect of the molecular structure on the inhibitor properties of azoles on mild steel corrosion in 1M hydrochloric acid. *Corrosion Science***49:**2131–2143.

Pradip, B.R. (2002). Design of tailor-made surfactants for industrial applications using a molecular modelling approach.*Coll. Surface A*: *Physicochem. Eng. Aspects*,**205 :**139–148.

Qafsaoui, W.,Blanc, C.,Roques, J.,Pebere, N.,Srhiri, A.,Mijoule, C.,Mankowski, G. (2001). Pitting corrosion of copper in sulphate solutions: inhibitive effect of different triazole derivative inhibitors. *Journal of Applied Electrochemistry* **31:** 223–231.

Quan, Z., Chen, S., Li, Y. and Cui, X. (2002). Adsorption behaviour of Schiff base and corrosion protection resulting film to copper substrate. *Corrosion Science***44:** 703-715.

Quraishi, M.A., and Sardar, R. (2002). Corrosion inhibition of mild steel in acid solutions by some aromatic oxadiazoles. *Material Chemistry and Physics 78: 703-231.*

Rahim, A.A.,Rocca, E.,Steinmetz, J.,Kassim, M.J.,Adnan, R andIbrahim, M.S. (2007). Mangrove tannins and their flavanoid monomers as alternative steel corrosion inhibitors in acidic medium. *Corrosion Science***49 :**402–407.

Rajendran, S., Joany, M.R., Apparao, B.V. and Palaniswamy, N. (2000). Synergistic effect of calcium gluconate and Zn^{2+}on the inhibition of corrosion of mild steel in neutral aqueous environment. *Transaction of the SEAST***35(3,4):**113-117.

Ramachandran, S., and Jovancicevic, V. (1999). Molecular modeling of the inhibition of mild steel carbon dioxide corrosion by imidazolines. *Corrosion Science.* (NACE) **55 :**259–267.

Ramachandran, S., Campbell, S. and Ward, M.B. (2001). Interaction and properties of corrosion inhibitors with by-product layers. *Corrosion***57(6):** 508-515

Rodríguez-Valdez, L.M.,Martínez-Villafane, A., and Glossman-Mitnik, D. (2005). Computational simulation of the molecular structure and properties of heterocyclic organic compounds with possible corrosion inhibition properties. *J. Mol. Struct*.(THEOCHEM) **713 :** 65–70.

Rodríguez-Valdez, L.M.,Martínez-Villafane, A., and Glossman-Mitnik, D. (2004). CHIH-DFT determination of the molecular structure, infrared and ultraviolet spectra of potentially organic corrosion inhibitors. *Journal of Molecular Structure* (THEOCHEM) **681 :**83–88.

Rodríguez-Valdez, L.M.,Villamisar, W.,Casales, M.,González-Rodríguez, J.G,Martínez-Villafane, A.,Martinez, L. and Glossman-Mitnik, D. (2006). Computational simulations of the molecular structure and corrosion properties of amidoethyl, aminoethyl and hydroxyethyl imidazolines inhibitors. *Corrosion Science***48 :** 4053–4064.

Sahin, M., Gece, G., Karci, F. and Bilgic, S. (2008). Experimental and theoretical study of the effect of some heterocyclic compounds on the corrosion of low carbon steel in 3.5 % NaCl medium. *Journal of Applied Electrochemistry***38:** 809-815.

Sastri, V.S. and Perumareddi, J.R. (1994). Selection of corrosion inhibitors for use in sour media. *Corrosion Science Sect.* (NACE) 432–437.

Sastri, V.S., and Perumareddi, J.R. (1997). Molecular orbital theoretical studies of some organic corrosion inhibitors. *Corrosion Science Sect*. (NACE) **53:**617–622.

Sayós, R.,González, M., andCosta, J.M. (1986). On the use of quantum chemical methods as an additional tool in studying corrosion inhibitor substances. *Corrosion Science***11:**927–934.

Scendo, M. (2005). Potassium ethyl xanthate as corrosion inhibitor for copper in acidic chloride solutions. *Corrosion Science***47 :**1738–1749.

Schmidt, M. W., Baldridge, K. K., Boatz, J. A., Elbert, S.T., Gordon, M.S.,Jensen, J.H., Koseki, S., Matsunaga, N., Nguyen, K.A., Su, S.J., Windus, T.L.,
Dupus, M.and Montgomery, J.A (1993). Games version 12*Journal of Computational Chemistry* 1347-1363.

Sein Jr., L.T.,Wei, Y., and Jansen, S.A. (2001). The role of adsorption of aniline trimers on the corrosion inhibition process : a ZINDO/1 study. *Computational and Theoretical Polymer Science***11 :** 83–88.

Sein Jr., L.T.,Wei, Y. and Jansen, S.A. (2004). Corrosion inhibition by aniline oligomers through charge transfer: a DFT approach. *Synthectic Method***143 :**1–12.

Sethuran, M.G. and Raja, P.B. (2005). Corrosion inhibition of mild steel by Datura metel in acidic medium. *Pigment and Resin Technol*ogy**34(6):**327-331.

Shapovalova, I.N.,Tatarchenko, G.O.,Zakharov,I.I. and Tyupalo, M.F. (2005). A quantum chemical model of active centers of electrochemical corrosion of metals. *Material Science***41:** 7–14.

Sheikhshoaie,I. and Mashhadizadeh, M.H. (2003). Syntheses, electronic structure and second-order optical nonlinearity of two new bidentate monoazo Schiff-base compounds. *Russian Journal of Coordination Chemistry***29:**710–713.

Silva, A. B, Agostinho, S. M. l., Barcia, O. E., Cordeiro, G. G. O. and D'Elia, E. (2006). The effect of cysteine on the corrosion of 304L stainless steel in sulphuric acid.*Corrosion Science***48:**3668–3674.

Soler, J.M.,Artacho, E.,Gale, J.D.,Garcia, A.,Junquera, J.,Ordejon, P. and Sanchez-Portal, D. (2002). The SIESTA method for ab initio order-N materials simulation. *J. Phys.- Condes. Matter*. **14:** 2745–2779.

Soliman, H.M.A and Abdel-Rahman, H.H. (2006). The use of rotating cylinder electrode to study the effect of 1,3-dihydoxypropane on the production of copper powder. *Journal of Brazilian Chemical Society***17(4):**705-714.

Solmaz, R., Kardas, G., Yaziei, B. and Erbil, M. (2005). Inhibition effect of rhodanine for corrosion of mild steel in HCl solution. *Protection of metals***41(6):**581-585.

Spah, M., Spah, D. C., Deshwal, B., Lee, S., Chae, Y. and Park, J. W. (2009). Thermodynamic studies on corrosion inhibition of aqueous solutions of amino/carboxylic acids toward copper by EMF measurement. *Corrosion Science***51:**1293–1298.

Steward, J. P. (2009) MOPAC Steward computational Chemistry, Version 9.069W. HTTP://OpenMOPAC.net

Stewart, J.J.P. (1989). Optimization of parameters for semiempirical methods.*Journal of Computational Chemistry***10:**209–220.

Stoyanov, S. R., Gusarov, S., Kuznick, S. M. and Kovalenko, A. (2008). Theoretical modelling of zeolite nanoparticle surface acidity for heavy oil upgrading. *Journal of Physical Chemistry***112:** 6794-6810.

Stoyanova, A.,Petkova, G., and Peyerimhoff,S.D. (2002). Correlation between the molecular structure and the corrosion inhibiting effect of some pyrophthalone compounds. *Chemistry and Physics***279 :**1–6.

Stoyanova, A.E. and Peyerimhoff, S.D. (2002). On the relationship between corrosion inhibiting effect and molecular structure. *Electrochimica Acta***47:** 1365 - 1371.

Stupnišek-Lisac, E.,Podbršc˘ek, S. and Soric´,T. (1994). Non-toxic organic zinc corrosion inhibitors in hydrochloric acid. *Journal of Applied Electrochemistry***24:**779–784.

Subramanyam, N.C.,Sheshardi, B.S. and Mayanna S.A. (1993). Thiourea and substituted thioureas as corrosion inhibitors for aluminium in sodium nitrite solution. *Corrosion Science***34:**563–571.

Sun, Y. (2003). Localized CO_2 corrosion in Horizontal wet gas flow. Ph.D. dissertation. Department of chemical engineering. ohioUniversity, Anthens, Ohio.

Szeptycka, B. (2005). Quantum chemical modeling (QCM) and quantum structureactivity relationship modeling (QSARM) of acid pickling inhibition. *Mater. Manuf. Proc*.,**20 :** 9–21.

Szeptycka, B. and Kwiatkowski, L. (2000). The applications of quantum mechanics calculations to the interpretation of corrosion inhibition mechanism in concentrated acid medium, in: Proceedings of the 9th European Symposium on Corrosion Inhibitors (9 SEIC). Ann. Univ. Ferrara, N.S., Sez. V, Suppl. N. **11:**161-171.

Tanak, H. and Yavuz, M. (2010). Density functional computational studies on (E)-2-[(2-hydroxy-5-nitrophenyl)-iminiomethyl[-4-nitrophenolate. *Journal of Molecular Modeling***16:** 235-241.

Tang, L.,Li, X.,Li, L.,Mu, G., and Liu, G. (2006). Interfacial behaviour of 4-(2-pyridylazo) resorcin between steel and hydrochloric acid. *Surface Coating Technology***201:**384–388.

Tavassoli-Salardini, P. (2004). Inhibition of corrosion of mild steel in aqueous solution. Ph.D. Thesis. University of Sydney.

Touhami, F.,Aouniti, A.,Abed, Y.,Hammouti, B.,Kertit, S., Ramdani A. and Elkacemi, K. (2000). Corrosion inhibition of armco iron in 1 M HCl media by new bipyrazolic derivatives. *Corrosion Science***42:**929–940.

Umoren, S.A. and Ebenso, E.E. (2007). The synergistic effect of polyacrylamide and iodided ions on the corrosion of mild steel in H_2SO_4. *Materials Chemistry and Physics***106:** 387-393.

Umoren, S.A. and Ebenso, E.E. (2008). Studies of anti-corrosive effect of Raphia hockeri exudates gum-halide mixtures for aluminiumcorrosion in acidic medium. *Pigment and Resin Technol*ogy**37(3):**173-182.

Umoren, S.A., Ogbobe, O., Igwe, I.E. and Ebenso, E.E. (2008b). Inhibition of mild steel corrosion in acidic medium using synthetic and naturally occurring polymers and synergistic halide additives. *Corrosion Science doi:* 10.1016/j.corsci.2008.04.015.

Umoren, S.A., Ebenso,E.E., Okafor, P.C., Ekpe, U.J. and Ogbobe, O. (2006a). Effect of halides on the corrosion inhibition of mild steel in alkaline medium using polyvinyl alcohol. *Journal of Applied Polymer Science*,**103:** 2810-2816.

Umoren, S.A., Obot, I.B. and Ebenso, E.E. (2008a). Corrosion inhibition of aluminium using exudate gum from Pacchylobus edulis in the presence of halide ions in HCl. *Electronic Journal of Chemistry*,**5(2):**355-364.

Umoren, S.A., Ogbobe, O., Ebenso,E.E., and Ekpe, U.J.(2006a). Effect of halides on the corrosion inhibition of mild steel in acidic medium using polyvinyl alcohol. *Pigment & Resin Technology***35(5):** 284-292.

Vosta J. and Eliásek J. (1971). Study on corrosion inhibition from aspect of quantum chemistry. *Corrosion Science***11:**223–229.

Wang, C.T.,Chen, S.H.,Ma, H.Y. andQi, C.S. (2003). Protection of copper corrosion by carbazole and N-vinylcarbazole self-assembled films in NaCl solution. *Journal of Applied Electrochemistry***33 :**179–186.

Wang, D.,Li, S.,Ying, Y.,Wang, M.,Xiao, H. andChen, Z. (1999). Theoretical and experimental studies of structure and inhibition efficiency of imidazoline derivatives. *Corrosion Science***41:**1911–1919.

Wang, H., Wang X., Wang, H., Wang, L. and Liu, A. (2007) DFT study of new bipyrazole derivatives and their potential activity as corrosion inhibitors. *Journal of Molecular Modeling***13:**147-153

Xiao-Ci, Y.,Hong, Z.,Ming-Dao, L.,Hong-Xuan, R. andLu-An, Y. (2000). Quantum chemical study of the inhibition properties of pyridine and its derivatives at an aluminium surface. *Corrosion Science***42:**645–653. 2990 G. Gece / Corrosion Science 50 (2008) 2981–2992

Xuejun, X.,Shuman, C.,Ling, P.,Xunjie, G. and Keru, P. (2004). A quantum chemistry calculation study on the inhibition efficiency of the para-chlorobenzene nitriles on carbon steel in hydrochloric acid. *Anti-corrosion Method***51 :**101–104.

Yan, L.J.,Niu, L.,Lin, H.C.,Wu, W.T. and Liu, S.Z. (1999). Quantum chemistry study on the effect of Cl^- on anodic dissolution of iron in H_2S-containing sulphuric acid solutions. *Corrosion Science***41:** 2303–2315.

Yan, Y.,Li, W.,Cai, L. and Hou, B. (2008). Electrochemical and quantum chemical study of purines as corrosion inhibitors for mild steel in 1 M HCl solution. *Electrochimica Acta***53 :** 5953–5960.

Young, D. C. (2001)*Computational Chemistry, A practical guide for applying techniques to real world problems.* Wiley Interscience, New York 324.

Yurt, A. ,Bütün, V. and Duran, B. (2007). Effect of the molecular weight and structure of some novel water-soluble triblock copolymers on the electrochemical behaviour of mild steel. *Material Chemistry and Physics***105 :**114–121.

Yurt, A.,Bereket, G. and Ög˘retir, C. (2005a). Quantum chemical studies on inhibition effect of amino acids and hydroxy carboxylic acids on pitting corrosion of aluminium alloy 7075 in NaCl solution. *Journal Molecular Structure* (THEOCHEM) **725:** 215–221.

Yurt, A.,Ulutas, S. and Dal, H. (2006). Electrochemical and theoretical investigation on the corrosion of aluminium in acidic solution containing some Schiff bases. *Applied Surface Science***253:**919–925.

Yurt, A., Balaban, A., Kandemer, S.U., Bereket,G and Erk, B. (2004). Investigation of some schiff bases as HCl corrosion inhibitors for carbon steel. *Material Chemistry and Physics***85:**420-426.

Yurt, A., Bereket, G., Rivrak, A., Balaban, A. and Erk, B. (2005). Effect of Schiff bases containing pyridyl group as corrosion inhibitors fro low carbon steel in 0.1M HCl. *Journal of Applied Electrochemistry***35:**1025-1032.

Zerfaoui, M. Ouddac, H., Hammouti, B. Kertit, S. and Benkaddourb, M. (2004) Inhibition of corrosion of iron in citric acid media by amino acids. *Progress in Organic Coatings* **51:**134–138.

Zhang, D.,An, Z.,Pan, Q.,Gao, L.,and Zhou, G. (2006). Comparative study of bispiperidiniummethyl- urea and mono-piperidiniummethyl-urea as volatile corrosion inhibitors for mild steel. *Corrosion Science***48:**1437–1448.

Zhang, D.,Gao, L., and Zhou, G. (2004). Inhibition of copper corrosion in aerated hydrochloric acid solution by heterocyclic compounds containing a mercapto group. *Corrosion Science***46:**3031–3040.

Zhang, J.,Zhang, Q.,Ren, H.,Zhao, W., and Zhang, H. (2007). Inhibition performance of 2-mercaptobenzothiazole derivatives in CO_2 saturated solution and its adsorption behavior at Fe surface. *Applied Surface Science***253:**7416–7422.

Zhang, S.G.,Lei, W.,Xia, M.Z. and Wang, F.Y. (2005). QSAR study on N-containing corrosion inhibitors: quantum chemical approach assisted by topological index. *Journal of Molecular Structure* (THEOCHEM) **732 :** 173–182.

Zhang, D., Cai, Q., He, X., Gao, L. and Zhou, G. (2008). Inhibition effect of some amino acids on copper corrosion in HCl solution. *Materials Chemistry and Physics***112:**353–358.

Zhao, P.,Liang, Q., and Li, Y. (2005). Electrochemical, SEM/EDS and quantum chemical study of phthalocyanines as corrosion inhibitors for mild steel in 1 mol/l HCl. *Applied Surface Science***252:**1596–1607.

Zhenlon, Q., Chen, S. and Li, S. (2004). Protection of Cu corrosion by modification of self-assembled films of Schiff bases with alkanethanol. *Corrosion Science***43:**1071-1080.

Zhou, Z. and Parr, R.G. (1990). Activation hardness:new index for describing the orientation of electrophilic aromatic substitution. *Journal of American Chemical Society***112:** 5720–5724.

Zuchi, F. and Omar, I.H. (1985). Plant extracts as corrosion inhibitors of mild steel in HClsolution. *Surface Technology***24(4):**391-399.

Zuchi, F., Trabanelli, G. and Gullari, G. (1978). Inhibitory action of some organic sulphides. *Electrochemica Material***34:**407-419.

APPENDIX

Appendix 1: Input file for MOPAC calculations involving CYS

* ==============================

* Input file for MOPAC

* ==============================

Hamiltonian 1SCF CHARGE=0 Singlet BONDS AUX

Mopac file generated by Dr. Nnabuk Okon Eddy

C 2.021478 1 0.663725 1 -0.462733 1

N 1.060625 1 -1.543166 1 -0.462733 1

C 0.744541 1 -0.140335 1 -0.462733 1

C -0.066633 1 0.196532 1 0.781472 1

S -1.680145 1 0.866595 1 0.289723 1

O 1.975153 1 1.870837 1 -0.462733 1

O 3.205023 1 0.039654 1 -0.462733 1

H 0.310985 1 -2.234859 1 -0.462733 1

H 2.034469 1 -1.846526 1 -0.462733 1

H 0.151153 1 0.106089 1 -1.371543 1

H -0.217183 1 -0.725494 1 1.386429 1

H 0.480289 1 0.953465 1 1.387027 1

H -2.569444 1 1.235905 1 1.228755 1

H 4.027543 1 0.557577 1 -0.462733 1

Appendix 2: Input file for MOPAC calculations involving CYS

```
* ================================
* Input file for MOPAC
* ================================
Hamiltonian 1SCF    CHARGE=0 Singlet  BONDS AUX
Mopac file generated by Dr. Eddy
C  0.768410  1 0.269345  1 -0.000045  1
N  -1.638536  1 0.254617  1 -0.000045  1
C  -0.473327  1 -0.588076  1 -0.000045  1
O  0.671002  1 1.473411  1 -0.000045  1
O  1.977324  1 -0.304041  1 -0.000045  1
H  -2.569444  1 -0.162288  1 -0.000045  1
H  -1.534132  1 1.269260  1 -0.000045  1
H  -0.480327  1 -1.229924  1 0.909213  1
H  -0.480334  1 -1.230559  1 -0.908855  1
H  2.777171  1 0.248254  1 -0.000045  1
```

Appendix 3: Input file for MOPAC calculations involving GLY

* ==============================

* Input file for MOPAC

* ==============================

PM6 1SCF CHARGE=0 Singlet BONDS AUX

Mopac file generated by Dr Eddy

C 2.586467 1 0.477521 1 0.458347 1

N 1.357319 1 -1.226509 1 1.632690 1

C 1.356425 1 -0.396593 1 0.458347 1

C 0.111287 1 0.480426 1 0.458347 1

C -0.717710 1 0.186315 1 -0.784952 1

C -1.130262 1 -1.279743 1 -0.785826 1

C -1.962856 1 1.063320 1 -0.783157 1

O 3.381480 1 0.401486 1 1.364679 1

O 2.796553 1 1.336799 1 -0.545521 1

H 0.593579 1 -1.883143 1 1.793726 1

H 2.121693 1 -1.158550 1 2.304638 1

H 1.358423 1 -1.039572 1 -0.450137 1

H -0.494102 1 0.264262 1 1.366942 1

H 0.412415 1 1.551916 1 0.458347 1

H -0.112398 1 0.401752 1 -1.693772 1

H -1.736089 1 -1.494678 1 -1.694422 1

H -0.220316 1 -1.920654 1 -0.787138 1

H -1.735574 1 -1.495180 1 0.122994 1

H -2.569444 1 0.849153 1 -1.691426 1

H -1.661365 1 2.134709 1 -0.783172 1

H -2.567405 1 0.847116 1 0.125988 1

H 3.588867 1 1.899847 1 -0.545521 1

Appendix 4: Input file for MOPAC calculations involving ALA

```
* ==============================
* Input file for MOPAC
* ==============================
Hamiltonian 1SCF    CHARGE=0 Singlet  BONDS AUX
Mopac file generated by Dr Eddy
C  0.812984  1 0.402629  1 -0.180437  1
N  -0.416165  1 -1.301401  1 0.993907  1
C  -0.417059  1 -0.471485  1 -0.180437  1
C  -1.662196  1 0.405535  1 -0.180437  1
O  1.607997  1 0.326593  1 0.725895  1
O  1.023070  1 1.261907  1 -1.184304  1
H  -1.179905  1 -1.958035  1 1.154943  1
H  0.348209  1 -1.233442  1 1.665854  1
H  -0.415061  1 -1.114464  1 -1.088920  1
H  -1.663867  1 1.048342  1 -1.089043  1
H  -2.569444  1 -0.239189  1 -0.181090  1
H  -1.663215  1 1.048055  1 0.728373  1
H  1.815384  1 1.824954  1 -1.184304  1
```

Appendix 5: Input file for GAMESS calculations involving CYS

```
! ============================================================
! This file was generated by Dr Nnabuk Okon Eddy
! ============================================================
 $CONTRL RUNTYP=Energy $END
 $CONTRL SCFTYP=RHF $END
 $DFT  DFTTYP=B3LYP $END
 $CONTRL ICHARG=0  MULT=1 $END
 $BASIS GBASIS=N31 NGAUSS=6 $END
$DATA
Molecule specification
C1
C  6.000000 2.021478 0.663725 -0.462733
N  7.000000 1.060625 -1.543166 -0.462733
C  6.000000 0.744541 -0.140335 -0.462733
C  6.000000 -0.066633 0.196532 0.781472
S  16.000000 -1.680145 0.866595 0.289723
O  8.000000 1.975153 1.870837 -0.462733
O  8.000000 3.205023 0.039654 -0.462733
H  1.000000 0.310985 -2.234859 -0.462733
H  1.000000 2.034469 -1.846526 -0.462733
H  1.000000 0.151153 0.106089 -1.371543
H  1.000000 -0.217183 -0.725494 1.386429
H  1.000000 0.480289 0.953465 1.387027
H  1.000000 -2.569444 1.235905 1.228755
H  1.000000 4.027543 0.557577 -0.462733
 $END
```

Appendix 6: Input file for GAMESS calculations involving GLY

```
! ============================================================
! This file was generated by Dr Eddy
! ============================================================
 $CONTRL RUNTYP=Energy $END
 $CONTRL SCFTYP=RHF $END
 $CONTRL MPLEVL=2 $END
 $CONTRL ICHARG=0  MULT=1 $END
 $BASIS GBASIS=STO NGAUSS=5 $END
$DATA
Molecule specification
C1
C  6.000000 0.768410 0.269345 -0.000045
N  7.000000 -1.638536 0.254617 -0.000045
C  6.000000 -0.473327 -0.588076 -0.000045
O  8.000000 0.671002 1.473411 -0.000045
O  8.000000 1.977324 -0.304041 -0.000045
H  1.000000 -2.569444 -0.162288 -0.000045
H  1.000000 -1.534132 1.269260 -0.000045
H  1.000000 -0.480327 -1.229924 0.909213
H  1.000000 -0.480334 -1.230559 -0.908855
H  1.000000 2.777171 0.248254 -0.000045
 $END
```

Appendix 7: Input file for GAMESS calculations involving LEU

```
! ============================================================
! This file was generated by Dr Eddy
! ============================================================
 $CONTRL RUNTYP=Energy $END
 $CONTRL SCFTYP=RHF $END
 $DFT  DFTTYP=B3LYP $END
 $CONTRL ICHARG=0  MULT=1 $END
 $BASIS GBASIS=N31 NGAUSS=6 $END
$DATA
Molecule specification
C1
C  6.000000 2.586467 0.477521 0.458347
N  7.000000 1.357319 -1.226509 1.632690
C  6.000000 1.356425 -0.396593 0.458347
C  6.000000 0.111287 0.480426 0.458347
C  6.000000 -0.717710 0.186315 -0.784952
C  6.000000 -1.130262 -1.279743 -0.785826
C  6.000000 -1.962856 1.063320 -0.783157
O  8.000000 3.381480 0.401486 1.364679
O  8.000000 2.796553 1.336799 -0.545521
H  1.000000 0.593579 -1.883143 1.793726
H  1.000000 2.121693 -1.158550 2.304638
H  1.000000 1.358423 -1.039572 -0.450137
H  1.000000 -0.494102 0.264262 1.366942
H  1.000000 0.412415 1.551916 0.458347
H  1.000000 -0.112398 0.401752 -1.693772
H  1.000000 -1.736089 -1.494678 -1.694422
```

H 1.000000 -0.220316 -1.920654 -0.787138

H 1.000000 -1.735574 -1.495180 0.122994

H 1.000000 -2.569444 0.849153 -1.691426

H 1.000000 -1.661365 2.134709 -0.783172

H 1.000000 -2.567405 0.847116 0.125988

H 1.000000 3.588867 1.899847 -0.545521

$END

Appendix 8: Input file for GAMESS calculations involving ALA

```
! ============================================================
! This file was generated by Dr Eddy
! ============================================================
 $CONTRL RUNTYP=Energy $END
 $CONTRL SCFTYP=RHF $END
 $CONTRL MPLEVL=2 $END
 $CONTRL ICHARG=0  MULT=1 $END
 $BASIS GBASIS=STO NGAUSS=5 $END
$DATA
Molecule specification
C1
C  6.000000 0.812984 0.402629 -0.180437
N  7.000000 -0.416165 -1.301401 0.993907
C  6.000000 -0.417059 -0.471485 -0.180437
C  6.000000 -1.662196 0.405535 -0.180437
O  8.000000 1.607997 0.326593 0.725895
O  8.000000 1.023070 1.261907 -1.184304
H  1.000000 -1.179905 -1.958035 1.154943
H  1.000000 0.348209 -1.233442 1.665854
H  1.000000 -0.415061 -1.114464 -1.088920
H  1.000000 -1.663867 1.048342 -1.089043
H  1.000000 -2.569444 -0.239189 -0.181090
H  1.000000 -1.663215 1.048055 0.728373
H  1.000000 1.815384 1.824954 -1.184304
 $END
```